Metal Incorporation in MCM-41 for Hydrodesulfurization

BY

Rizwan Ahmed Khan

A Thesis Presented to the

DEANSHIP OF GRADUATE STUDIES

KING FAHD UNIVERSITY OF PETROLEUM & MINERALS

DHAHRAN, SAUDI ARABIA

In Partial Fulfillment of the
Requirements for the Degree of

MASTER OF SCIENCE

In

CHEMICAL ENGINEERING

January, 2003

ProQuest Information and Learning Company
300 North Zeeb Road
P.O. Box 1346
Ann Arbor, MI 48106-1346

King Fahd University of Petroleum & Minerals
DHAHRAN 31261, SAUDI ARABIA

DEANSHIP OF GRADUATE STUDIES

This thesis, written by Rizwan Ahmed Khan under the direction of his thesis advisor and approved by his thesis committee, has been presented to and accepted by the Dean of Graduate Studies, in partial fulfillment of the requirements for the degree of MASTER OF SCIENCE IN CHEMICAL ENGINEERING.

Thesis Committee

Prof. M. A. Al-Saleh
(Thesis Advisor)

Prof. M. A. Shalabi
(Co-Advisor)

Dr. Shakeel Ahmed
(Member)

Dr. Habib Al-Ali
(Member)

Dr. S.M. Zaidi
(Member)

Prof. Mohamed B. Amin 20/1/2003
(Department Chairman)

Prof. Osama Ahmed Jannadi
(Dean of Graduate Studies)

عمادة الدراسات العليا
DEANSHIP OF GRADUATE STUDIES

Date 05/2/2003

DEDICATION

This work is dedicated to
my parents,
brother, and sisters.

ACKNOWLEDGMENT

In the name of Allah, the Most Beneficient, the Most Merciful.

"Read, In the name of thy Lord and Cherisher, Who Created. Created man from a [Leech-like] clot. Read, and thy Lord is most Bountiful, He who taught [the use of] pen. Taught man which he knew not. Nay, but man doth transgress all bounds. In that he looketh upon himself as self-sufficient. Verily, to thy Lord is the return [of all]."(The Holy Quran, Surah # 196,Verses 1-5)

All praises are due to Allah, subhaanahu wa ta'aala, for his blessings on me and members of my family. I feel privileged to glorify his name in the sincerest way through this small accomplishment. I seek his mercy, favor, and forgiveness. I ask him to accept this little effort as an act of worship. May the peace and blessings of Allah be upon his prophet, Muhammad (Salla Allahu 'Alaehi was-sallam).

The support provided by King Fahd University of Petroleum & Minerals (KFUPM) is highly acknowledged. My appreciation goes to CRP, KFUPM-RI for allowing me to work in their laboratories and use their facilities.

With deep sense of gratitude and appreciation, I would like to express my sincere thanks to my thesis advisor, Prof M. A. Al- Saleh for his inspiring guidance, and help and excellent cooperation in supervising this research work. I am also very grateful to my co-advisor, Prof M. A. Shalabi for his great help, continuous encouragement and several discussions.

I owe special thanks to Dr. Shakeel Ahmed, Research Engineer III and a member of my thesis committee for his continous guidance & assistance during the course of my work. I was fortunate to have worked with him.

I would like to offer my sincere thanks to my learned thesis committee, Dr. H. Al – Ali, Dr. Javed Zaidi for their review and comments.

I would also like to thank the laboratory staffs and technicians at CRP, KFUPM-RI, especially Mr. K. Alam, Mozahar and Mr. Khalid Al- Nawad for their help and service during the experimental works.

Finally I would like to thank my friends Sohail bhai, Saif, Mazhar, Ifadat, Iqbal, Faiz, Al-Khater, Nabeel, Sohail, Munawar & Afzal who are brothers to me and my cousin brothers Farooque, Iqbal, Naser, Haroon. I would also like to thank BABA group Mujtaba, Imran, Abdullah. I would also like to thank all 903 building friends & especially the 34 flat group & all chemical R.A.'s & my room partner.

I am thankful to chairman of chemical engineering department Dr. Mohammed B. Amin for his help and cooperation. I am also thankful to all faculty and Staff members for their kind and cheerful cooperation.

Finally and humbly, I offer my sincere thanks to my parents and other family members for their encouragement, support and prayers.

(RIZWAN AHMED KHAN)

CONTENTS

LIST OF TABLES

LIST OF FIGURES

ABSTRACT

Name:	**RIZWAN AHMED KHAN**
Title:	**METAL INCORPORATION IN MCM-41 FOR HYDRODESULFURIZATION**
Degree:	**MASTER OF SCIENCE**
Major field:	**CHEMICAL ENGINEERING**
Date of degree:	**JANUARY 2003**

This thesis presents synthesis, characterization and catalytic testing of metal incorporated MCM-41 catalysts for hydrodesulfurization. Co, Ni, and Mo are incorporated in the MCM-41 with Si/Co = 50, Si/Ni= 50, Si/Mo= 10 ratios. Aluminum was also incorporated in the structure so as to increase the acidity of MCM-41 based catalysts. These catalysts were characterized by temperature programmed reduction, atomic absorption spectrometer and X-ray diffraction.

Nitrogen isotherm, pore size distribution and XRD of these catalysts are those characteristic of MCM-41 confirming that the prepared catalysts are MCM-41. Temperature programmed reduction techniques were used to find out metal interaction and incorporation in the support, which clearly indicated that metal is getting incorporated in the structure. It can be concluded from the pulse reactor results that impregnation of metal on these metal incorporated catalysts increased the activity of these catalysts. It can be also concluded from batch reactor evaluations that MCM-41 based catalysts perform better than the zeolite based catalysts. MCM-41 based catalysts have shown high conversion per metal mole as compared to commercial catalyst in batch reactor.

Master of Science Degree

King Fahd University of Petroleum & Minerals

Dhahran, Saudi Arabia

January 2003

مـــــــــلخص الرسالة

الاسم : رضوان أحمد خان
العنوان : دمج المعادن مع (MCM-41) للإزالة الهيدروجينية للكبريت
الدرجة : ماجستير
التخصص: هندسة كيميائية
التاريخ : يناير ٢٠٠٣

تناقش هذه الرسالة تصنيع وتحديد الخواص للحفاز المعدني المدعم المعادن مع (MCM-41). لإزالة الكبريت واستخدمت المعادن لتحضير الحفاز: الكوبالت(Co)؛ النيكل(Ni) والموليبدينوم (Mo) ونسبها هي كالآتي: Si/Co = ٥٠؛ Si/Ni = ٥٠؛ Si/Mo = ١٠. تم اضافة الألمونيوم لـ (MCM-41) لزيادة درجته الحامضية. وتم تحديد الخواص الحفزية للحفازات الجديدة باستخدام: الإختزال الحراري؛ ومقياس الطيف الذري وانحراف الأشعة السينية.

أثبتت اختبارات النيتروجين وتوزيع المسام و (XRD) للحفازات الجيدة انها جميعاً أنها تركيبة (MCM-41). وتم تقييم تفاعل المعادن المضافة و جودة الدمج بمساعدة اختبار الإختزال والذي اعطى نتائج ايجابية دلت على وجود دمج للمعادن في تركيبة (MCM-41). أكدت النتائج التي تم الحصول عليها بإستخدام المفاعل ان المعادن المضافة قد زادت من النشاط الحفزي للحفازات الجديدة بينما أظهرت النتائج الأخرى المتحصل عليها من المفاعل (batch) ان أداءها افضل من الزيولايت. كما ان الـ (MCM-41) لديها معدل تحويل عالي مقارنة بالحفازات التجارية.

درجة الماجستير

جامعة الملك فهد للبترول والمعادن

الظهران ، المملكة العربية السعودية

يناير ٢٠٠٣

1

Introduction and History

1.1 Introduction

Catalysis is the focal point where many chemical disciplines inorganic, organic, metal organic, colloidal, and, more generally, physical chemistry, chemical engineering and material science connect strongly together. Therefore, catalysis plays a fundamental role for these sciences and in the evolution of industrial technology, whether looking for scientific, technical or practical point of view. The growing constraints imposed by requirements of energy saving and environmental protection will accelerate these trends. Material science is a prime driver for innovation or field of catalytic processes. Developments on material science, particularly in the last decade have yielded a broad range of porous solids, which have found application in the industrially important area of catalysis.

In catalytic reactions, the reactants must diffuse through the pores to reach the catalyst surface for reaction. Transport through these pores occurs mainly by diffusion and often affects or even controls the overall reaction rate of the process. The mechanisms by which diffusion may proceed are highly affected by the nature of the diffusing molecules and their interactions with the surroundings. The following in-series steps can occur during a heterogeneous reaction:

(a) Diffusion of reactants to the exterior of the crystal surface (external diffusion) from the flowing stream.

(b) Diffusion of the reactants through the crystal pores.

(c) Adsorption of the reactants on the crystal active sites, which is the result of the collision between the reactant molecules and active sites.

(d) Chemical reaction at the active sites.

(e) Desorption of the products.

(f) Diffusion of the products through the crystal pores to the external surface of the crystal.

(g) Transfer of the product from the external surface of the zeolite crystal to the flowing stream.

In zeolites, the micropores are small (<10 A) and diffusing molecules must be smaller than pore diameter to get in to the zeolite cage. The larger the molecule size the larger the activation energy to diffuse through the pores. If the molecules are larger than the pore diameter then it may not diffuse into the micropores and majority of the catalytic surface area (97% area in the pellet) will not involved in the reaction and we may not have the desired yield.

Porous materials are classified into 3 groups by International Union of Pure & Applied Chemistry (IUPAC). Figure 1-1.

- Microporous < 2nm
- Mesoporous (2 – 50 nm)
- Macroporous > 50 nm

Well known members of microporous class are zeolites, which provide excellent catalytic properties by virtue of their crystalline aluminosilicate network. Breakthrough in

mesoporous catalyst came in 1992 in the form of family of materials called M41S. M41S family contains MCM41 which is hexagonal in shape and MCM48 which is 3 d cubic in structure and MCM50 which has lamellar structure.

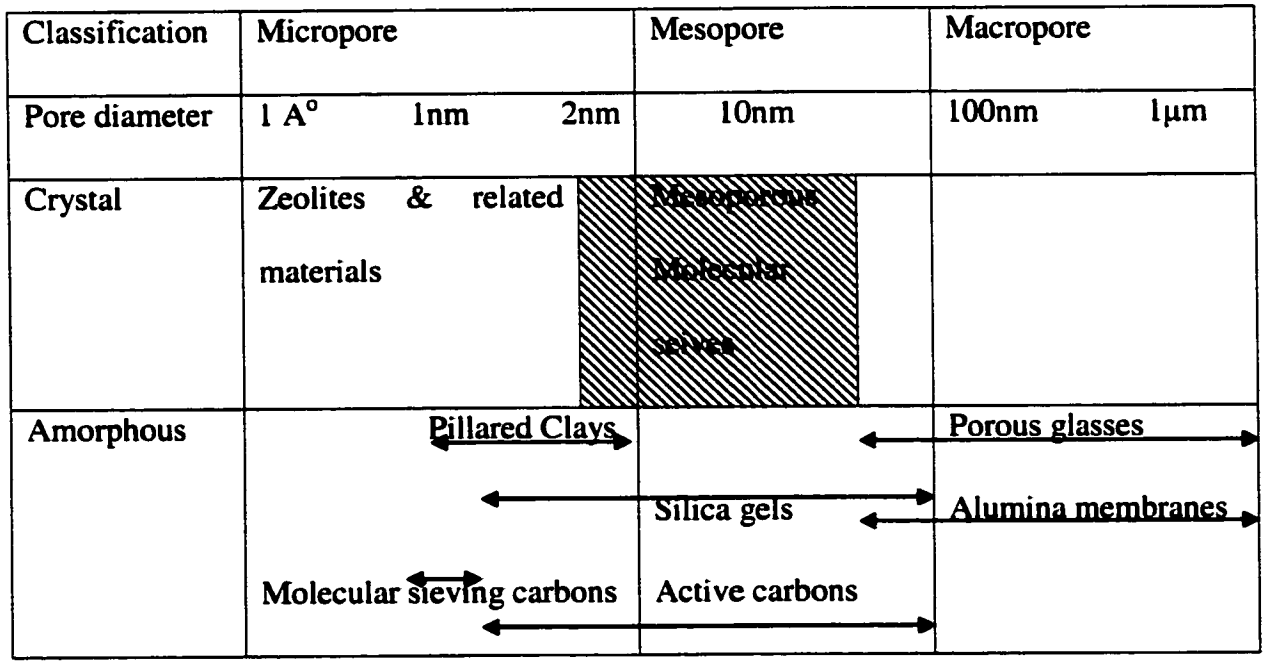

FIGURE 1-1 Classification of porous materials.

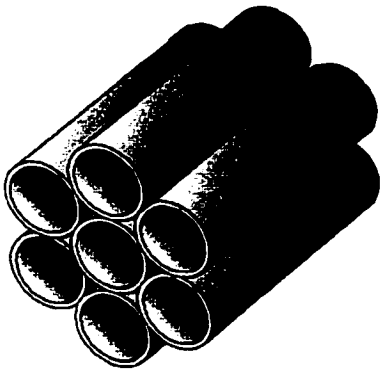

MCM41

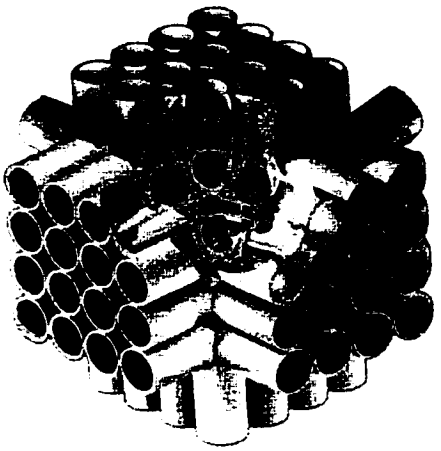

MCM-48

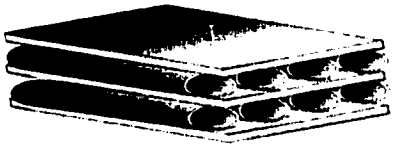

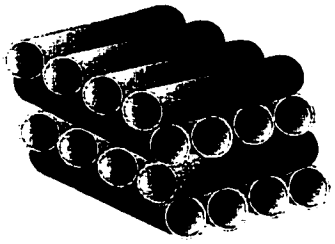

MCM-50

FIGURE 1-2 M41S family containing MCM41, MCM48, MCM50

1.2 Motivation

The challenge of producing enough liquid hydrocarbon fuels to fulfill the world's growing transportation needs is accentuated by demands that these fuels be clean and least polluting. Gas oil for automotive use (Diesel fuel) is an example of an oil product where clean air considerations have led to drastic reductions in maximum sulfur levels in recent years. Prior to 1990, sulfur in crude gas oil was removed from a level of, e.g. 1-2 wt% in the straight run gas oil to a typical level of 0.3-0.5 wt% as specified in most industrial countries around the world. (For instance, U.S.A., Japan, U.K., France, Germany, Netherlands) In 1994, maximum sulfur level was reduced to 0.05 wt% in the U.S.A., to be followed by Japan and other countries that adopted the same level a few years later (1996). The council of European ministers for environmental affairs and the European parliament have led to adoption of a maximum sulfur level of 0.035 wt% by 2000 and an even lower sulfur level of 0.005wt% by the year 2005 is foreseen. These increasingly stringent sulfur content requirements are driven by the need to limit emissions of the oxides of sulfur which lead to acid rain, atmospheric problems, and smog. Automobile manufacturers are also demanding low sulfur liquid hydrocarbons because only then would their advanced, sulfur sensitive technology achieves their potential of reducing emissions of the oxides of N_2 and particulate matter.

Sweet crude oil prices and its availability can be expected to come under increasing pressure because developing countries are also moving towards clean fuels. For example, The Indian Supreme court recently directed refineries to produce diesel with no more than 500-ppm sulfur (*Srinivasan*)[1]. India plans to reduce sulfur in diesel down to 350

ppm by the year 2005. Diesel fuel sulfur specifications all over the world are represented in a figure 1-3.

Although development of slightly improved catalysts of the established types is still possible and this remains a worthwhile goal, it is not likely to drastically change the hydrotreating process. Increasing the operating temperature to meet increased severity requirements has its limitations. Higher temperature may cause formation of polyaromatics by dehydrogenation while increased catalyst deactivation rate in combination with narrower workable operating temperature span results in shorter operating cycle and higher catalyst consumption.

Knudsen *et al.*[2] in 1999 estimated the need for catalysts at least 4 times active than present catalyst in order to reduce sulfur content of diesel from 500 ppm to 50 ppm. Thus, industry at present is facing problem of deep desulfurization, which should be overcome. The potential significance of the application of MMS as supports for hydrotreatment catalysts is vividly reflected by the patents.[3, 4, 5, 6, 7, 8]

1.3 Need for Mesoporous Catalyst

Zeolite and in general microporous molecular sieves have shown wide range of applications. Reason for success of zeolites in catalytic processes are attributed to the following features

- High surface area and adsorption capacity
- Controllable adsorption properties from hydrophobic to hydrophilic type materials.
- Strength and concentration of acid sites can be tailored for particular application.
- Can be activated to produce very stable materials against heat and chemical attack.

- Size of the channels and cavities.
- Uniform pore diameter and Intricate channel structure.

Even possessing these catalytically desirable properties, zeolites are not of use when reactants of sizes larger than pore dimensions are processed. Therefore the research was on to explore materials like zeolites having same porous structure but with an increase in pore diameter.

M41S family of materials have opened new possibilities for preparing catalyst with uniform pores in mesoporous region that can be easily accessed by bulky molecules that are present in crude oils. Pore size distribution is nearly as sharp as that of conventional zeolites type. Possibility to introduce different atoms in these mesoporous materials can generate catalytically active centers together with high surface areas. Tunable pore size and pore size distribution enables one to use these materials in acid base and redox catalysis as well as high surface area supports for acid, bases, metal oxides and transition metal complexes.

1.4 MCM41

MCM41 consists of parallel one-dimensional channels, which form hexagonal array. Scientists have postulated that the formation of these molecular sieve materials concerns the concepts of structural directing agent or template. Templating has been defined, in a general sense, as a process in which an organic species functions as a central structure about which oxide moieties organize into a crystalline lattice. Strictly speaking, a template is a structure (usually organic) around which a material (often inorganic) nucleates and grows in a skin-tight fashion, so that upon removal of the templating

structure, its geometric and electronic characteristics are replicated in the (inorganic) materials. The above definition has been elaborated to include the role of the organic molecules as:

(a) Space filling species.

(b) Structural directing agents.

(c) Templates.

In the simplest case of space filling, the organic species merely serves to occupy a void about which the oxide crystallizes. Therefore, the same organic molecule can be used to synthesize a variety of structures or vice versa. Structural direction requires that a specific framework is formed from a unique organic compound. And this does not imply that resulting oxide structure mimics identically the form of the organic molecule. In true templating, however, in addition to the structural directing component, there is an intimate relationship between oxide lattice and the organic form such that the synthesized lattice contains the organic locked into position. Thus, the lattice reflects identical geometry of the organic molecule.

Synthesis of this material employs organic surfactant molecules, which alter the inorganic structure and can be cationic, anionic, neutral surfactants. Surfactant molecules are dispersed as monomers in water when concentration is low. At some point solubility limit is reached and excess surfactant precipitates and form aggregates in which hydrophobic part of molecules is hidden in interior to minimize contact with water. These aggregates are in equilibrium with monomers and monomer concentration remains close to limit called CAC (critical aggregate concentration). Hydrophobic parts is made of CH_2 chains and if n is too large (n=no. Of CH_2 units) aggregates are not formed and excess

surfactants precipitates, solubilization limit is called Kraft point .For CTAB (cetyl trimethyl ammonium bromide) micelles are obtained at higher temperature above 25°C. The pore size in MCM41 materials can be controlled from 1.5 nm to 10 nm by the hydrophobic alkyl chain length of ionic surfactants. MCM41 exhibit catalytic ability for macromolecular reaction because of the larger surface area (>1000 m^2/gm) and tunable pore sizes and pore volumes (>1.0 cm^3/gm) and narrow pore size distributions and high sorption capacity. MCM41 show low hydrothermal stability and low mechanical strength and lacks acidity as compared to amorphous aluminosilicates. However addition of aluminium increases its acidity. Size of the pores combined with acidic nature of inorganic walls was expected to catalyze cracking of large organic molecules, but mere success was achieved even when transition metals were introduced in the formation of MCM41. Figure 1-4 gives a computational view of relative sizes of MCM41 pores and DBT. To increase catalytic activity, sieves were modified by ion exchange, grafting of the pore walls with organic functions, build–in of redox centers, coating of the walls with inorganic oxides, partial recrystallization.

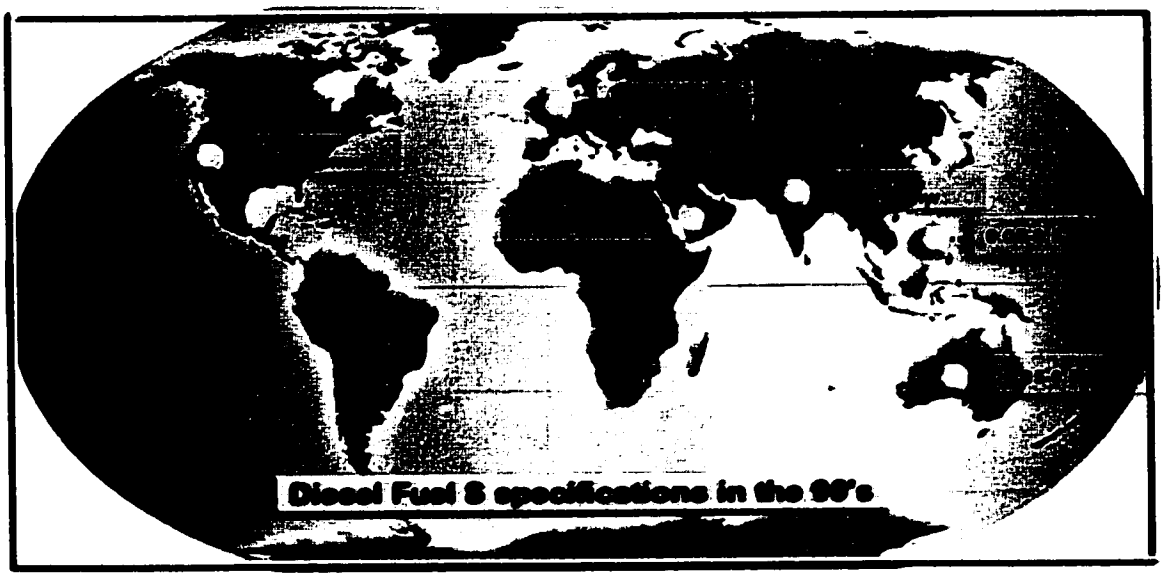

FIGURE 1-3 Diesel fuel sulfur specifications in the 90's.

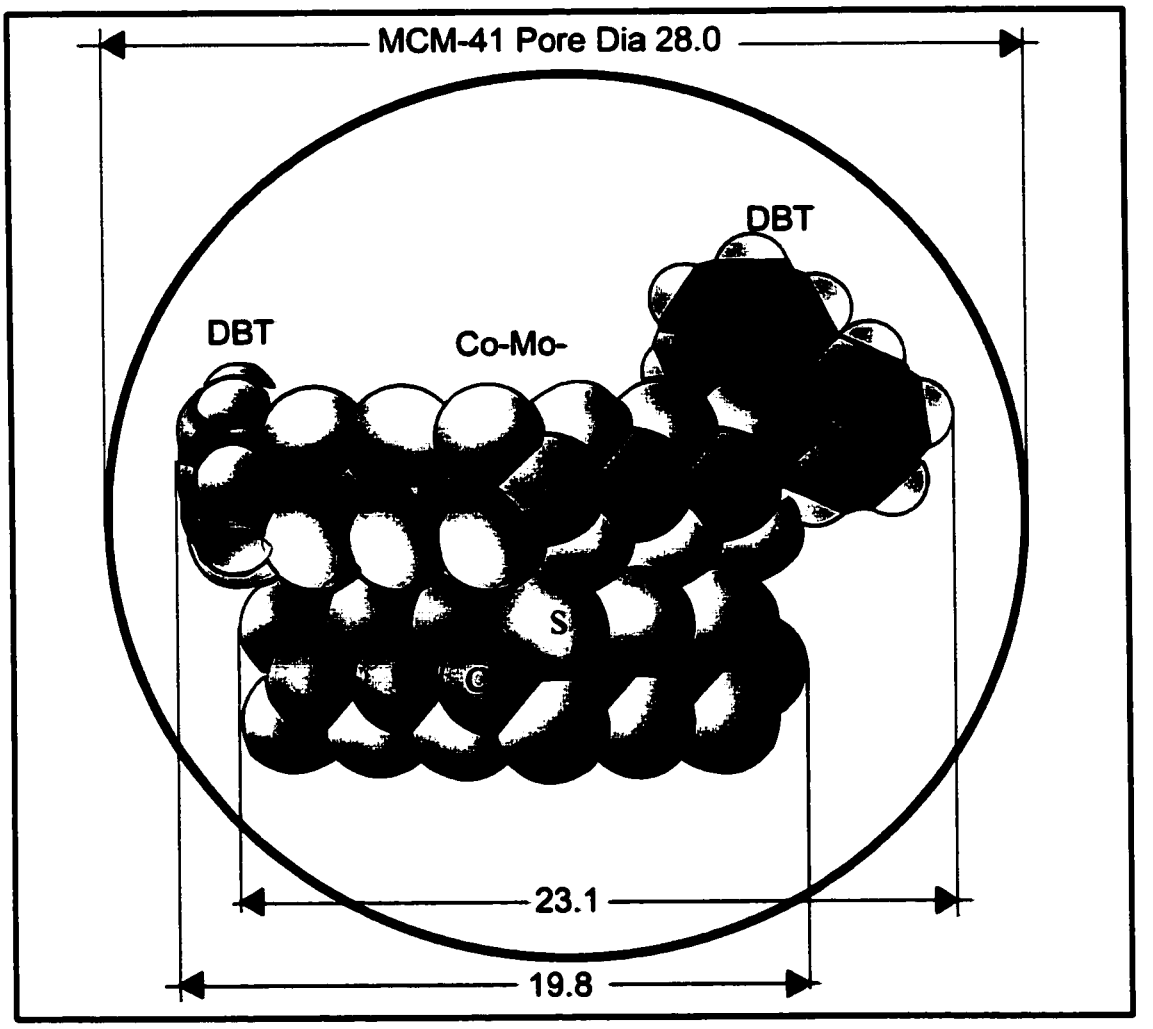

FIGURE 1-4 Computational view of the relative sizes of the MCM41 pores, DBT, and two slabs of the Co-Mo-S active phase (Ma *et al*[9])

1.5 Hydrotreating

Hydrotreating is a catalytic process that simultaneously dehydrogenates, cracks and hydrogenates the feedstocks, removing nitrogen, sulfur, oxygen, metal and aromatic constituents. Hydrotreating is a part of a complex process to remove undesirable impurities and lower the molecular weight of heavy petroleum feed stocks in presence of hydrogen and suitable catalyst. Technique of removing sulfur is known as hydrodesulfurization. Analogous procedure for nitrogen and metal removal are hydrodenitrogenation and hydrodemetallation respectively. Chemical and structural feature of MCM41, when metals are incorporated into the network for desulfurization will have

- Easy diffusion of Polyaromatic sulfur compounds within its mesopores & capable of preventing undesirable cracking and probably just isomerizing polyaromatic sulfur compounds to more reactive variants.
- Capabilities of processing wide range of feedstocks and reducing the sulfur content to a minimum as desired.

1.5.1 Chemistry of Hydrodesulfurization

Sulfur is the most abundant hetroatom in crude oils. Sulfur is in the form of thiols (mercaptanes), sulfides, disulfides, thiophene and thiophene derivatives.

Order of reactivity is RSH> R-S-S-R^{I}> R-S-R^{I}>thiophene>thiophene derivatives

R and R^{I} are various hydrocarbon groups. Reactivity of these compound decreases with increasing molecular size and varies depending on whether R is a aliphatic or aromatic group.[10] The reactivity of thiophene decreases in the order of

Thiophene> benzothiophene>dibenzothiophene> thiophenederivatives.

Group 1 Benzothiophene with no substituents in the 2 or 7

relative K=1

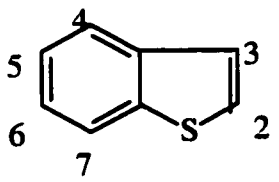

Group 2 Dibenzothiophenes with no substituents in 4 & 6

relative K=0.23

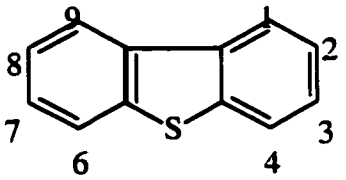

Group 3 Dibenzothiophenes with one substituent in the 4

relative K=0.08

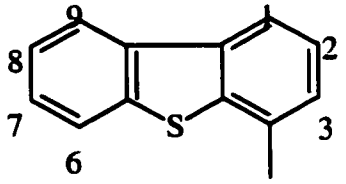

Group 4 Dibenzothiophenes with two substituents in the 4 & 6

relative K=0.028

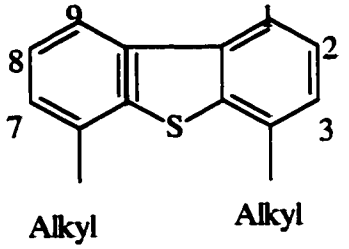

FIGURE 1-5 HDS relativity groups (Whitehurst *et al.*[11] in 1998)

1.5.1.1 The HDS Mechanism

Thiols and sulfides react to form hydrogen sulfides and hydrocarbon[12].

Sulphur Class	Reaction
Mercaptanes	$R\text{-}SH + H_2 \longrightarrow RH + H_2S$
Sulfides	$R\text{-}S\text{-}R + 2\,H_2 \longrightarrow 2\,RH + H_2S$
Disulfides	$R\text{-}S\text{-}S\text{-}R + 3H_2 \longrightarrow 2\,RH + H_2S$
Thiophene	 $+ 4\,H_2 \longrightarrow CH_3(CH_2)_2CH_3 + H_2S$
Benzothiophene	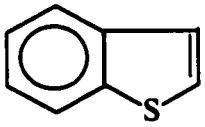 $+ 3H_2 \longrightarrow$ 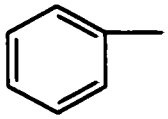 $+H_2S$

Figure 1-5 provides the structure of thiophene derivatives with their relative HDS rate constants. For highly substituted dibenzothiophene, ring dissociation prior to sulfur extrusion is the major route to hydrocarbon production as, relative to the parent molecules, aliphatic substituents on aromatic ring carbons adjacent to the sulfur atom impose severe steric hindrance towards bonding to the catalyst surface and to the production of appropriate intermediate species. Individual rate constants if determined, can be same if product are produced either by hydrogenating one of sulfur compounds

aromatic rings (K_{HS1}) followed by desulfurization (K_{D1}) or by removal of sulfur without ring hydrogenation (K_{D0}) followed by hydrogenation of one of the phenyl rings of the desulfurized product (K_{HP1})[13].

Rate constant	Reaction occurred
(K_{D0})	Desulfurization without ring hydrogenation.
(K_{D1})	Desulfurization of one ring of the hydrogenated sulfur compound.
(K_{D2})	Desulfurization of the fully saturated sulfur compound.
(K_{HS1})	Hydrogenation of one ring of the sulfur compound.
(K_{HS2})	Hydrogenation of the second ring of the sulfur compound.
(K_{HP1})	Hydrogenation of one phenyl ring of desulfurized biphenyl.
(K_{HP2})	Hydrogenation of second phenyl ring of biphenyl.

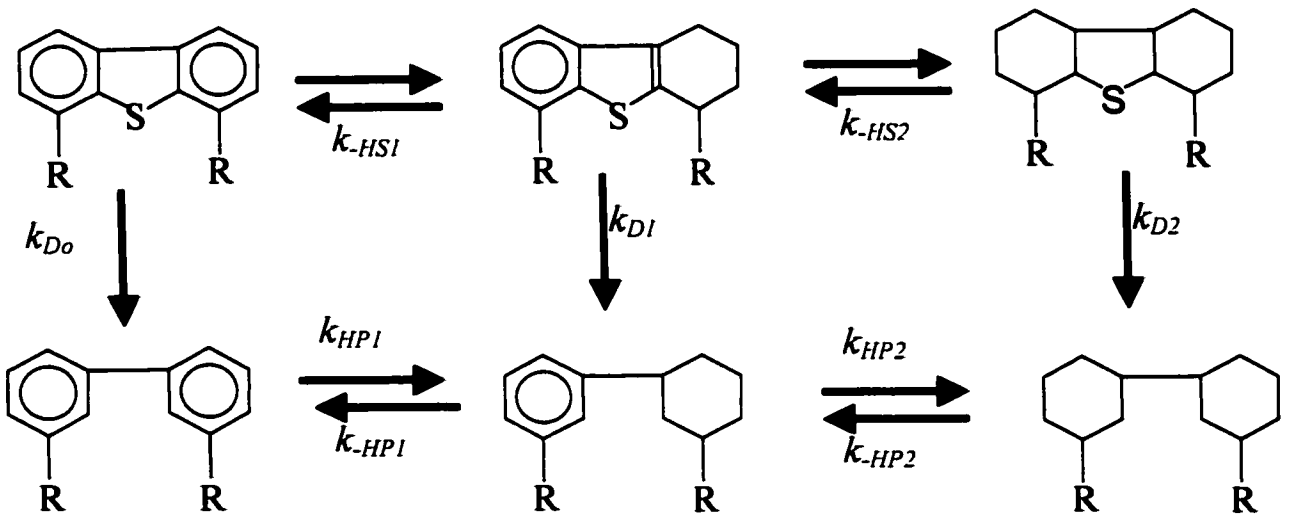

1.5.1.2 The HDS catalytic active phase

Hydrodesulfurization is carried out over sulfides of molybdenum or tungsten, and promoted with cobalt or nickel. Hydrodesulfurization represents a number of different reactions, which are discussed in previous sections.

Molybdenum sulfide alone shows high activity for direct sulfur extrusion from sulfur compounds such as thiophene[14,15]. Molybdenum sulfide has graphite-like stacked lamellar structure. Molybdenum sulfide can be visualized as a sandwich of the metal between two sulfur layers. The chemical reactivity of molybdenum sulfide is attributed to molybdenum cations. Sulfur anions in the basal planes of molybdenum sulfide are more difficult to remove than anions at corners and edges. There will, therefore, be a greater number of exposed molybdenum ions at the edges and corners of the molybdenum sulfide sandwich. The sulfur atom of the sulfur-containing compound adsorbs to the exposed molybdenum ion at a sulfur vacancy through a one-point attachment. This is followed by hydrogen transfer and sulfur elimination to complete desulfurization[16,17]. Daage and Chianelli[18] on the basis of studies on un-promoted molybdenum sulfide, proposed the rim-edge model. The model is supposed to be more relevant for large PASCs like DBT, 4-MDBT, and 4, 6-DMDBT. According to this model hydrogenation of DBT occurs exclusively on rim sites, while HDS (C-S bond hydrogenolysis) takes place on both the rim and the edge sites. Adjacent layers hinder the adsorption of large molecules like DBT on the edge sites and, thus, hydrogenation takes place on the rim sites. Thus, the rim-edge model predicts that rim sites dominate hydrogenation, and the selectivity for hydrogenation should be related to the ratio of rim to edge sites. That the addition of small amounts of the sulfides of a second metal such as cobalt or nickel

enhances activity of molybdenum sulfide was established in as early as 1928[11]. The monolayer model, attributing activity to highly dispersed molybdenum oxy-sulfides bound strongly to the support, was the first explanation offered by Lipsch and Schuit[19] and Massoth[20]. The monolayer model suggests that cobalt is located deep inside the support. This was followed by the pseudo-intercalation model which believed that cobalt when intercalcated at the edges of the layers of molybdenum sulfide created the active phase[21] . Hagenbach *et. al.*[22, 23] proposed the contact-synergy model (also known as the remote control model) which identified the interface of molybdenum sulfide (where the sulfur containing organic molecule adsorbs) and Co_9S_8 structures (which dissociate hydrogen) as the active phase. It should be noted that molybdenum sulfide (MoS_2) and Co_9S_8 are the thermodynamically stable sulfides of molybdenum and cobalt, respectively. However, none of these models were proven definitively.

The most widely accepted model of the HDS active phase, now, is the Co-Mo-S model postulated on the basis of Mossbaauer spectroscopic experiments by Topsoe *et. al.*[24] and Wivel[25]. The catalytically active Co-Mo-S phase consists of small stacks of molybdenum sulfide with cobalt atoms decorating the edges of the layered molybdenum sulfide structures. It may also contain cobalt ions firmly bound to the support and crystallites of Co_9S_8 which has a lower activity for HDS. Depending on the relative proportions of cobalt and molybdenum and on the pretreatment, a sulfided catalyst contains either a relatively large amount of Co_9S_8 or a large amount of the Co-Mo-S phase[26]. Notwithstanding debate on the role of the promoter, molybdenum sulfide is widely accepted as the basic active phase for HDS catalysis. Daage and Chianelli[18] proposed the rim-edge model for un-promoted molybdenum sulfide crystals, which

consolidated the validity of molybdenum sulfide being the active phase for large PASCs also. Several researchers believe that a high dispersion of molybdenum sulfide will make effective deep desulfurization catalysts[26, 27, 11].

A hydrogenolysis catalytic circle during HDS over sulfided Co-Mo catalysts is proposed by Hensen *et. al.*[28], which is as shown in figure 1-6. The mechanism briefly describes the possible reaction steps involved on the local sites. It is assumed that gaseous hydrogen adsorbs dissociatively on the surface of the catalysts and that the hydrogen species consumed in the reaction are supplemented by means of spillover on the surface. Similarly, the HDS reaction mechanism over Mo/MCM41 is as shown in figure 1-7. The cleavage and formation of bonds take place between the edged Mo atom and its neighboring Mo atom. Since the strength of Mo-S bond is higher than the Co-S bond, Mo-S attached to the edged Mo atom is more difficultly cleaved than the Co-S bond. Consequently, the HDS reaction rate over Mo catalyst is lower than that over Co promoted Mo catalyst.

Nagai[29] proposed a mechanism for Ni-Mo sulfides in figure 1-8, which briefly describes the possible reaction steps involved on the local site. It was assumed that gaseous hydrogen adsorbed dissociatively on the surface of catalysts and that the hydrogen species consumed in the reaction were supplemented by means of spillover on the surface.

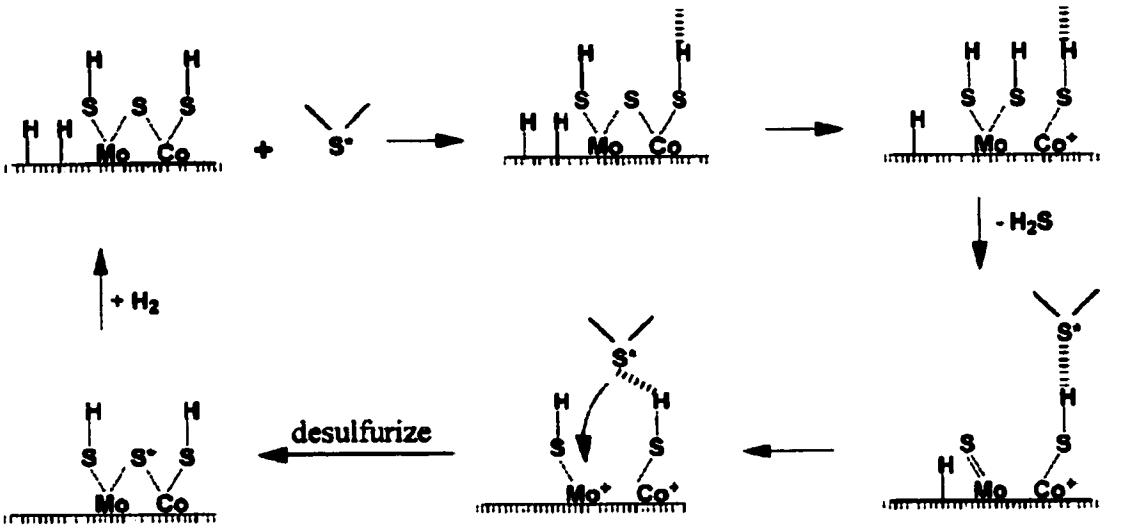

stands for H_2S, thiophene, benzothiophene, dibenzothiophene or their derivatives

FIGURE 1-6 Mechanism of hydrodesulfurization of DBT over sulfided Co-Mo catalysts.

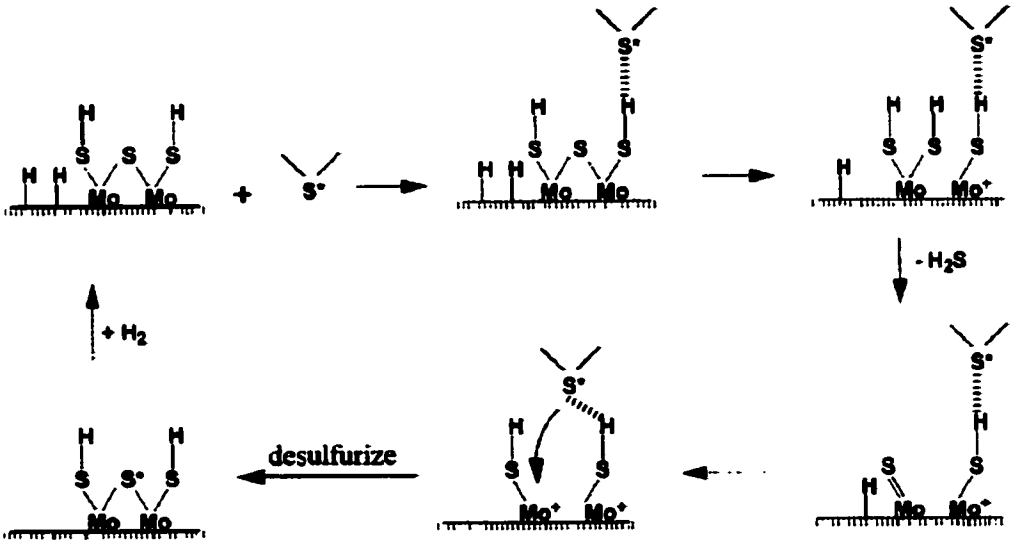

stands for H_2S, thiophene, benzothiophene, dibenzothiophene or their derivatives

FIGURE 1-7 Mechanism of hydrodesulfurization of DBT over sulfided Mo catalysts.

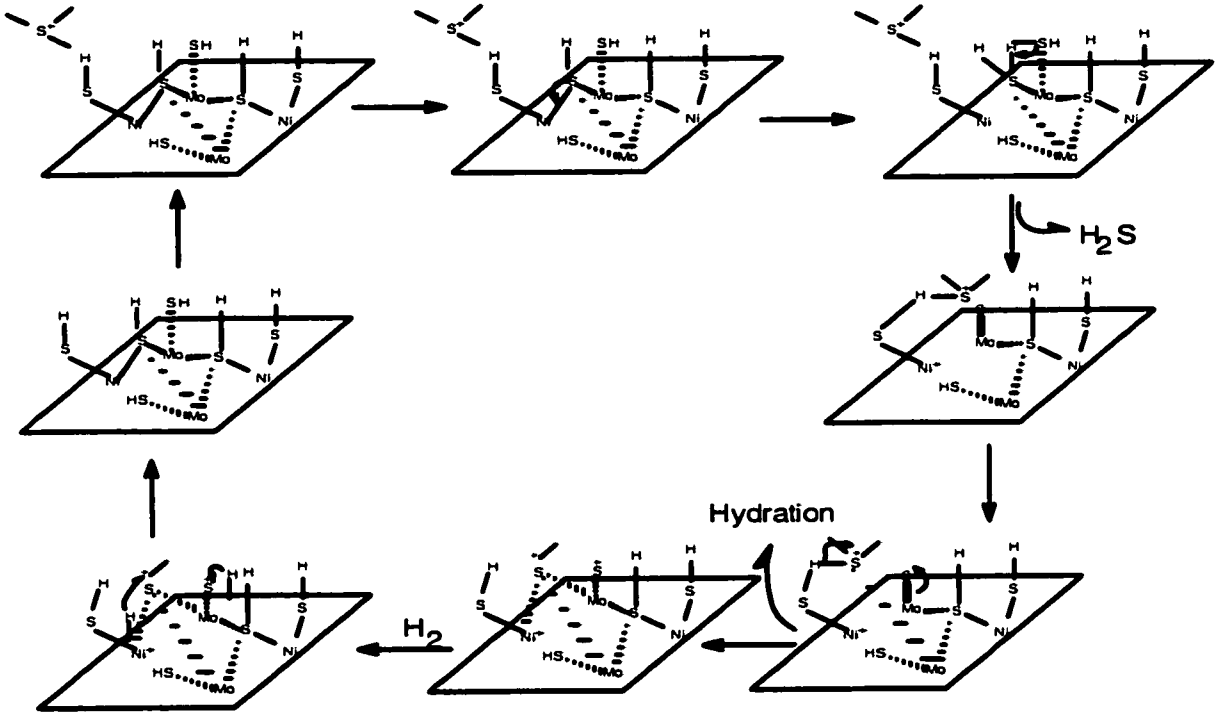

FIGURE 1-8 Mechanism of hydrodesulfurization of DBT over sulfided Ni-Mo sulfides.

1.6 Objectives

The objectives of the study are to prepare metal incorporated MCM41 molecular sieves and characterize with different techniques and evaluate its performance.

However specific objectives are as follows

- Incorporation of Ni, Co, and Mo in MCM41.
- Impregnating other metal on these metal incorporated MCM41 to prepare other MCM41 based species.
- Characterizing these MCM41 based samples with techniques like temperature programmed reduction (TPR), X- ray diffraction (XRD), Atomic absorption analyzer (Porosity measurements).
- Pulse evaluation of these catalysts at atmospheric pressure and at range of temperatures.
- Batch evaluation of these catalysts using DBT in dodecane as model feed.

Literature Survey

2.1 Zeolite Supported HDS Catalysts

In heterogeneous field of catalysis, zeolites known as crystalline aluminosilicates are widely used in industry. Discovered in 1756, zeolites were first commercially used for catalytic cracking in 1964.Zeolites have pores with one or more discrete sizes and diameter of less than 10°A. Exchangeable cations in zeolites allows introduction of cations with catalytic properties. Cationic sites can also be exchanged to H^+, by which they can have more number of strong acid sites.

Vasudevan and Fierro[27] showed that ion exchange used for metal incorporated zeolite based hydrogenation catalysts is not suitable as there is absence of cationic form of molybdenum. Other catalyst preparation technique like incipient wetness impregnation is found to be better. However even incorporation and stabilization of active phase within zeolite, akin to reactant diffusion, has been limited by the support's microporosity.

Fierro *et. al.*[30] in 1987 were able to redisperse molybdenum species within NaY zeolite pores through thermal decomposition (non conventional procedure), which uses constant rate decomposition at a very low water vapor pressure. In contrast to this, Leglise *et. al.*[31] reported problems in completely sulfiding redispersed molybdenum species.Cid *et. al.*[32] attribute incomplete sulfidation to excessively strong interaction between acidic zeolite and molybdenum.

Yitzhaki *et. al.*[33] in 1995 have studied hydrodesulfurization and identified reactant diffusion within zeolite as the key problem. Corma[34] in 1997 reported that zeolite pore diameters can be increased by dealumination. Large number of defects in a small area leads to coalescence of small pores into mesopores. Modified zeolites has mesoporous region but it lacks uniform pore size and catalytic functionalities. i.e. acidity. Organic templates were then used to synthesize zeolites that affected gel chemistry and they acted as void fillers in porous solids. Results did not give positive signs of mesoporosity even after employing larger organic templates.

In conclusion, it can be said that despite the outstanding progress made in producing large pore zeolites, the materials so far synthesized are still not suitable to be used in the context of current catalytic processes.

2.2 MCM41

Mobil Oil Corporation reported their invention of MCM41 in 1992 as a silicate in basic media using cationic alkyl tri methylammonium surfactant system that showed limited catalytic activity applications because of stability problems. Beck *et. al.*[35] in 1992 proposed a liquid crystal templating mechanism (LCT). They proposed that structure is defined by the organization of surfactant molecules into liquid crystals, which serves as a template for the formation of MCM41 structure. First step in the synthesis leads to the formation of the micellar rod around surfactant micelle which in second step will produce hexagonal array of rods, followed by incorporation of inorganic array (silica,silica - alumina) around the rod like structure (figure 2-1). Cong Yan *et. al.*[36] in 1993concluded that the liquid crystalline phase is not present in the synthesis medium during the formation of MCM41, and consequently, this phase cannot be structure directing for the

synthesis of mesoporous material in agreement with already proposed mechanism through route 2.

Thus, the randomly ordered rod like organic micelles interacts with silicate species to yield 2 or 3 monolayers of silica around the external surface of the micelles. These composite species spontaneously form long-range order characteristic of MCM41 as shown in figure 2-2.

2.2.1 Factors affecting synthesis of MCM41

2.2.1.1 Drying

Although the pore structure and connectivity of a solid material are essentially fixed after being isolated from mother liquor, drying can affect porosity (Raman *et. al.*[37],1996). During the drying process, water is being significantly removed and shrinkage of the network is taking place to a small extent .In this procedure, care should be taken to avoid long-time exposure to air since this might lead to hydrolysis of some bare siloxane bridges, in particular for MCM-41 materials.

2.2.1.2 Template Removal

The as-synthesized materials contain a large portion of organic template inside pores. To enable accessible pores, templates must be removed. The methods and conditions used to remove the template have a strong impact on the final porosity, the pore size, and even the pore connectivity under some extreme conditions. Two methods are normally used to achieve this, i.e. Calcination and solvent extraction.

2.2.1.2.1 Calcination

Calcination was carried out in a furnace in air. During this process, surfactant molecules are decomposed of according to Hoffman elimination reaction. At the same time, surface silanol groups are formed and further condensed (Chen *et. al.*[38],1993b). Significant shrinkage of the pore network can be observed (Raman *et. al.*[37],1996)due to condensation of SiOH groups. One of the most important factors in calcinations is heating rate. In this research, calcination was conducted in steps.

2.2.2 Research on MCM41

Jaenicke *et. al.*[39] in 1997 showed that Ti MCM41 is more thermally stable than Si-MCM41 and Al-MCM41.Addition of Lanthanum (La_2O_3) improved its thermal stability at lower temperatures. Ryong and Jun[40] in 1997 investigated on stability and concluded that addition of some salts (NaCl, KCl, sodiumacetate) can improve hydrothermal crystallization process. Zhixiang *et. al.*[41] in 1999 proved that physical properties can be designed by controlled synthesis and by variation of alkyl chain length of surfactant. Thomson[42] in 1993 incorporated aluminium in framework which proved to be effective hydrocracking and isomerization catalyst. Haller and Cesteros[43] discovered that nature of aluminium source is critical factor in determining the location and coordination of Al in MCM41 framework and use of antifoaming agent before addition before addition of surfactant and a previous aging of the mixture of silica and aluminum sources prior to the synthesis improve the structure of Al-MCM41. Tetrahedral incorporation of aluminum imparts molecular sieves their acidic catalytic functionality. However not all aluminum incorporation in MCM41 is tetrahedral as octahedral incorporation also occurs. Some of tetrahedrally incorporated aluminum is known to come out of material framework and

assume octahedral coordination during calcinations. MCM41 has moderate acidity between two extremes of γ-alumina (support for commercial HDS catalyst) and Y-zeolite (Usually used for hydrocracking). Dong Hoo *et. al.*[44] in 1999 loaded cobalt by incipient wetness method and concluded that octahedral cobalt species containing phosphate species get dispersed onto the surface of mesoporous molecular sieve as a tetrahedral species. Rohit and Vishwanathan[45] showed molybdenum could be incorporated into MCM41, which can be used for oxidation reactions. Deung Hee *et. al.*[46] in 2000 worked on increasing molybdenum loading and concluded that Si/Mo upto 10 can be loaded as at higher ratios catalysts become amorphous. This catalysis showed good oxidation activity. Corma *et. al.*[47] in 1994 showed that MCM41 can be readily dealuminated upon thermal treatment and after calcinations has good acidity as compared to USY zeolite.

Based on the literature survey, it can be concluded that several mechanisms were proposed for formation of MCM41 and metals (Mo, Ni, Co, Ti, Fe, and W) can be loaded to make it catalytically active. It can be said that mesoporous molecular sieves have attracted the attention of many researchers due to the novelty of material and perspectives of applications. The future of this mesopores may prove to be more flourishing than zeolites.

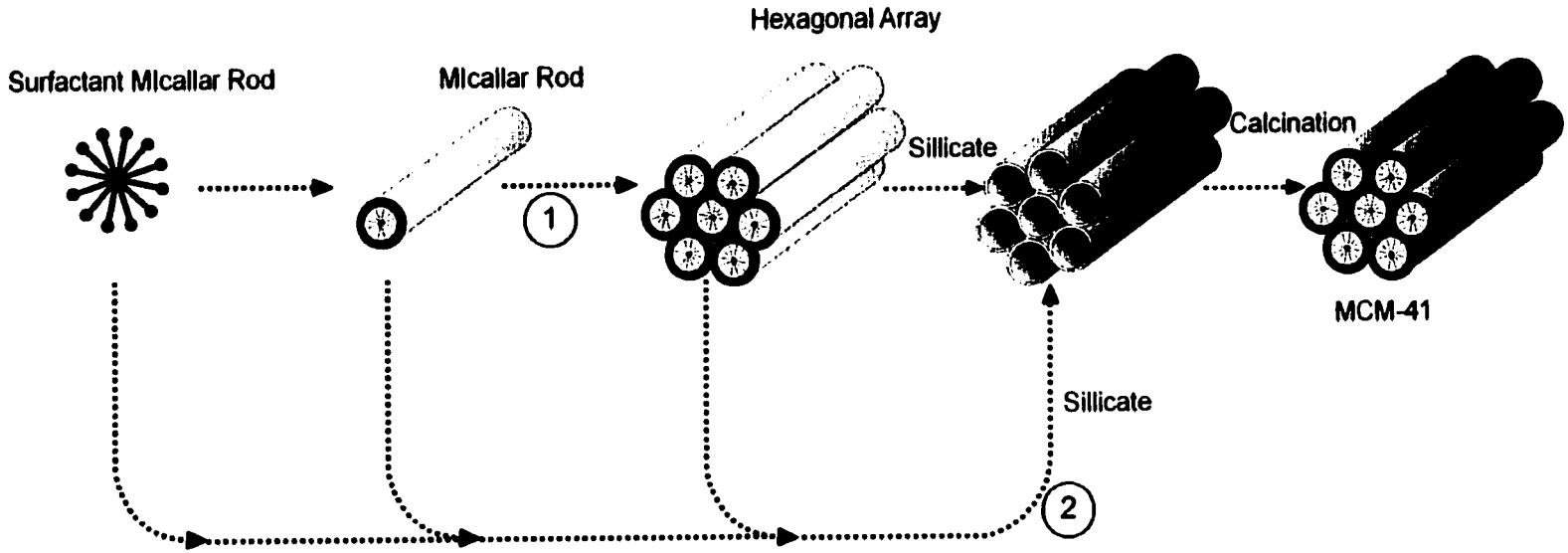

FIGURE 2-1 Liquid crystal templating mechanism (LCT) proposed Beck *et al.* showing two possible pathways for the formation of MCM41: Liquid crystal initiated & Silica initiated.

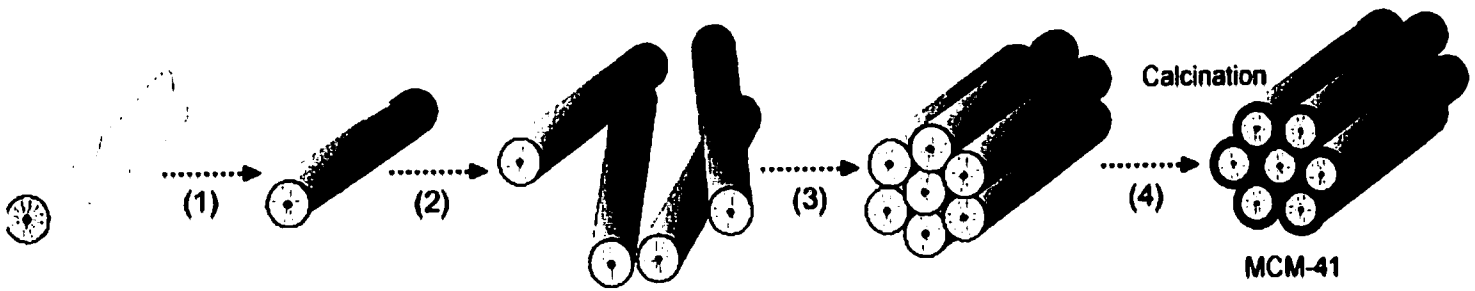

FIGURE 2-2 Alternative formation mechanism of the formation of MCM41.

2.3 MCM41 Supported Hydrotreating Catalysts

Corma *et. al.*[48] in 1995 compared NiMo/MCM41 with NiMo/SiO_2-Al_2O_3 and NiMo/USY in simultaneous one-step HDS, HDN and MHC of vacuum gas oil at temperature ranging from 350 to 450°C. A secondary hydrocracking of the hydrotreated products was also studied. Results indicate superior activity of the MCM41 supported catalyst in both HDS and HDN.A higher activity for MHC s with better selectivity toward middle distillate and other reported results indicate that the mild acidity of MCM41 support comparable to SiO_2-Al_2O_3 allows to avoid the over cracking observed with USY. Results showed that large pores of MCM41 allow fast diffusion of the products out of the pore lattice. Song & Reddy[49,50] in 1999 provided preliminary proof of the potential of mesoporous molecular sieves for HDS catalysis. They carried out hydrodesulfurization of dibenzothiophene at two metal loading levels on MCM41(Low & High). Low metal loading had 13.5 wt% Mo_2O_3 and 2.9 wt% CoO whereas high metal loading had 27 wt% Mo_2O_3 and 5.8 wt% CoO. Catalysts supported on γ-alumina showed no increase in activity whereas MCM41 supported catalysts with high metal loading were almost twice more active than γ-alumina supported catalysts. It is evident that because of high surface area of MCM41 there exists tremendous potential to load increasing amount of active phase in a highly dispersed manner and substantially increase activity per unit mass or volume of catalyst.

Reddy *et. al.*[51] proved that MCM41 could be used as effective supports for desulfurization catalysts. However the results for the upgrading of atmospheric and vacuum reside suggested that Co-Mo /MCM41 are not effective as Co-Mo/Al_2O_3 for resids containing asphaltene due to pore size limitations of MCM41.Removing

asphaltene from the resid prior to HDS improved the catalytic activity of Co-Mo/MCM41.

Vartuli *et. al.*[52] have examined the demetallation and asphaltene removal of residuum over a series of Ni-Mo/MCM41 of diameters ranging between 30 and 80 A°. The 80 A° pore catalyst was more active than a conventional demetallation catalyst. Yue *et. al.*[53] studied Ni/MCM41, Mo/MCM41, and MoNi/MCM41 in HDS of thiophene and found that Mo/MCM41 is most active owing to better Mo dispersion in the silica MCM41 support. T. Klimova *et. al.*[54] in 1998 concluded that incorporation of MCM41 into alumina support in NiMo hydrotreating catalyst leads to an increase in HDS activity compared with catalysts supported on a pure alumina. In the Mo un-promoted catalysts, an increase in content of MCM41 caused a decrease in thiophene conversion. They reported that hydrodesulfurization to hydrogenation ratio in NiMo catalysts increases with increase in MCM41 content.

Ramirez *et. al.*[55] in 2000 found that incorporation of MCM41 to the catalyst formulation leads to higher catalytic activity in the dibenzothiophene hydrodesulfurization reaction than the catalyst supported on pure alumina. MCM41 incorporation also leads to diminished interaction between the Co and Mo phases with support, compared to those existing in alumina supported catalyst, which in turn causes formation of great amount of polymeric Mo octahedral species and decrease in the population of tetrahedral Co as $CoAl_2O_4$. He also reported that the strong acidity in MCM41 was detrimental to the HDS activity of the catalyst. Wang *et. al.*[56,57] confirmed the fact by reporting that high surface area and mild acidity of the support improves the HDS activity by preparing siliceous MCM41 supported Co-Mo or Ni-W sulfides which

showed significant improvement in the HDS of DBT. Wang *et. al.*[58] showed by depositing Ni-Mo sulfides over siliceous MCM41 that Ni-Mo/MCM41 is better in performance as compared to Co-MoMCM41 in the HDS of DBT because of the enhanced hydrogenation ability of Ni-Mo sulfides.

As a conclusion MCM41 based catalyst are good prospectives for hydrodesulfurization for big sulfur molecules.

Experimental Approach

3.1 Experimental Design

For successful completion of a project, plan was chalked out before starting the actual work. In this work the plan was to

(a) Synthesis and characterization of MCM41.

(b) Synthesis and characterization of metal incorporated MCM41 molecular sieve.

(c) Impregnation of metal on metal incorporated MCM41 molecular sieves to prepare the remaining samples and characterizing it.

(d) Evaluation of these catalysts in pulse reactor to find the promising ones.

(e) Evaluation of promising catalysts in batch reactor.

3.2 Synthesis of metal incorporated molecular sieves

3.2.1 Synthesis

Syntheses of MCM41 based molecular sieves were done in alkaline medium. One of main steps in preparing metal incorporated molecular sieves is preparation of the gel i.e. mixture of inorganic species and template and metal. A number of parameters in a gel preparation process can affect the resultant phases. These include pH, molar ratio of reactants, aging, stirring, adding sequence of reactants, etc. In this research work, syntheses of MCM41 based mesopores were conducted using different metals.

Catalysts preparation recipes are included at the end. In Cobalt and Nickel incorporated MCM41 ratio of Si/Co and Si/Ni is kept at 50 molar ratios while as for molybdenum it is kept at 10 molar ratio.

After the preparation of the homogeneous gel, it needs to be transferred into an reactor (temperature resistant bottle) which is then heated to a 370°K temperature for 4 days. During these 4 days pH is maintained at 10.5. Upon the reaction being completed, the reactor is cooled down, and the mixture is separated normally by filtration with extensive washing in order to remove any unwanted species such as sodium ions, chloride, nitrate etc.

For clarity, MCM41 based samples are denoted as follows:

Metal Incorporated MCM41:

MoMCM41 means Molybdenum incorporated MCM41 and similar convention for NiMCM41 and CoMCM41.

Metal impregnated on metal incorporated MCM41:

Co-MoMCM41 means cobalt is impregnated on the molybdenum incorporated MCM41. Some catalyst samples were ion exchanged before impregnation and some were not. Flow chart is given in figure 3-1.

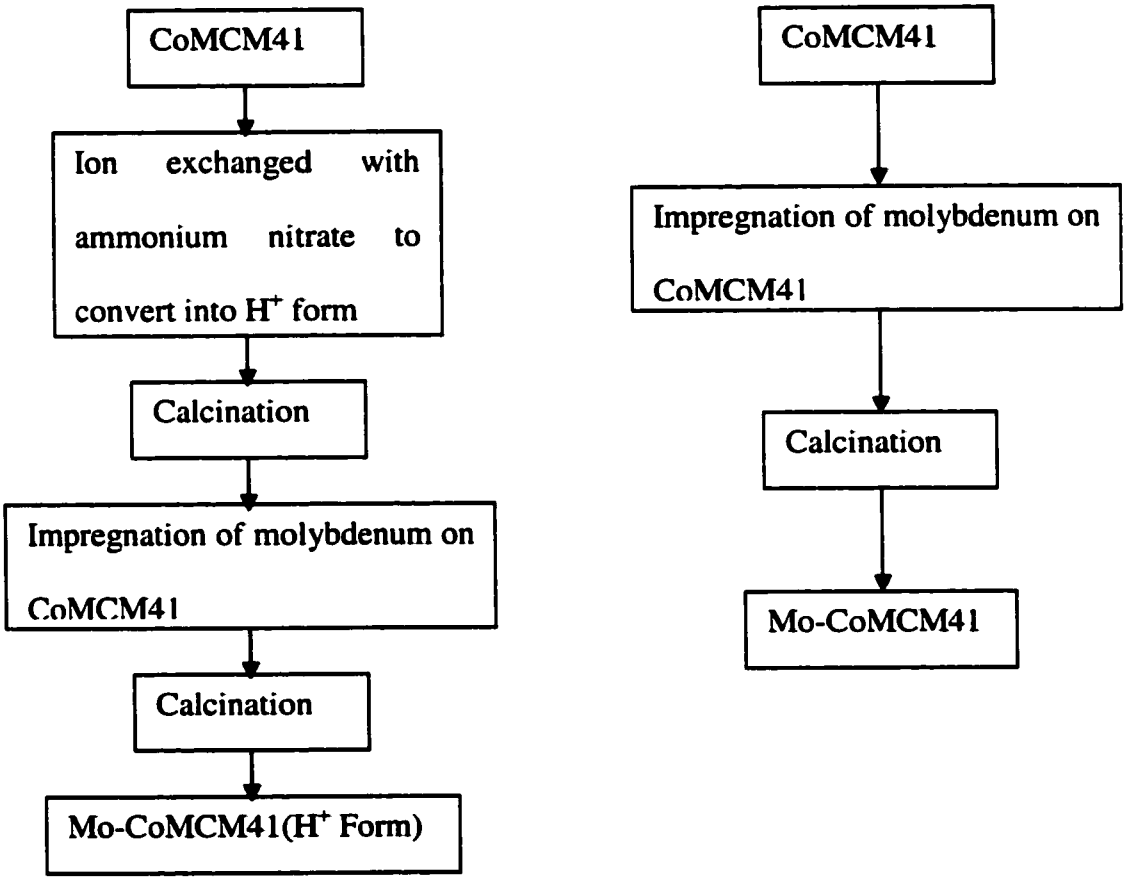

FIGURE 3-1 Synthesis steps in ion exchanged and calcined samples

3.2.2 Drying

After the solution is filtered we get a cake like solid, which was dried in an oven at 373 K at atmospheric pressure, overnight. Prolonged drying of MCM-41 based materials might result in partial removal of the template molecules.

3.2.3 Template Removal

Template removal was done by calcination. The procedure for calcination of as-synthesized sample is as follows:

1. Temperature increased from room temperature to 1200C at 10C /min and maintained for 30 min.
2. Temperature increased from 120^0C to 250^0C at 2^0C /min and maintained for 30 min.
3. Temperature increased from 250^0C to 550^0C at 10^0C /min and maintained for 6 hours.

3.2.4 Ion-Exchange

To make catalysts catalytically active, catalysts were ion exchanged with 0.1 M ammonium nitrate solution. Ion exchange process is as follows:

1. Add catalyst to ammonium nitrate solution in a beaker and solution is stirred continuously. E.g. for every 10 gm of catalyst, 150 ml of ammonium nitrate is used.
2. Change ammonium nitrate solution after every 24 hours. Keep stirring.
3. After 3 days filter the sample and dry it in oven overnight.

4. Calcine the sample with temperature program similar to template removal except that temperature was increased till 500°C only.

3.2.5 Impregnation

In impregnation, a solution of a metal salt of sufficient concentration to give the desired loading is added to the support, after which the system is aged, usually for a short time only, dried, and calcined. Each metal incorporated MCM41 is impregnated with other metal with desired loading.

TABLE 3-1 Metal Impregnated on different catalysts.

No.	Catalyst	Wt% of metal incorporated	Wt% of metal impregnated
1	Mo-NiMCM41 (cal)	1.6 Wt% Ni	2.5 Wt% Mo
2	Mo-NiMCM41 (H^+Form)	1.4 Wt% Ni	2.5 Wt% Mo
3	Mo-CoMCM41 (cal)	1.6 Wt% Co	2.5 Wt% Mo
4	Mo-CoMCM41 (H^+Form)	1.5 Wt% Co	2.5 Wt% Mo
5	Ni-MoMCM41 (cal)	2.5 Wt% Mo	1.6 Wt% Ni
6	Ni-MoMCM41 (H^+Form)	1.7 Wt% Mo	1.6 Wt% Ni
7	Co-MoMCM41 (cal)	2.5 Wt% Mo	1.6 Wt% Co
8	Co-MoMCM41 (H^+Form)	1.7 Wt% Mo	1.6 Wt% Co

3.3 Catalyst characterization

The condition or characteristics of catalyst can be determined by different techniques, which somehow relates to the success of the catalyst. Techniques are X-ray powder diffraction (XRD), electron microscopy (EMR), photoelectron spectroscopy, infrared spectroscopy, temperature programmed reduction (TPR), temperature programmed desorption (TPD), and temperature programmed sulfiding (TPS). Temperature programmed methods (TPR, TPD, TPS) form a class of techniques in which a chemical

reaction is monitored while the temperature increases linearly with time and this is how characterization of the hyrotreating catalyst in terms of hydrogenation functionality and acidity function is done.

3.3.1 X-Ray Diffraction

The various samples of MCM41, being crystalline, have characteristic X-ray powder diffraction patterns, which are used for their identification. X ray diffraction patterns of as-synthesized and calcined mesoporous samples show characteristic peaks of 100, 110 and 200.X-ray diffraction patterns from typical catalyst powders give information about interplanar lattice spacing through Bragg's equation.

$$2*d*sin\theta=n\lambda$$

Where

d is interplanar spacing.

Θ is angle between lattice plane and both the incident and diffracted X ray beam.

n is order of Braggs reflection.

Λ is the wavelength of the X-rays.

Combined with fact that intensities of diffraction lines depend on the arrangement of atoms in unit cell of crystal lattice, this information in principle provides an almost unique description of nature of the crystalline phases present. However in practice the interpretation of diffraction patterns may not always be trivial as catalysts often contain many different phases. The equipment is used to measure the crystalline pattern of the synthesized sample by step measurement method. The diffraction pattern is generated by a 2-theta/ theta scanning diffractometer.

The operating conditions of XRD analysis is:

Cu broad focus tube at 40 Kv and _30ma.

Scanning speed and interval of data collection was 0.01 degree two theta/sec.

Angle scanned: 1 to 10 two theta.

3.3.1.1 XRD setup

X ray Diffraction (XRD) experiments were done on system supplied by *Jeol Ltd.*, (model JDX-3530) employing a multicomputer system, 32-bit engineering workstation as a core of the system, for improving the data processing capability. The multi-task and multi-window allows parallel execution of measurement and data processing, and serial execution of measurement, data processing and result output. Measured results are displaced on the high-resolution color CRT for easy observation of measurement results. Outline of diffraction optics is given in figure comprising of arrangement of X ray source, X ray source side soller slit, divergence slit, receiving slit, scattering slit, X ray detector. Outline of diffraction optics is given in figure 3-2 .

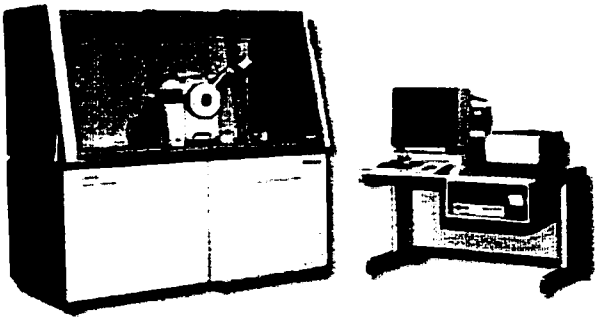

FIGURE 3-2 Setup of XRD

3.3.2 Temperature Programmed Reduction (TPR)

TPR is used to monitor metal support interactions .It also provides useful information about the temperatures needed for the complete reduction of a catalyst. For bimetallic catalysts, TPR patterns often indicate whether two components are mixed or not.

Reduction is an inevitable step in the preparation of metallic catalysts. The reduction of metal oxide MO_n by H_2 is described by the equation.

$$MO_n + nH_2 \longrightarrow M + n\,H_2O$$

Reaction of metal oxides by hydrogen, start with dissocative adsorption of H_2, which is a much more difficult process on oxides than on metals. Rate expression for the reduction reaction under conditions where the reverse reaction from metal to oxide can be ignored, is

$$-\frac{d[MO_n]}{dt} = k_{red}[H_2]^p f([MO_n])$$

In which

$[MO_n]$ is the concentration of metal oxide.

$[H_2]$ is the concentration of hydrogen gas.

k_{red} is the rate constant of the reduction reaction.

p is the order of the reaction in hydrogen gas.

f is the function, which describes the dependence of the rate of reduction on the concentration of metal oxide.

t is the time

3.3.2.1 Setup of Temperature programmed reduction (TPR)

Temperature programmed reduction (TPR) experiments were carried out in a system supplied by *Ohkura Riken Co. Ltd.*, (model TP-200). A schematic flow diagram of apparatus is given in figure 3-3 .The equipment is developed to enable user to obtain data related to reduction and sulfiding characteristics of metal oxides or catalysts containing metals.

3.3.2.2 Operational Procedure for TPR:

The operational procedure can be divided into two parts:

3.3.2.2.1 Pretreatment

150 mg of catalyst sample (particle size 600-212 μm) is weighed and placed in a quartz tube (8 mm O.D.) reactor in such a way that it is close to the thermocouple with the help of quartz wool plugs. Temperature is raised to 400° C at a rate of 10° C for 2 hr, then cooled to ambient temperature. Air is purged by flowing dry air (22 cm^3/min) for 30 min at ambient temperature.

3.3.2.2.2 Reduction

Gas mixture used for reduction was 5 % H_2 in Argon at a flow rate of 30 cm^3/min. Temperature of the reactor is programmed to increase linearly from room temperature to 1030°C at a heating rate of 10°C/min and then retained at this temperature for 15 minutes. A 5A molecular sieve is used to trap the water formed either by reduction or from dehydration process. The hydrogen concentration is determined with a thermal conductivity detector (TCD). The temperature of the catalyst and the TCD current

response is monitored and recorded continuously on a personal computer (NEC Model PC9821-Xe10).

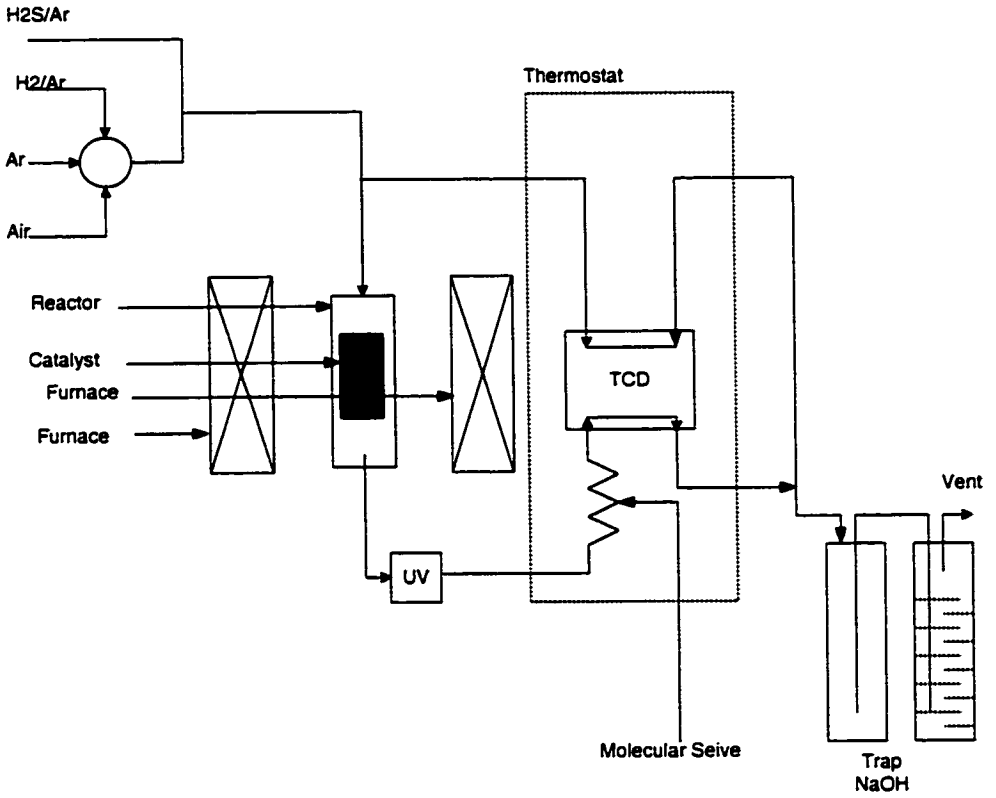

FIGURE 3-3 Temperature programmed reduction apparatus

3.3.3 Gas Sorption Analyser

Accurate sorption measurements of a gas on solids surface were carried out in NOVA-1200 system supplied by *Quantachrome Corporation.* A schematic flow diagram of apparatus is given. NOVA is a acronym for NO VOID ANALYSIS which measure multipoint BET surface area, single point BET surface area, total pore volume, average pore radius, sample volume, density, twenty five point adsorption isotherms, twenty five point desorption isotherms. A schematic flow diagram of apparatus is given in figure 3-4.

3.3.3.1 Operational Procedure for gas sorption analyser

Procedure for pretreatment and subsequent experiment is as follows:

0.25 gm of catalyst sample is weighed and is placed in a sample cell assembly which heated to 90°C in 10 min and temperature is maintained for 1 hr then the temperature is raised to 350°C and is maintained for 2 hr. Adsorbate source used is Nitrogen as it serves to be most common adsorbate source and well characterized one. All measurements are done as it is programmed (fully automated).

Mesopore size calculations are done assuming cylindrical pore geometry using the Kelvin equation[59].

$$r_k = \frac{-2\gamma V_m}{RT \ln(P/P_0)}$$

Where γ is the surface tension of nitrogen at its boiling point (8.85 ergs/cm^2 at 77K).

V_m is molar volume of liquid nitrogen (34.65cm^3/mol).

R is gas constant (8.314x10^{7}ergs/deg mol).

T is boiling point of nitrogen.

P/P_0 is relative pressure of nitrogen.

r_k is the Kelvin radius of the pore.

Kelvin radius r_K is the radius of pore in which condensation occurs at a relative pressure of P/P_o. Since prior to condensation some adsorption has taken place on the walls of the pore r_K is not actual pore radius. Actual pore radius is given by $r_p = r_K + t$

t is the thickness of the adsorbed layer.

t is given by

$$t(A^0) = 3.54\left[\frac{5}{2.303\log(P_0 / P)}\right]^{1/3}$$

Total pore volume is derived from the amount of vapor adsorbed at a relative pressure by assuming that pores are filled with liquid adsorbate. Most common method in determining the total surface area of the catalyst is that developed by Braunner, Emmet and Teller (called BET method).

BET equation is given by

$$\frac{P}{V_a(P_o - P)} = \frac{1}{V_m C} + \frac{c-1}{V_m C}\left(\frac{P}{P_o}\right)$$

V_a is the quantity of gas adsorbed at a relative pressure P/P_0.

V_m is the quantity of adsorbate constituting a monolayer of surface coverage.

C (BET constant) is related to energy of adsorption in the first adsorbed layer and indicates the magnitude of the adsorbate /adsorbent interactions. In this technique, amount of nitrogen adsorbed at equilibrium at its normal boiling point (-195.8°C) is measured over a range of partial pressure below 1 atmosphere. The volume of gas

adsorbed is calculated by measuring pressure variation resulting from adsorption of known volume of N_2 gas by test sample.

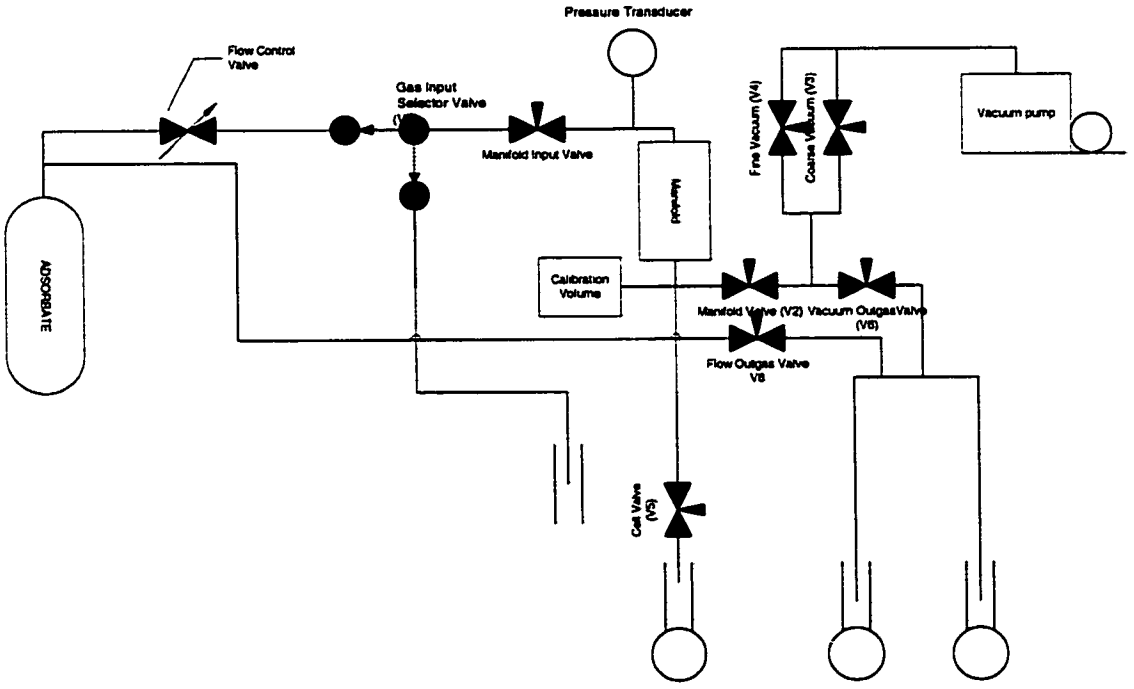

FIGURE 3-4 Schematic flow diagram of Nova sorption analyzer

3.4 CATALYST EVALUATION

3.4.1 Pulse Micro Reactor

For quantitative and qualitative investigations of heterogeneous catalytic reactions, Pulse micro reactor is easy and most widely used tool for evaluating catalysts.

3.4.1.1 Pulse reactor setup

Pulse micro reactor is designed by PEC and fabricated by Okhura Riken Co., Ltd., Japan. It consists of two identical, parallel units, A and B. Each unit comprises a gas inlet, injection port, microreactor, and gas chromatograph (GC). A well design control panel is also attached with the system to control and monitor reactor temperature, pressure and flow rates.

3.4.1.2 Pulse reactor operational procedure

The microreactor is filled with 0.1 gm of catalyst. Quartz wool is inserted at both ends of the reactor tube to make sure that catalyst bed is located at the middle of the tube. Before starting run catalyst is pretreated for 6 hours. The pretreatment is done by hydrogen/hydrogen sulfide mixture. During pretreatment the reactor temperature is programmed to increase from room temperature to 400^0C. Inert gas is introduced to purge the system.

To start the run, adjust gas flow rate, pressure, temperature of the column oven and detector oven and start GC. Four-way valve is adjusted according to the required direction of the flow. Reactant is injected into port by using a syringe, which comes into contact of catalyst, and reacts. GC measures composition of the reactor outlet and

analysis of which will give conversion. Figure 3-5 shows the schematic flow diagram of pulse microreactor system.

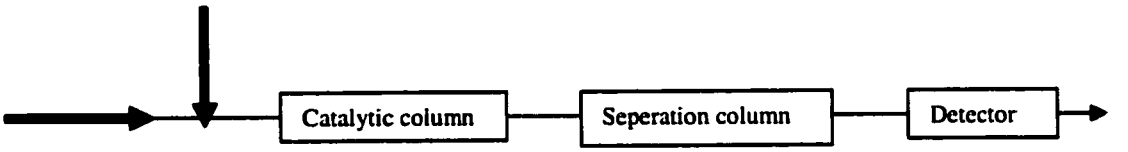

FIGURE 3-5 Micro catalytic pulse method

3.4.2 BATCH AUTOCLAVE REACTOR

Batch autoclave reactor is suitable for studying high exothermic hydrocracking reactions. With advantage of excellent fluid contacts, isothermicity within reactor, simple to operate, it also provides information about cracking activity, selectivity and stability of catalyst and kinetic data that can be used to determine the intrinsic reaction order and activation energy.

3.4.2.1 Batch Reactor setup

The size of autoclave reactor is 300 ml. The reactor is housed in furnace. There is programmed control system for controlling temperature, speed of the stirrer. Pressure and flows is controlled manually. A schematic flow diagram of this system is shown in figure 3-6.

3.4.2.2 Batch Reactor feed

Feed is dibenzothiophene dissolved in dodecane. First dibenzothiophene amount in the feed was 1000 ppm then it was increased 0.25 wt% as conversions were coming high

3.4.2.3 Batch Reactor operational procedure

Pre-sulfided catalyst from pulse micro reactor is used to test its hydrocracking and hydrodesulfurization activity.

75 gm of feed and 3 % of sulfided catalyst is loaded inside the reactor. Reactant and catalyst is purged in N_2 and H_2 and leak is checked by H_2 detector. Pressure of 67 kgf/m^2 at room temperature and temperature increasing rate is 5^0C/min. The system is allowed to react for 3 ½ hours. System is allowed to cool down to room temperature and then it is purged by N_2 after removing the product gas sample. Liquid product is analyzed by GC 14-B Shimadzu with FPD (flame photo-ionization detector) sulfur detector.

System	Catalyst Wt%	Dibenzothiophene wt %
1	3	0.1
2	2	0.1
3	0.5	0.25

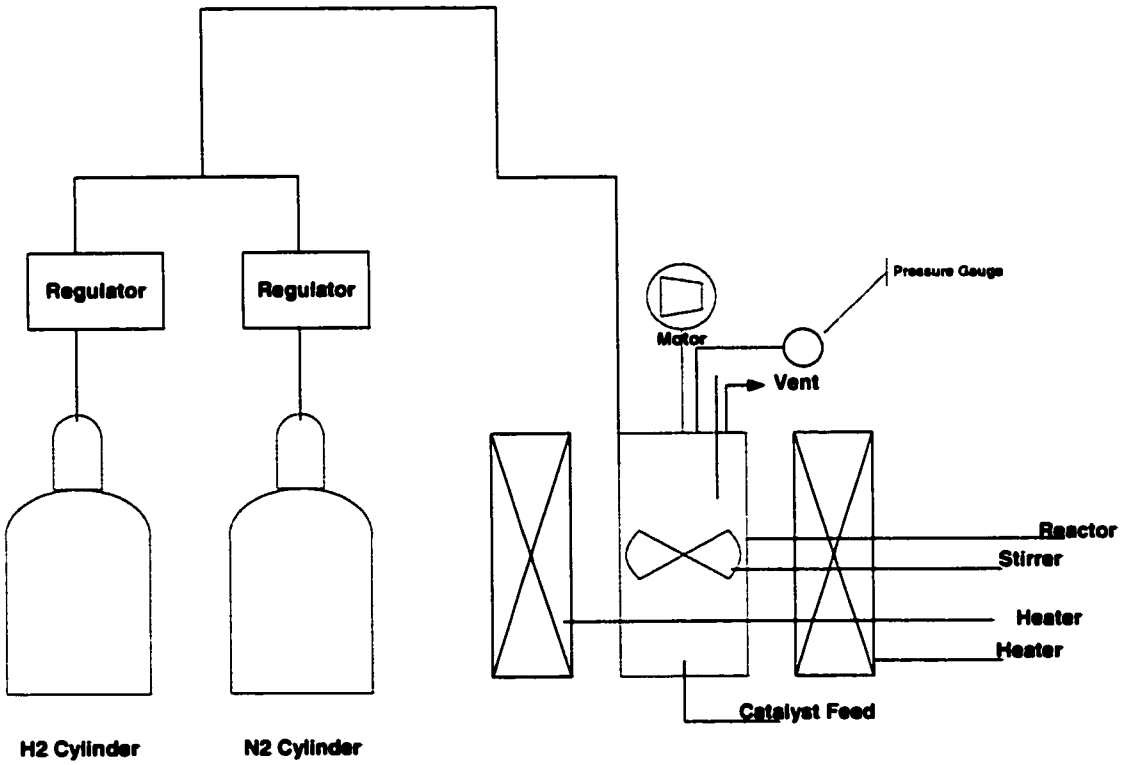

FIGURE 3-6 Experimental setup of batch autoclave reactor

RESULTS AND DISCUSSION

In this chapter, experimental results are presented and discussed. In all thirteen samples were synthesized and characterized as MCM41 based samples. Out of these thirteen samples, eleven samples were characterized and evaluated. Experimental results are presented in the following sequence

1 X-Ray Diffraction.

2 Gas Sorption Analyser.

3 Temperature Programmed Reduction.

4 Elemental Analysis.

5 Pulse microreactor evaluation

6 Batch reactor evaluation

4.1 X-ray Diffraction (XRD)

After synthesizing MCM41 samples, the measurements were carried out in order to confirm that the mesopores material has been crystallized as MCM41.

From d_{100}, calculation of parameter a_o in a hexagonal lattice is done by using the formula

$$a_o = 2*d_{100}/\sqrt{3}$$

As shown in figure 4-1 unit cell parameter a_o and d_{100} is clear.

Framework thickness D can be calculated from the formula given below

$$D = a - 2*r$$

Where r is pore radius.

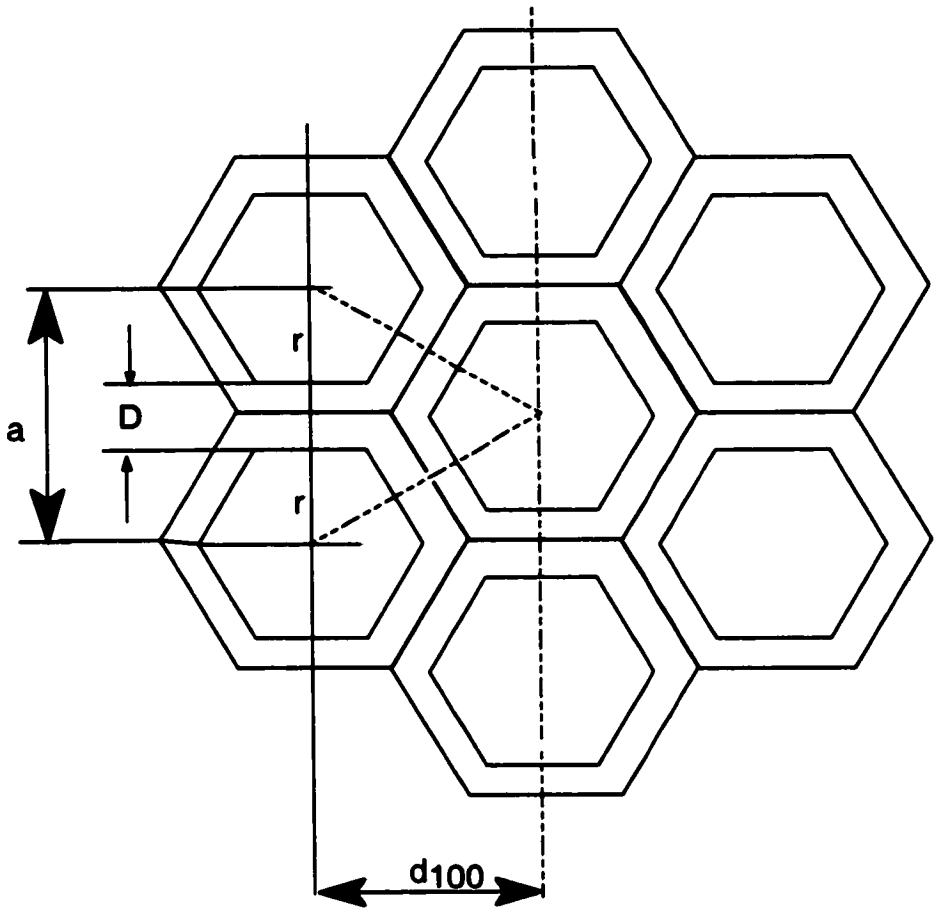

FIGURE 4-1 Figure showing d_{100}, a (unit cell size), D (Framework thickness), r (radius of the pore) and 2*r represents the pore size.

TABLE 4-1 Table showing D_{100} and a_o values for different catalysts.

Catalyst	D_{100}	a_o
MCM41	40.7	47.0
NiMCM41	42.0	48.5
CoMCM41	39.4	45.5
MoMCM41	55.8	64.5

As shown in figure 4-2, XRD of the calcined MCM41 show higher ordered pore structure similar to typical hexagonal lattice reported by Beck[60]. It shows four low angle peaks in the region 2θ=1.5-10, corresponding to the (100), (110), (200), and (210) reflections.

The XRD patterns as observed in figure 4-3 for cobalt incorporated MCM41 and in figure 4-4 for nickel-incorporated MCM41 and in figure 4-5 for molybdenum incorporated MCM41 showed a decrease in crystallanity as compared to MCM41. The decrease in crystallanity is more pronounced in MoMCM41 as shown in figure 4-5, which is in accordance with the results obtained by Deung[46]. As compared to nickel and molybdenum incorporated MCM41, cobalt incorporated MCM41 is showing high crystallanity with all the characteristic peaks. Luan *et. al.*[61] [62] who incorporated aluminium in the framework proved that by incorporating metal in the structure will result in low ordered pore structure. Similarly incorporation of metal (Ni, Co or Mo) in the framework of MCM41 resulted in low ordered pore structure. In addition to the metal (Ni, Co or Mo), aluminium was also added to these MCM41 based samples to increase the acidity of MCM41, which again would have added to the effect of decreasing the crystallanity.

Remarkable difference was observed in when these metal incorporated catalysts were impregnated with one more metal. For molybdenum impregnated samples with cobalt and nickel incorporated the trend is same as shown in figure 4-6. For cobalt and nickel impregnated samples where molybdenum was incorporated trend is like as shown in figure 4-7. Overall it can be said, after impregnation the crystallanity reduced markedly

in all the impregnated samples especially in the ones where molybdenum was incorporated.

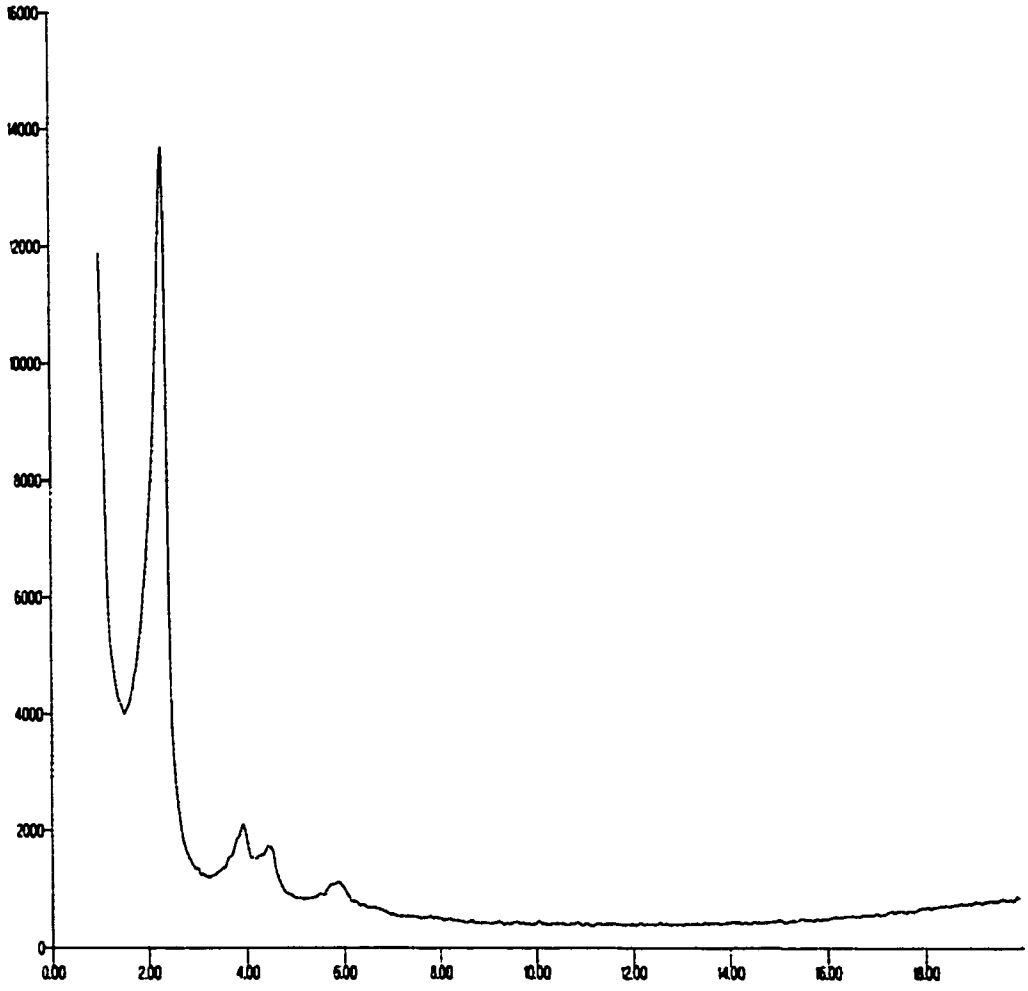

FIGURE 4-2 XRD pattern of calcined MCM41

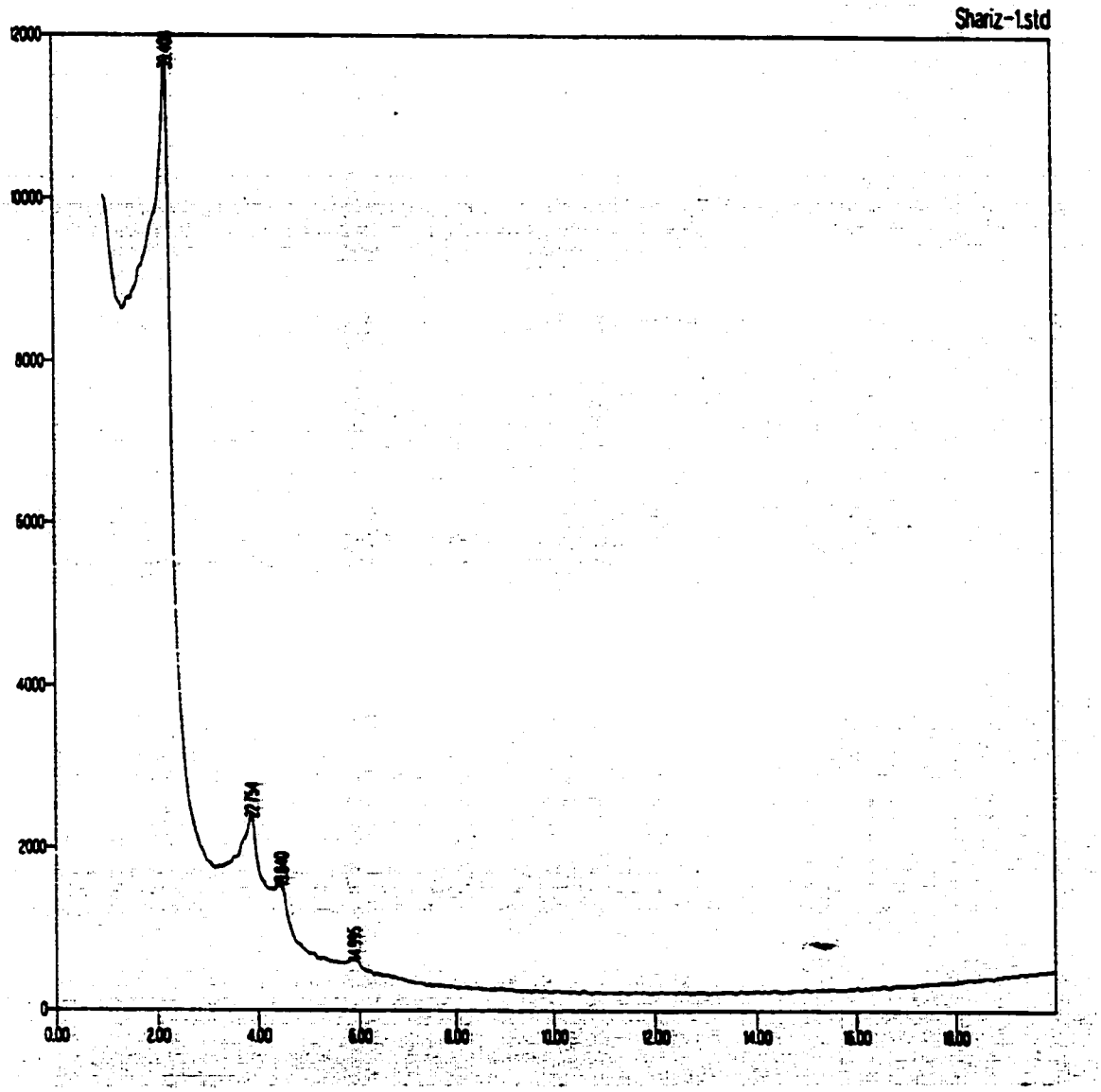

FIGURE 4-3 XRD pattern of CoMCM41

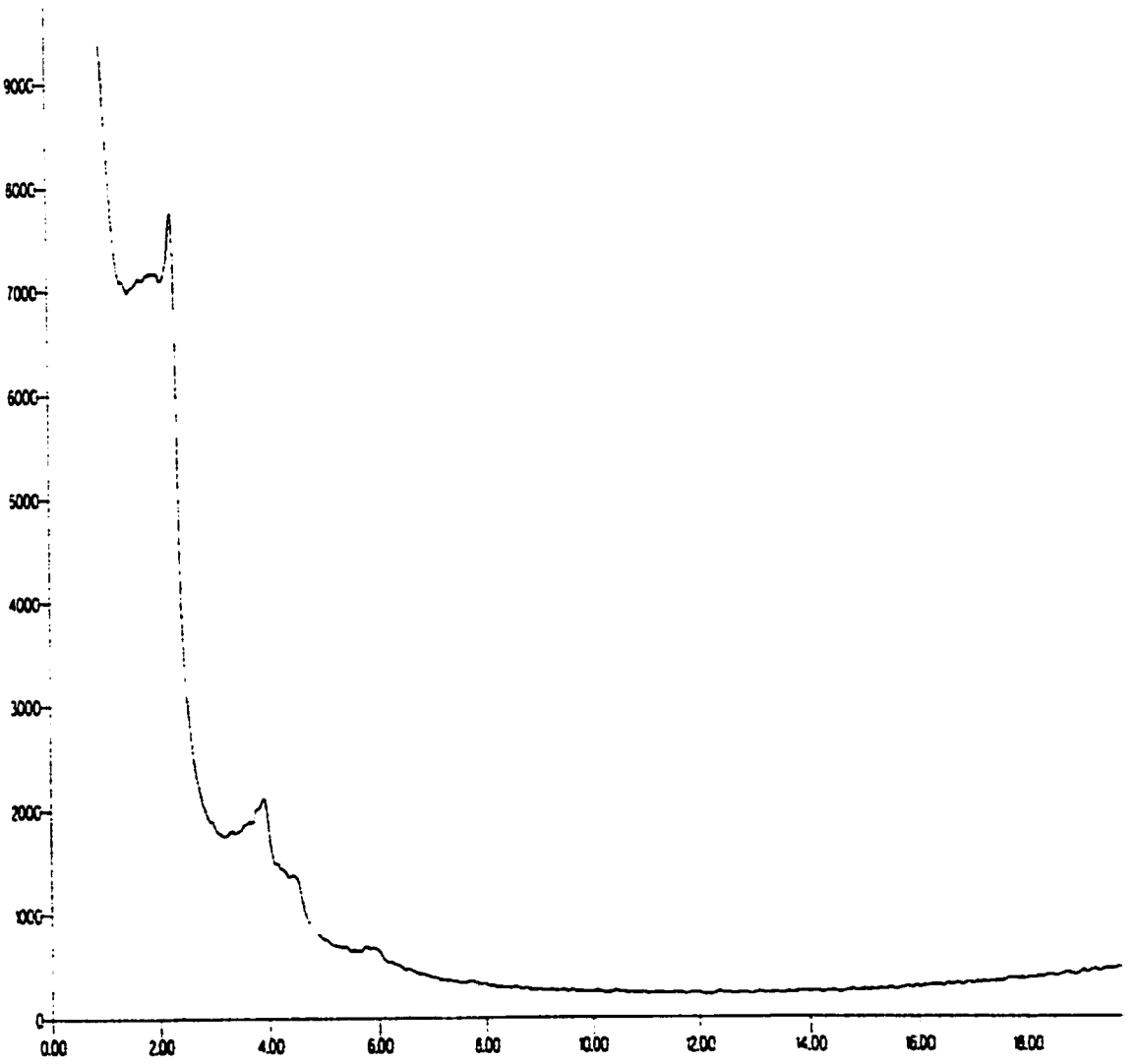

FIGURE 4-4 XRD pattern of NiMCM41

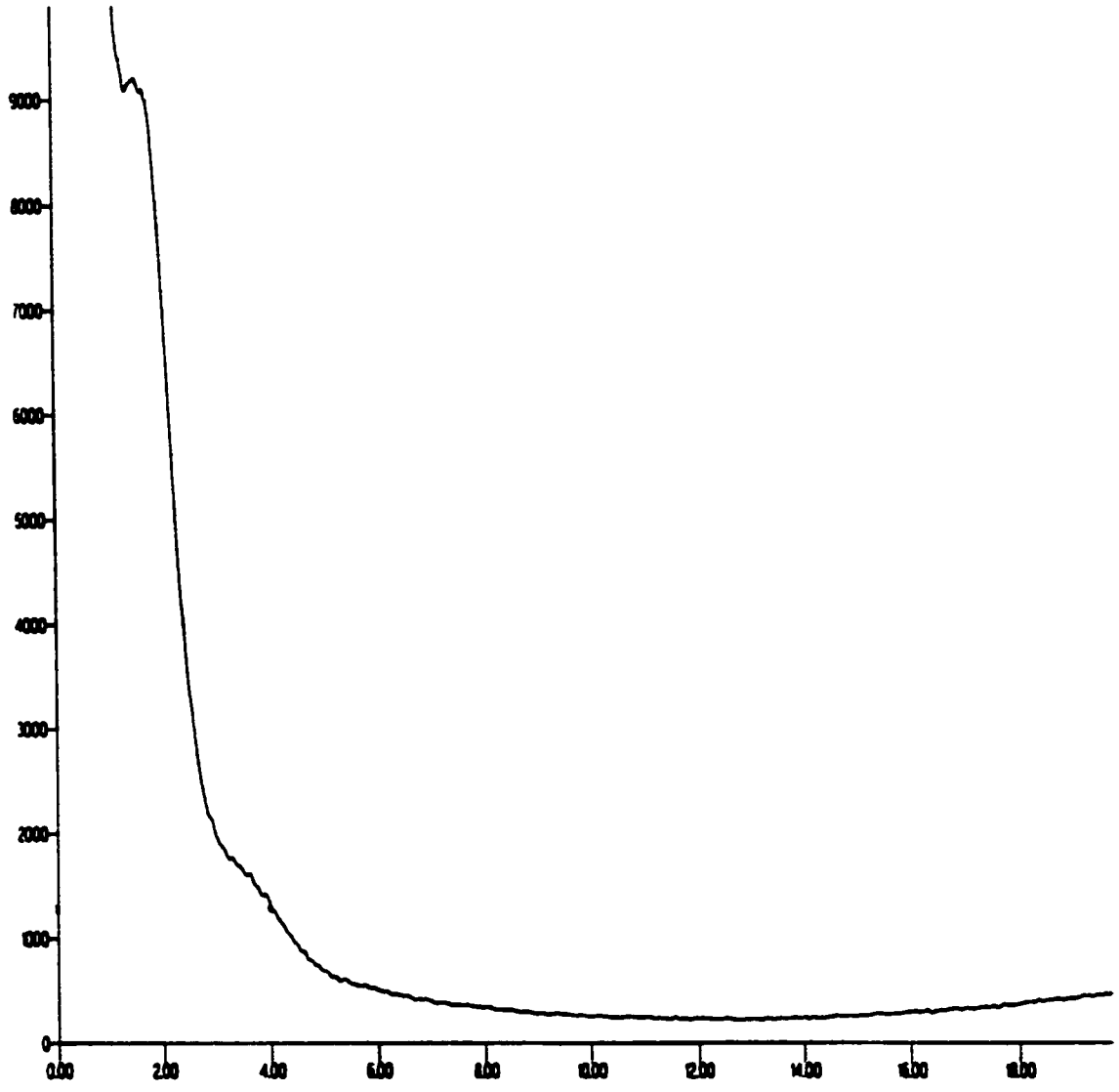

FIGURE 4-5 XRD patterns of MoMCM41

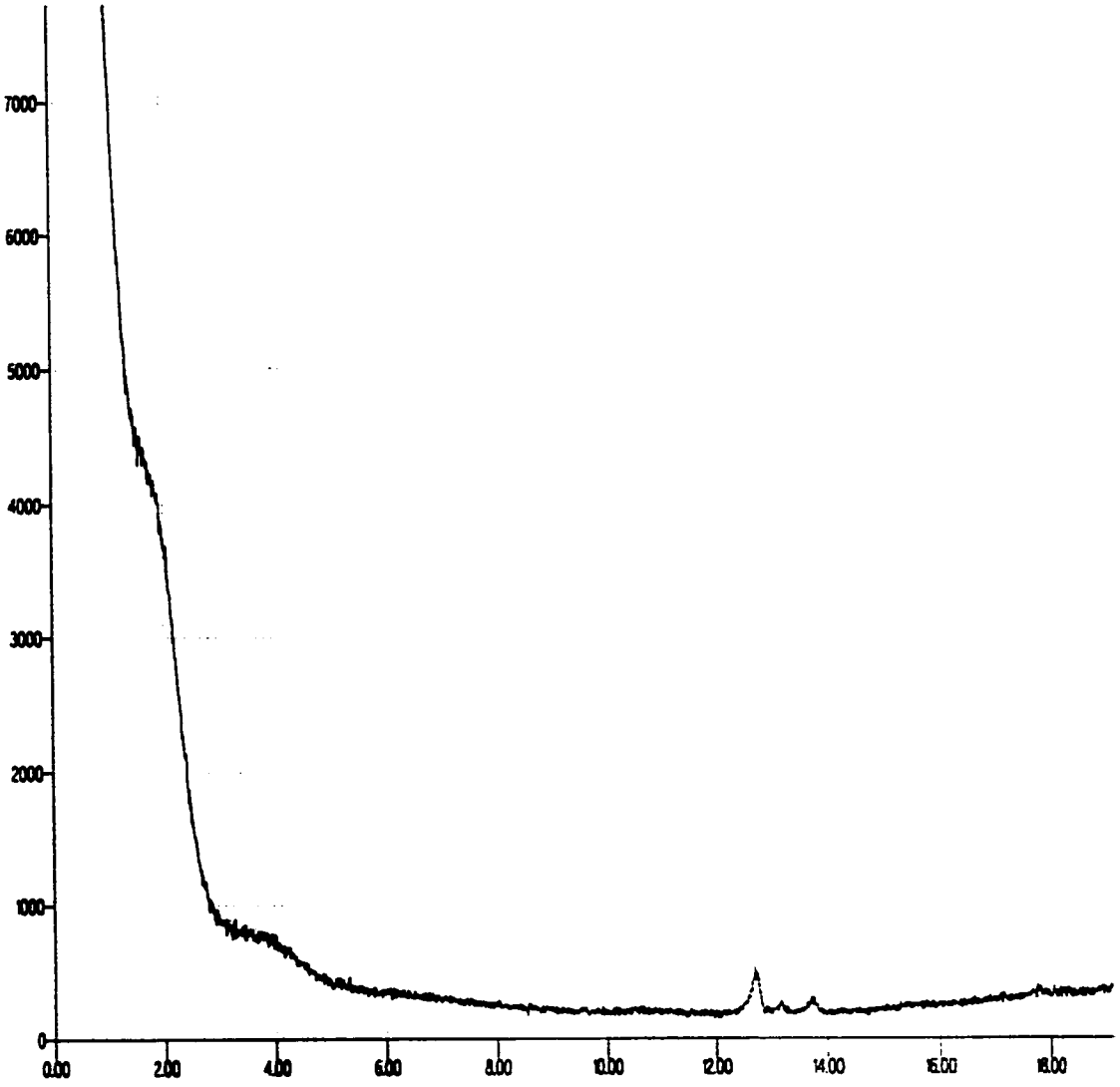

FIGURE 4-6 XRD pattern of Mo-NiMCM41

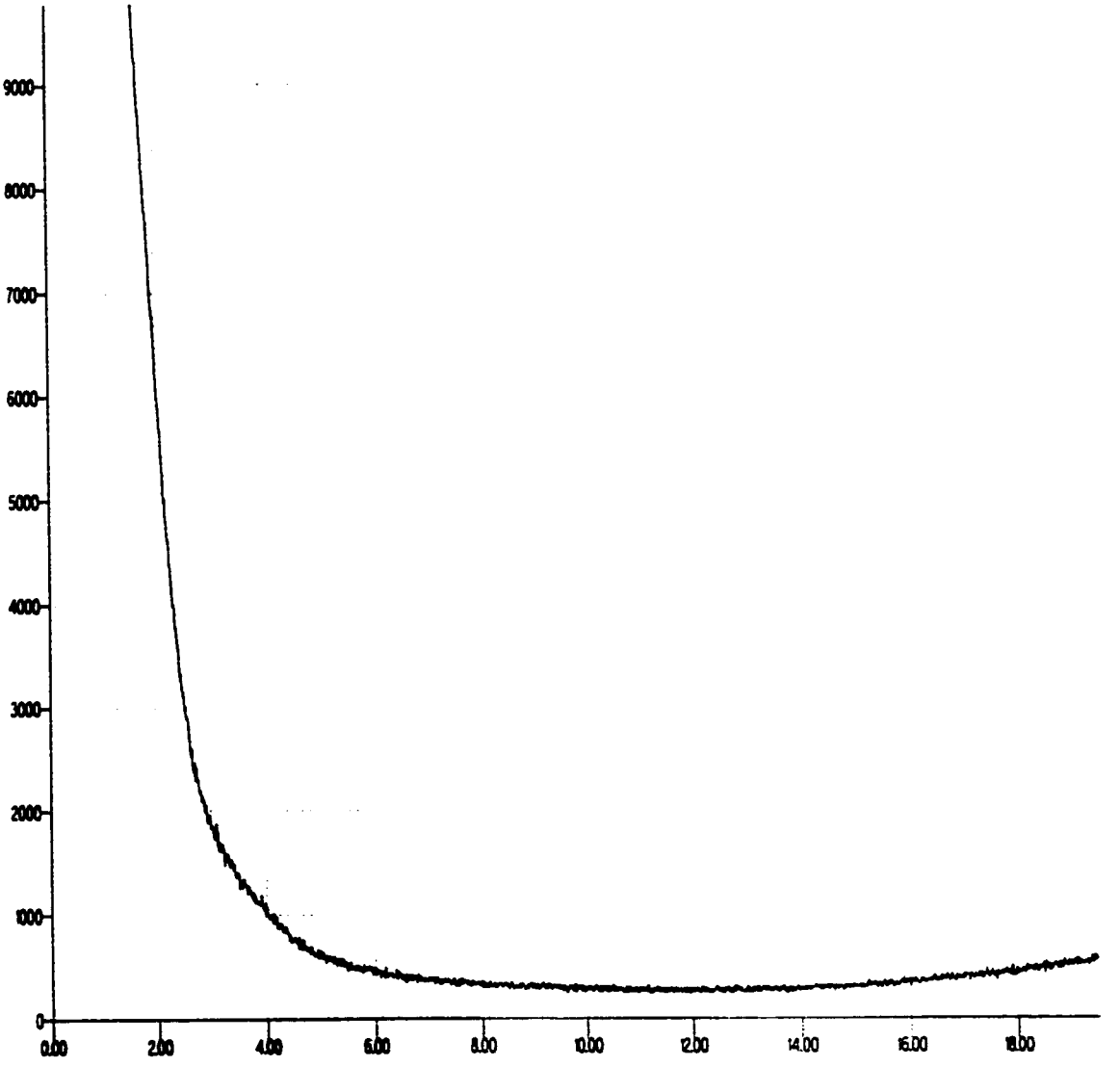

FIGURE 4-7 XRD pattern of Ni-MoMCM41

4.2 Gas Sorption Analyser

Surface area and porosity are important properties in the field of catalyst design and heterogeneous catalysis. Total surface area is a crucial criterion for solid catalysts since it determines accessibility of active sites and is thus often related to catalytic activity. The pore architecture of a heterogeneous catalyst controls transport phenomenon and governs selectivity in catalyzed reactions. Properties such as pore volume and pore-size distribution are therefore essential parameters especially in shape selective catalysis.

4.2.1 Isotherms

The first important information about surface and porosity obtained from the experiment is the isotherm. It can reveal the kind of porosity present in unknown samples. Brauner *et. al.*[63] has defined five different types of isotherms. Type I isotherms are characteristic for microscopic adsorbents, such as zeolites. Type IV isotherms are typical for mesoporous catalyst. Important features are the increase in volume adsorbed at higher p/p_o caused by adsorption in mesopores as well as a hysteresis loop. A distinct increase in adsorbate volume in the low p/p_o region in type IV isotherms indicates the presence of micropores associated with mesopores. For MCM41 type materials type IV isotherm is encountered with typical adsorbate uptake starting at 0.3 p/p_o. Capillary condensation is a secondary process that requires the preformation of an adsorbed layer on the pore walls formed by multilayer adsorption. A fluid confined in a pore condenses at a pressure lower than the saturation pressure at a given temperature. The condensation pressure depends on the pore size and shape and also on the strength of the interaction between the fluid and pore walls. It is assumed that for the pores of a given shape and surface chemistry, there exists

a one to one correspondence between the condensation pressure and the pore diameter. The occurrence of a wider, more pronounced hysteresis loop indicates that the evaporation from a pore is a distinctly different process from condensation within it. When gas condenses in a pore, the condensate builds from the walls inward toward a central core of decreasing diameter. However, it must evaporate from a liquid surface with a different curvature. This inhibits the evaporation and causes the decreasing portion of the loop to lag behind until all pores have emptied. Thus the adsorption isotherm that represents the amount of adsorbed fluid as a function of the vapor pressure contains direct information about the pore size distribution in the sample.

4.2.1.1 Metal Incorporated MCM41

Nitrogen adsorption-desorption isotherms of MCM41 prepared is as shown in figure 4-8. Similarly for MCM41 based samples, isotherms are shown in figures from 4-8 to 4-19. Four steps can be seen in type IV isotherm. Step A, monolayer-multilayer adsorption process rather than micropore filling can be seen, which increased sharply with increasing relative pressure. Step B, capillary condensation process, exhibits a sharp increase in the adsorption amounts. Step C, adsorption over the external surfaces. Step D, capillary condensation within the interparticles. After incorporation of Cobalt and nickel, isotherm obtained is same, type IV isotherm as shown in figure 4-9, 4-10. Molybdenum incorporation results into disturbed isotherm as shown in figure 4-11, that could be attributed to less crystallanity, which was confirmed by XRD results. Sudden increase in the adsorption of N_2 indicates that some macropores are present which are indicated in pore size distribution results. Uptake of N_2 decreases with the incorporation of the metal in the MCM41. The incorporation of metal leads to the reduction of the N_2 adsorption on

the surface, probably due to the blocking of the pores. However it is worth noting that NiMCM41 showed high adsorption capacity as compared to CoMCM41, suggesting that chemical adsorption of N_2 on Ni species may have occurred. Same result was got by Wang *et. al.*[58] when they impregnated Ni on MCM41. After ion exchanging metal incorporated MCM41, catalysts were impregnated with second metal, the isotherms then obtained are disturbed type IV isotherms as shown in figure 4-12, 4-13, 4-14, 4-15. Adsorption capacity of all the catalysts again decreased after impregnation of second metal, which might be because of pore blocking. Isotherm obtained for these catalysts are not showing all the characteristic features of the MCM41 materials. This might be because of the less crystallanity of these samples, which can be seen in XRD results. If impregnation is done without ion exchange, isotherms obtained are as shown in figure 4-16, 4-17, 4-18, 4-19. Isotherms obtained are comparatively better than ion-exchanged catalyst in terms of the characteristic nature of the isotherm obtained for MCM41 materials. In all MoMCM41 based samples when impregnated showed sudden increase in the adsorption capacity near $p/p_o = 1$ indicating formation of macropores.

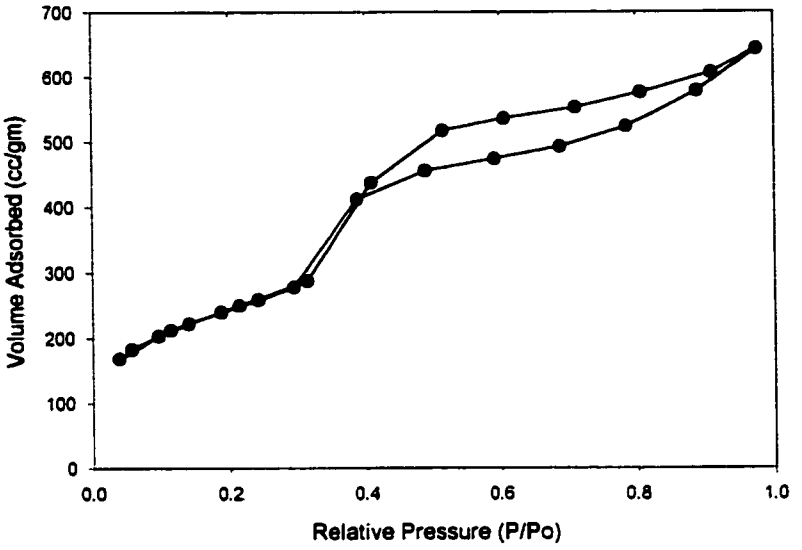

FIGURE 4-8 Nitrogen adsorption-desorption isotherms of MCM41.

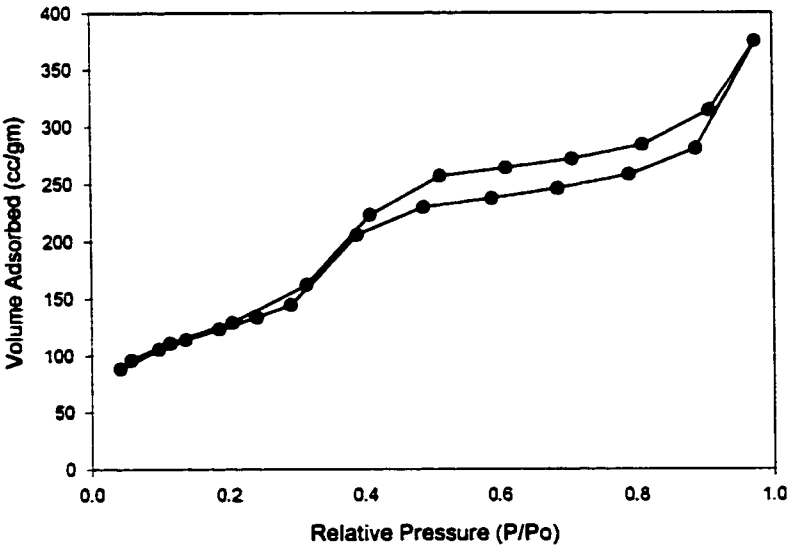

FIGURE 4-9 Nitrogen adsorption-desorption isotherms of cobalt incorporated MCM41. (CoMCM41)

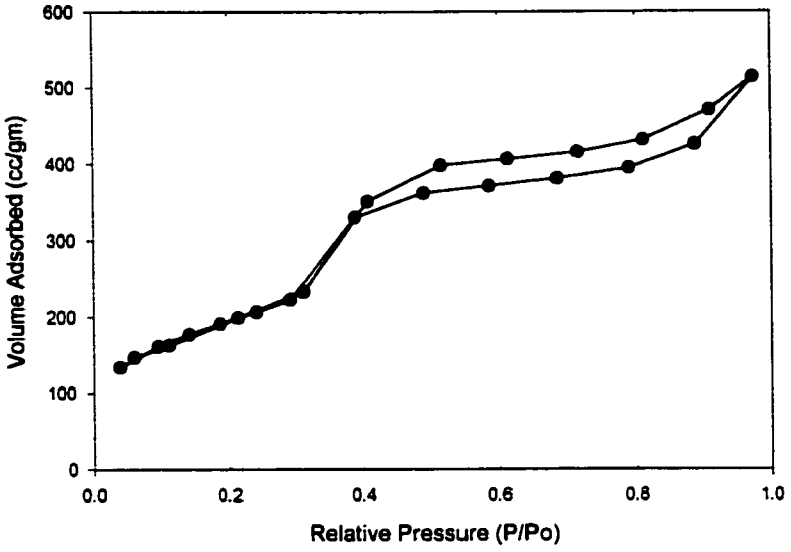

FIGURE 4-10 Nitrogen adsorption-desorption isotherms of nickel incorporated MCM41.(NiMCM41)

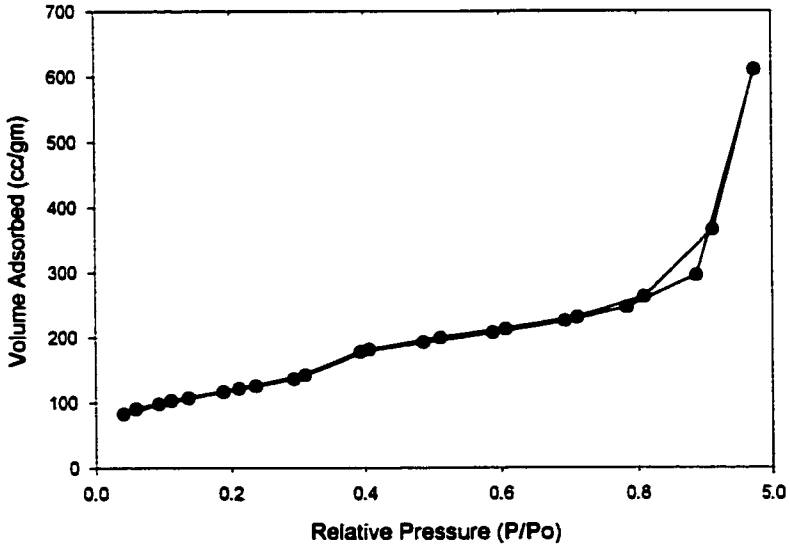

FIGURE 4-11 Nitrogen adsorption-desorption isotherms of molybdenum incorporated MCM41. (MoMCM41)

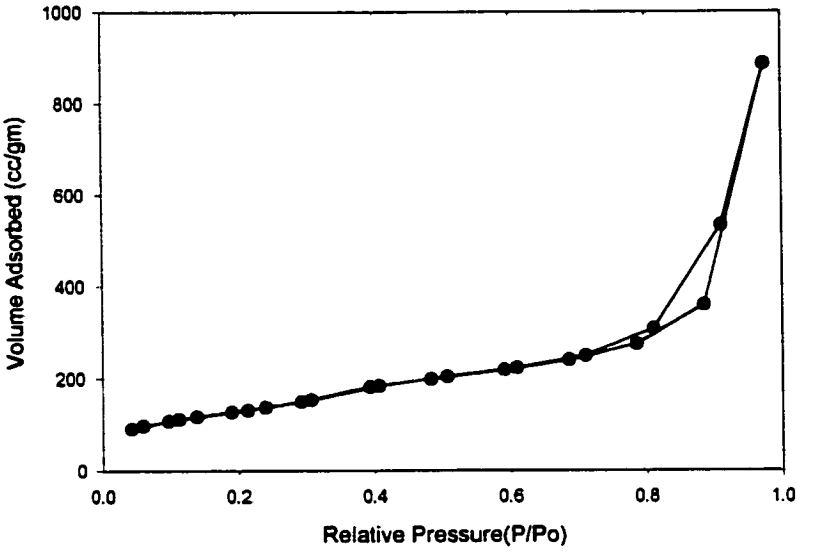

FIGURE 4-12 Nitrogen adsorption-desorption isotherms of cobalt impregnated on molybdenum incorporated MCM41. (Co-MoMCM41)

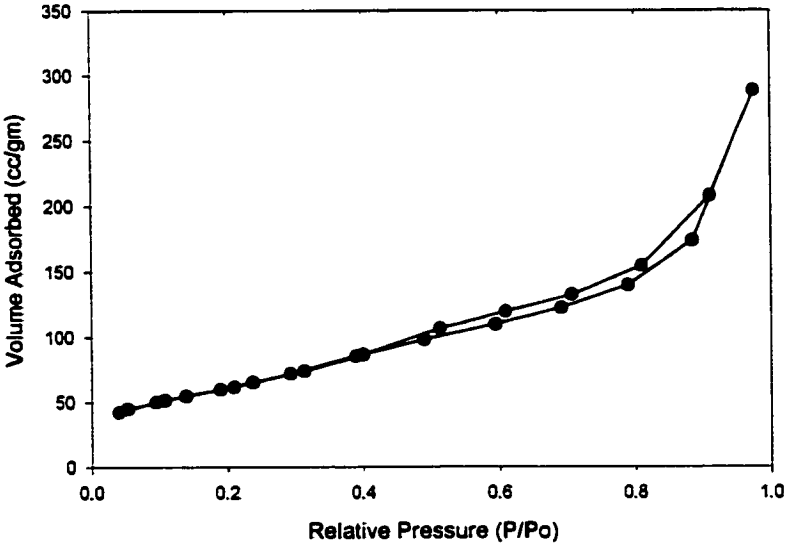

FIGURE 4-13 Nitrogen adsorption-desorption isotherms of molybdenum impregnated on cobalt incorporated MCM41. (Mo-CoMCM41)

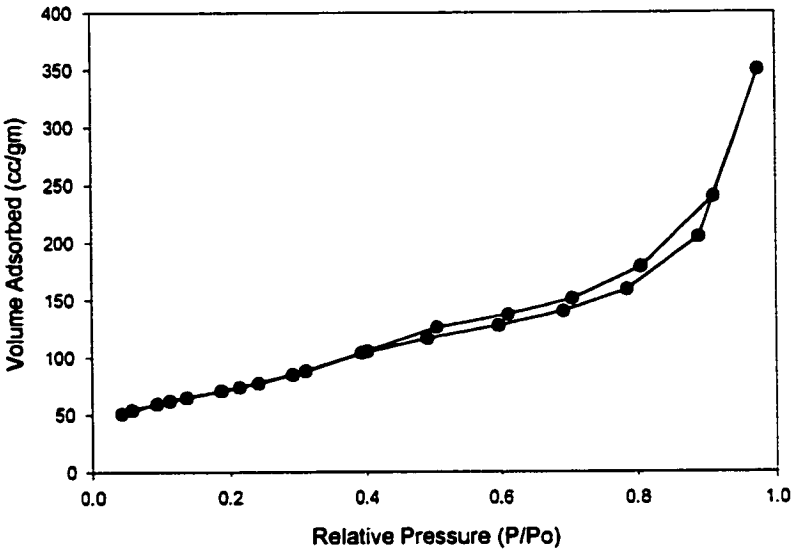

FIGURE 4-14 Nitrogen adsorption-desorption isotherms of molybdenum impregnated on nickel incorporated MCM41. (Mo-NiMCM41)

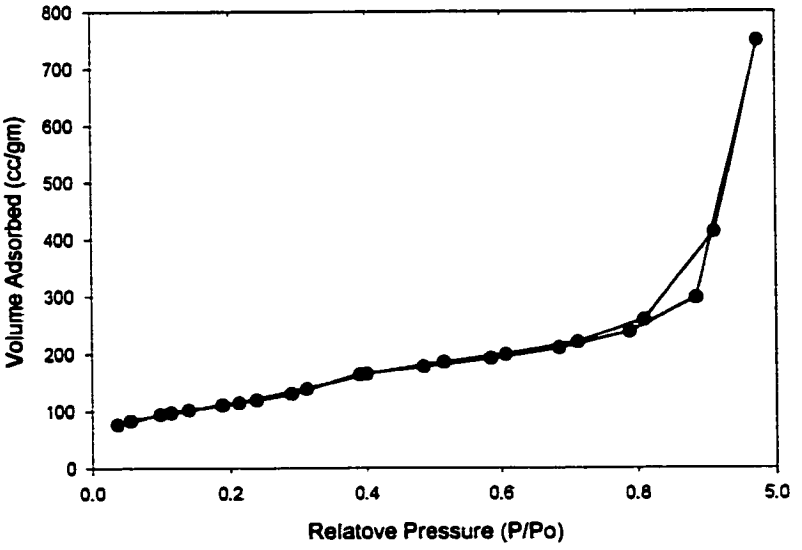

FIGURE 4-15 Nitrogen adsorption-desorption isotherms of nickel impregnated on molybdenum incorporated MCM41. (Ni-MoMCM41)

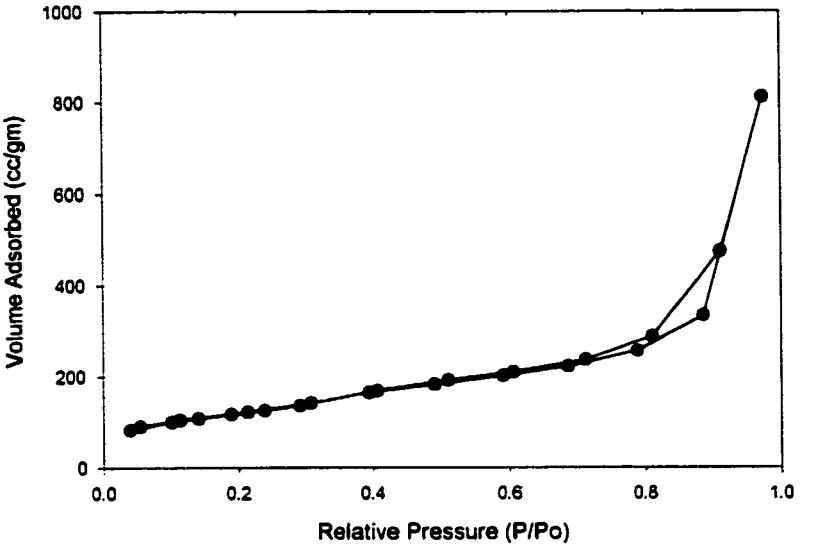

FIGURE 4-16 Nitrogen adsorption-desorption isotherms of cobalt impregnated on molybdenum incorporated MCM41. (Co-MoMCM41)

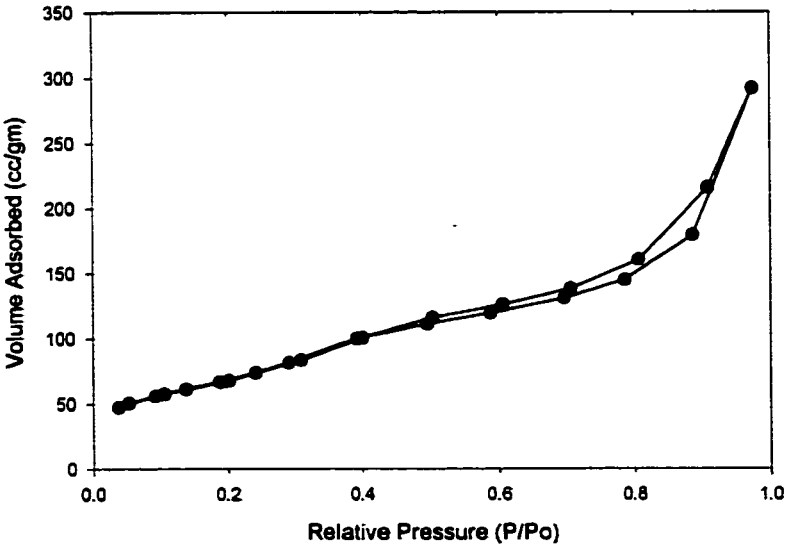

FIGURE 4-17 Nitrogen adsorption-desorption isotherms of molybdenum impregnated on cobalt incorporated MCM41. (Mo-CoMCM41)

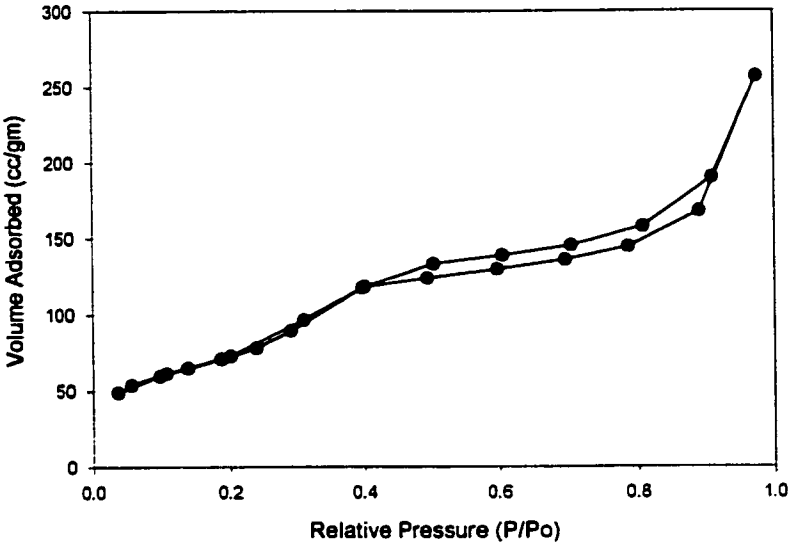

FIGURE 4-18 Nitrogen adsorption-desorption isotherms of molybdenum impregnated on nickel-incorporated MCM41. (Mo-NiMCM41)

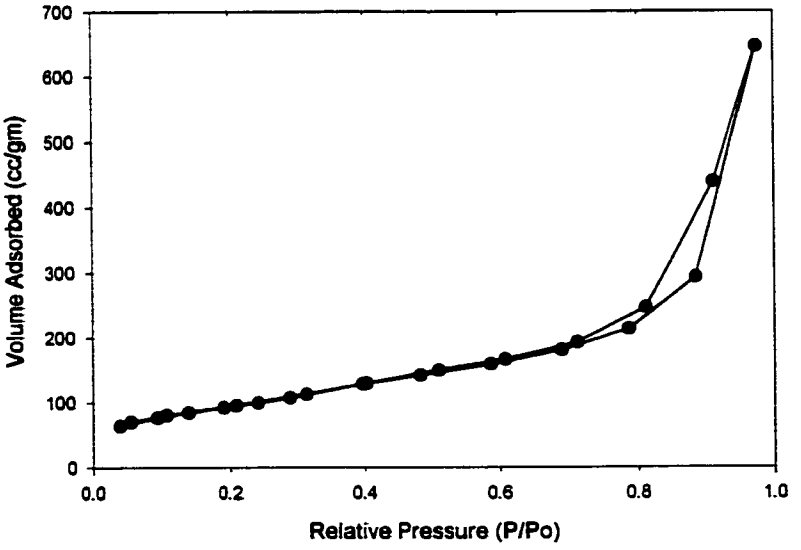

FIGURE 4-19 Nitrogen adsorption-desorption isotherms of nickel impregnated on molybdenum incorporated MCM41. (Ni-MoMCM41)

4.2.1.2 Y-Zeolite

Isotherm obtained for Y-zeolite is type I isotherm as shown in figure 4-20. Isotherm obtained is like other microporous material. Initially there is vertical rise, which instrument was unable to detect, then this rise levels out to a long nearly horizontal section and then to rise as saturation is approached and bulk condensation begins to occur.

Nickel and molybdenum were impregnated on Y-zeolite, isotherm for which is as shown in figure 4-21. As compared to MCM41, impregnated Y-zeolite has very less pore volume. Nickel was impregnated 1.6 wt% and molybdenum 2.5 wt%. Nickel was impregnated first. It can be seen clearly that adsorption capacity of zeolite is far less than MCM41 based catalyst.

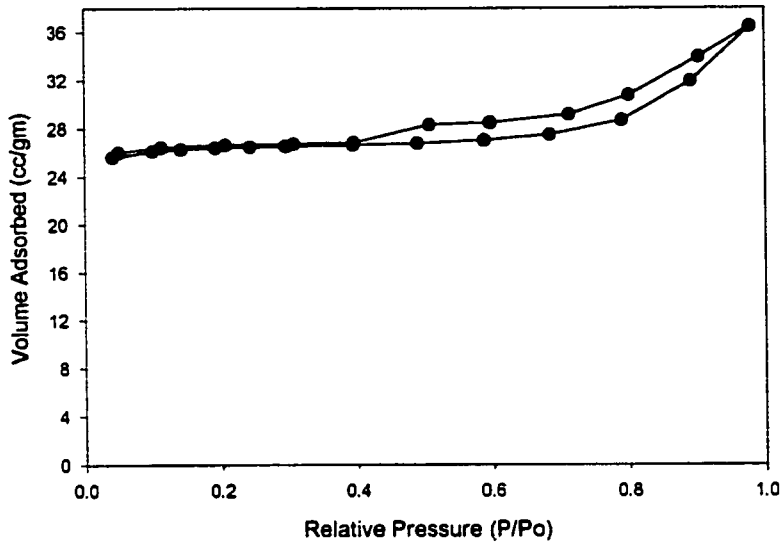

FIGURE 4-20 Nitrogen adsorption-desorption isotherms of Y zeolite.

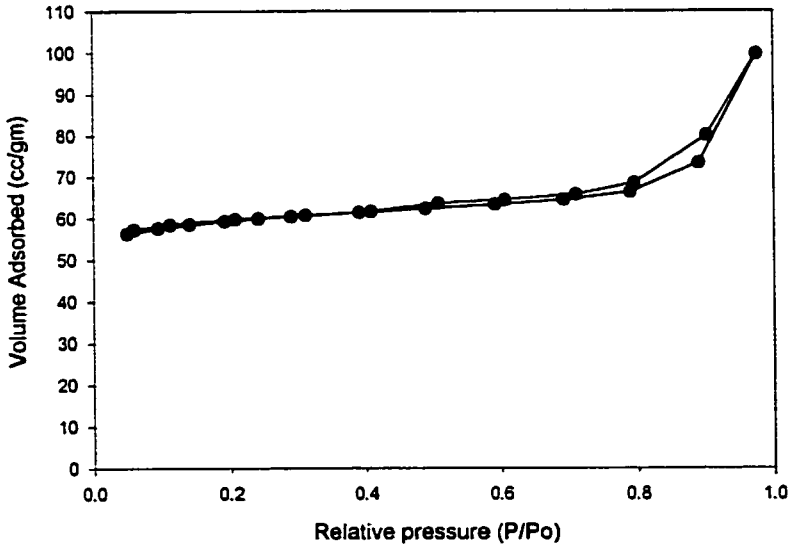

FIGURE 4-21 Nitrogen adsorption-desorption isotherms of nickel and molybdenum impregnated on Y zeolite. (Ni-Mo/Y Zeolite)

4.2.2 Pore Size Distribution

Pore size distribution of MCM41 is narrow and unique as shown in figure 4-22. All pores are uniform and poresize of 15 A^{o}. Pore size distribution of metal incorporated MCM41 is unimodal and narrow as shown in figure 4-23, 4-24, 4-25. After ion exchanging these metal incorporated catalysts, another metal was impregnated and pore size distribution for these are shown in figures 4-26, 4-27, 4-28, 4-29. Co-MoMCM41 and Ni-MoMCM41 pore size distributions shows that macropores bigger than mesopores are formed which can be because of less crystallanity, which was seen in isotherm result and confirmed by XRD. Pore size distribution for metal impregnated on metal incorporated MCM41 without ion exchange are shown in figure 4-30, 4-31, 4-32, 4-33.

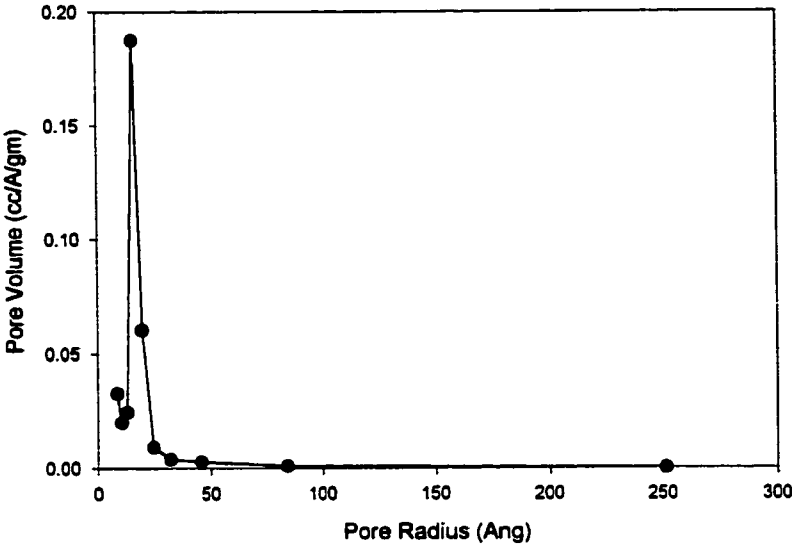

FIGURE 4-22 Pore size distribution of MCM41

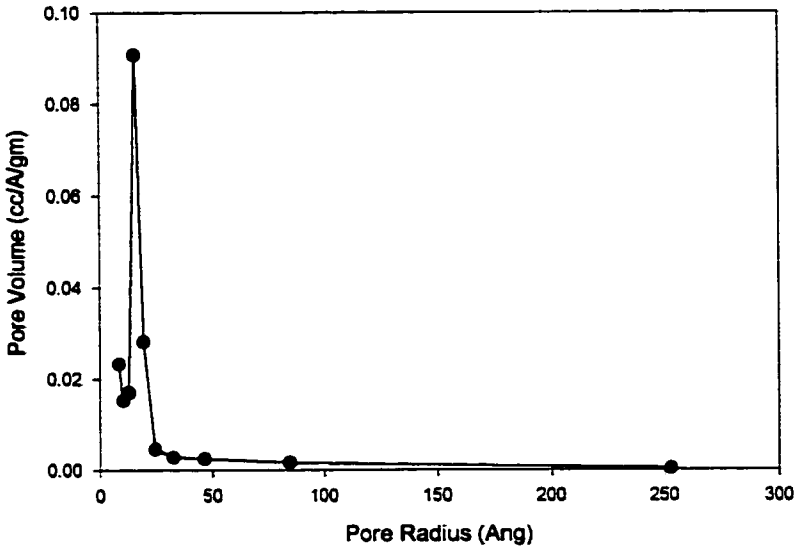

FIGURE 4-23 Pore size distribution of cobalt incorporated MCM41

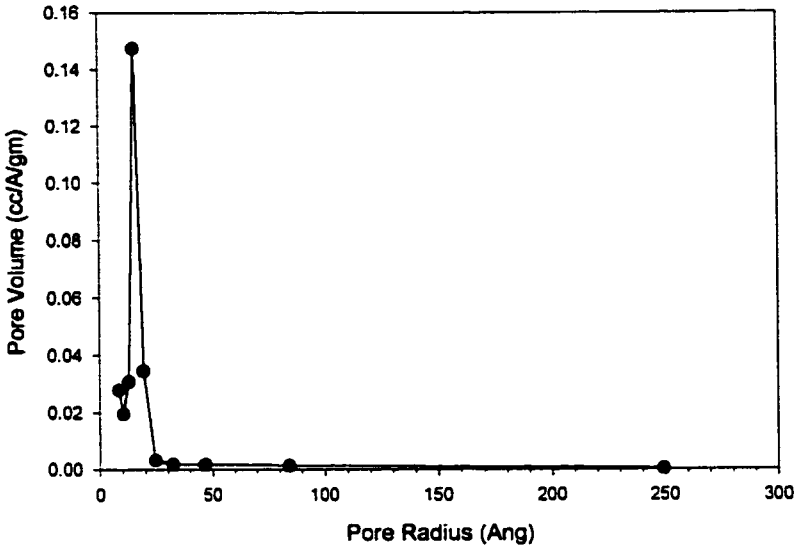

FIGURE 4-24 Pore size distribution of nickel incorporated MCM41

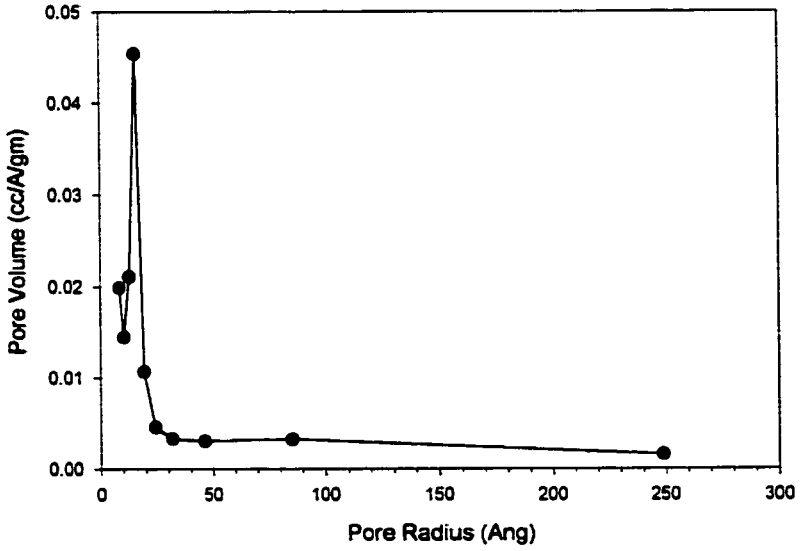

FIGURE 4-25 Pore size distribution of molybdenum incorporated MCM41

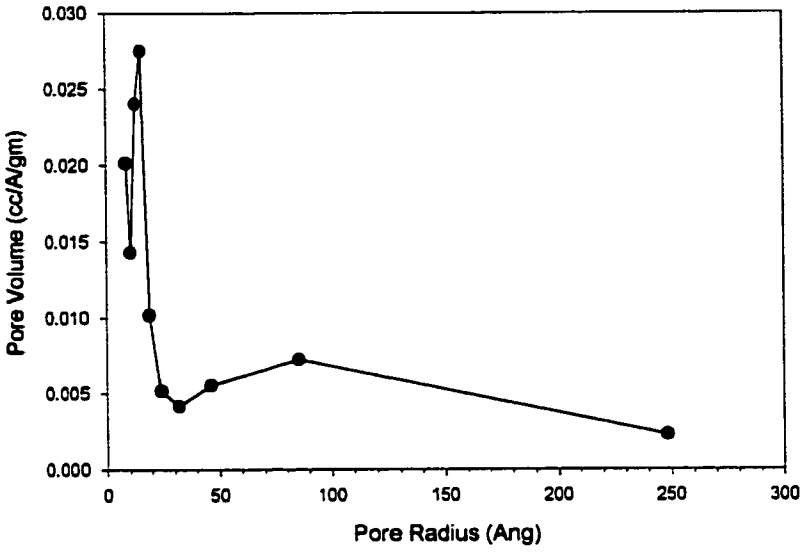

FIGURE 4-26 Pore size distribution for cobalt impregnated on molybdenum incorporated MCM41 (H^+form) Co-MoMCM41

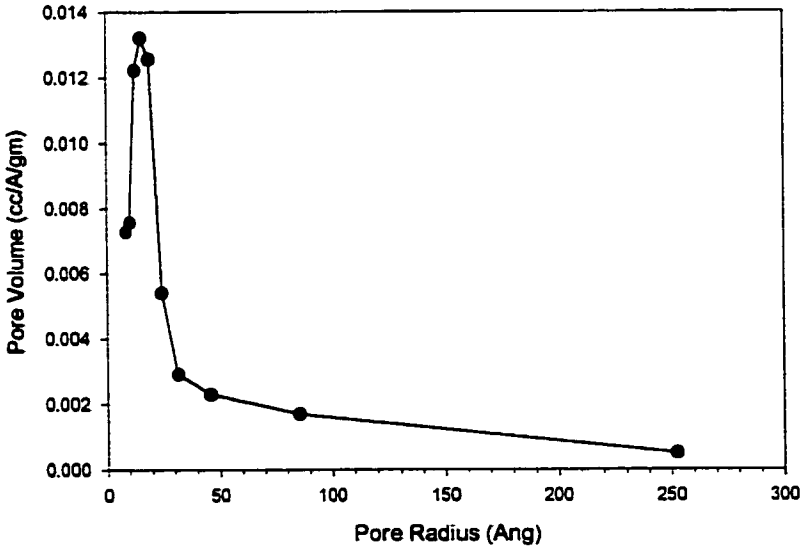

FIGURE 4-27 Pore size distribution for molybdenum impregnated on cobalt incorporated MCM41 (H^+form) Mo-CoMCM41

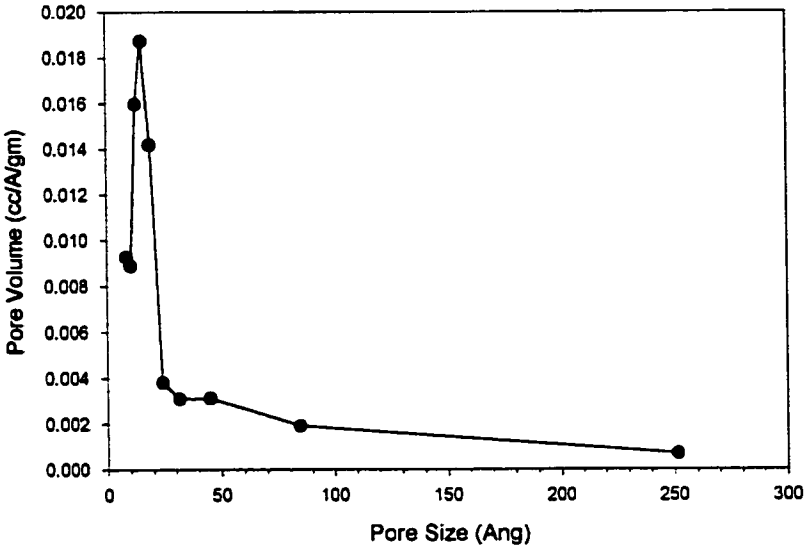

FIGURE 4-28 Pore size distribution for molybdenum impregnated on nickel incorporated MCM41 (H^+form) Mo-NiMCM41

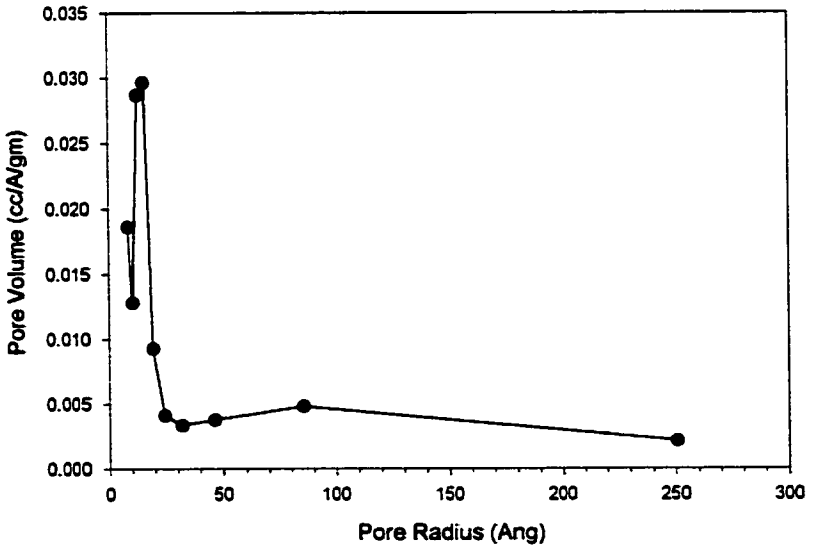

FIGURE 4-29 Pore size distribution for nickel impregnated on molybdenum incorporated MCM41 (H^+form) Ni-MoMCM41

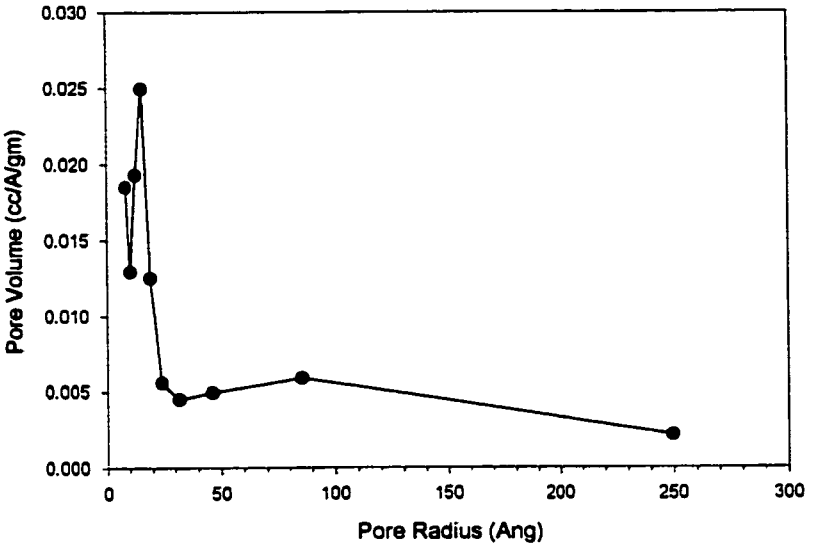

FIGURE 4-30 Pore size distribution for cobalt impregnated on molybdenum incorporated MCM41 (Calcined) Co-MoMCM41

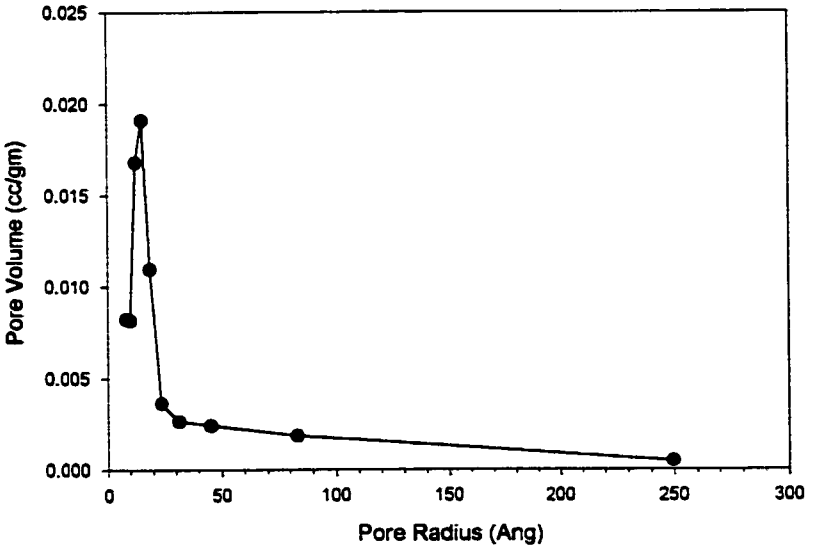

FIGURE 4-31 Pore size distribution for molybdenum impregnated on cobalt incorporated MCM41 (Calcined) Mo-CoMCM41

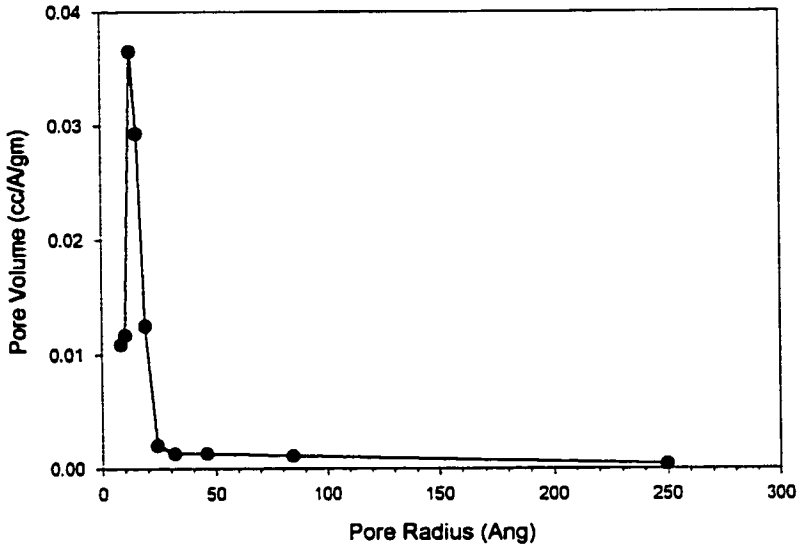

FIGURE 4-32 Pore size distribution for molybdenum impregnated on nickel incorporated MCM41 (Calcined) Mo-NiMCM41

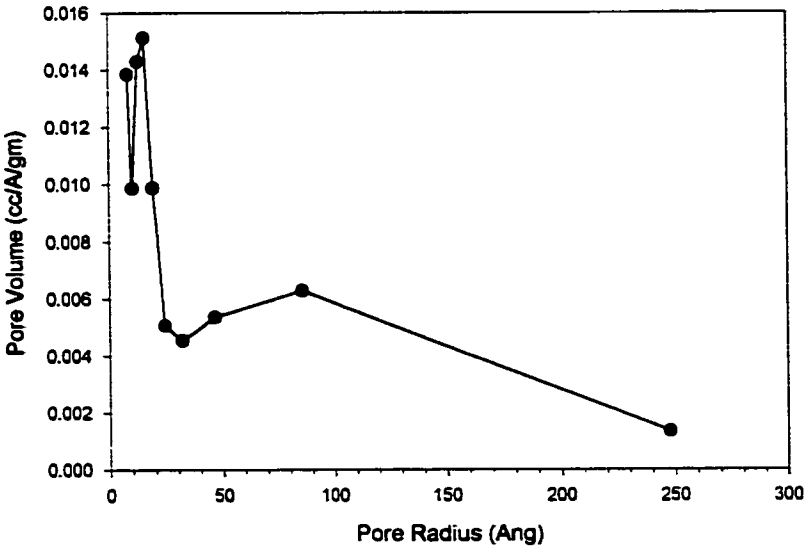

FIGURE 4-33 Pore size distribution for nickel impregnated on molybdenum incorporated MCM41 (Calcined) Ni-MoMCM41

4.2.2.1 Y zeolite

Pore size distribution of Y-zeolite is shown in figure 4-34. It can be seen from figure that pores less than 10 A^{o} are not seen, which is because of the limitation of the instrument.

Pore size distribution of impregnated y zeolite is as shown in figure 4-35. Mesopores, formed due to treatment to catalysts are seen in pore size distribution.

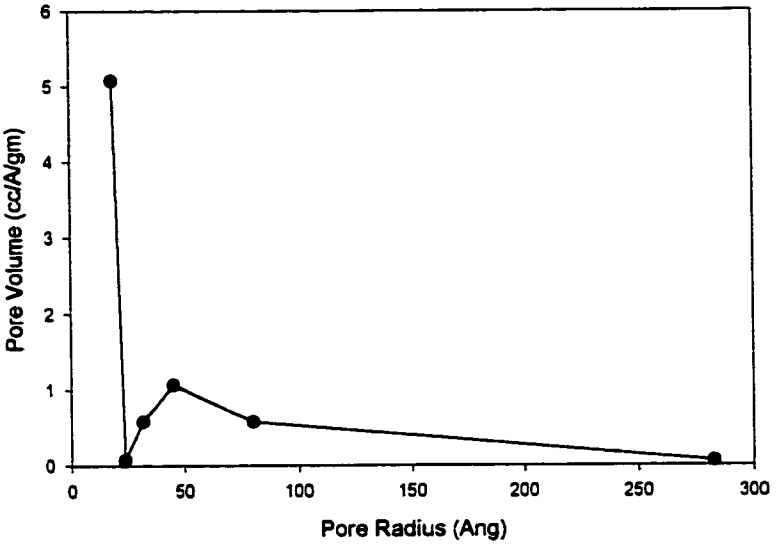

FIGURE 4-34 Pore size distribution of Y-zeolite

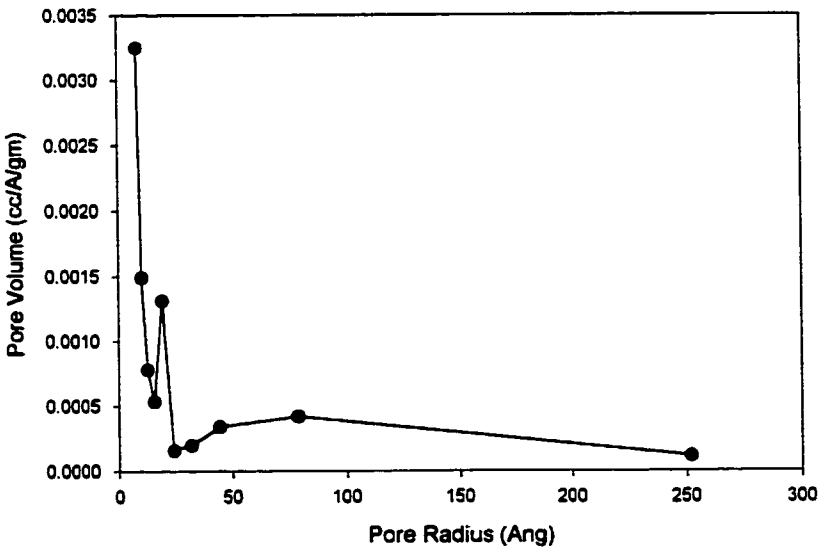

FIGURE 4-35 Pore size distribution for nickel and molybdenum impregnated Y-zeolite (Nickel first) (Ni-Mo/Yzeolite)

TABLE 4-2 Pore radius of different catalysts obtained.

Catalyst	Average Pore Radius (A^o)	Pore Volume (cc/gm)	Surface Area m^2/gm
MCM41	22.5	0.99	883.22
NiMCM41	27.0	0.65	459.00
CoMCM41	25.3	0.58	457.00
MoMCM41	43.8	0.94	430.20
Co/MoMCM41(H^+Form)	58.0	1.37	472.20
Mo/CoMCM41(H^+Form)	39.8	0.44	223.90
Mo/NiMCM41(H^+Form)	40.9	0.54	264.60
Ni/MoMCM41(H^+Form)	57.0	1.12	409.00
Co/MoMCM41 (cal)	58.3	1.25	430.40
Mo/CoMCM41 (cal)	36.0	0.45	251.10
Mo/NiMCM41 (cal)	29.6	0.40	268.40
Ni/MoMCM41 (cal)	58.6	0.99	341.00
Y Zeolite	7.0	0.28	428.50
Mo-Ni/ Yzeolite	15.9	0.15	193.4

As observed from table 4-2 average pore radius of all MCM41 based catalysts are high compared to zeolite based catalyst with MCM41 based catalyst in the range of 22 A°-58 A° while zeolite from 7 A°-15 A°. Surface area of MCM41 and metal incorporated MCM41 (NiMCM41, CoMCM41, MoMCM41) and metal impregnated on metal incorporated MCM41 is very much high as compared to zeolite and zeolite impregnated catalyst, with MCM41 based catalysts in the range of 250-900 m^2/gm and zeolites 190-400 m^2/gm. Similarly pore volume of MCM41 based catalysts ranging from 0.4-1.4 cc/gm and for zeolites 0.15-0.28 cc/gm. Clearly from above it can be concluded that MCM41 based catalysts are far superior as compared to zeolites in terms of surface area, pore volume, and pore radius.

After incorporating metals in MCM41 like Ni, Co, Mo the surface area reduces by a large extent from 883.2 m^2/gm for MCM41 to 459.00, 477.5 and 453.1 m^2/gm respectively. Incorporation of aluminium in the structure also adds to the decrease in the surface area as discussed by Luan *et. al.*[61, 62] . Decrease in surface area of metal incorporated MCM41 indicates less crystallanity, which was confirmed by XRD. CoMCM41 and NiMCM41 when impregnated with molybdenum, surface area reduces to almost half, which can be because of the blockage of the pores by the big atomic size molybdenum. MoMCM41 when impregnated with Ni and Co, there are some minor changes in surface area and pore volume, which can be attributed to calcining and drying step at that stage. Similar reason can be given for the difference in the surface area and pore volume in ion-exchanged and union-exchanged samples. Average pore radius for molybdenum incorporated MCM41 (MoMCM41) is more as compared to nickel and

cobalt incorporated MCM41 as atomic radius for molybdenum is high. Due to big atomic radius molybdenum faces difficulty in getting incorporated in the structure.

Reproducibility of the prepared catalyst with respect to pore size for 6 different catalyst is as represented in table 4-3.

TABLE 4-3 Pore radius of different catalysts obtained. (Reproducibility test)

Runs	Catalyst	Average pore radius (A^o)	Pore Volume (cc/gm)	Surface Area m^2/gm
Run1	MCM41	22.5	0.99	883.22
Run2	MCM41	20.5	0.79	788.62
Run1	NiMCM41	27.0	0.65	459.00
Run2	NiMCM41	26	0.62	439.00
Run1	CoMCM41	25.3	0.58	457.00
Run2	CoMCM41	25.1	0.66	525.00
Run1	MoMCM41	43.8	0.94	430.20
Run2	MoMCM41	52.7	0.83	453.10
Run1	Co/MoMCM41	58.0	1.37	472.20
Run2	Co/MoMCM41	55.4	1.07	492.60
Run1	Mo/CoMCM41	39.8	0.44	223.90
Run2	Mo/CoMCM41	36.6	0.52	233.70

4.3 Temperature Programmed Reduction (TPR)

Temperature programmed reduction (TPR) has been widely used for the investigation and characterization of metal incorporated and metal supported catalysts. TPR peak area represents the amount of hydrogen consumption and peak temperature represents the reducibility of the metal oxide or oxides. Thus TPR results can therefore be interpreted quantitatively as estimates of the distribution of various metal oxide phases as well as the metal support interaction for supported metal oxide catalysts.

The TPR profiles of MCM41 catalyst and metal incorporated MCM41 (Ni, Co, Mo) are shown in figure 4-36. It has been reported by Arnoldy and Moulijn[64] that at least four oxidic Co phases could be distinguished which differ widely in their reducibility and which could be divided into eight sub phases. It has been reported that the peak of Cobalt in CoMCM41 at 676°C is the reduction of surface phase of Co^{2+} ions. Brynmor *et. al.*[65] reported that peak I (270°C) of NiMCM41 can be assigned to reduction of traces of the higher Ni (III) oxide, while peak II (448°C) results from much more reduced Ni (II) species. Ni (II) can be either a surface nickel silicate or NiO present as very small, difficultly reducible particles. Arnoldy *et. al.*[66] reported that first peak at low temperature is reduction peak of octahedrally surrounded Mo^{+6} multilayer, and second peak at higher temperature is attributed to reduction of tetrahedrally and octahedrally surrounded Mo^{+6} monolayer species.

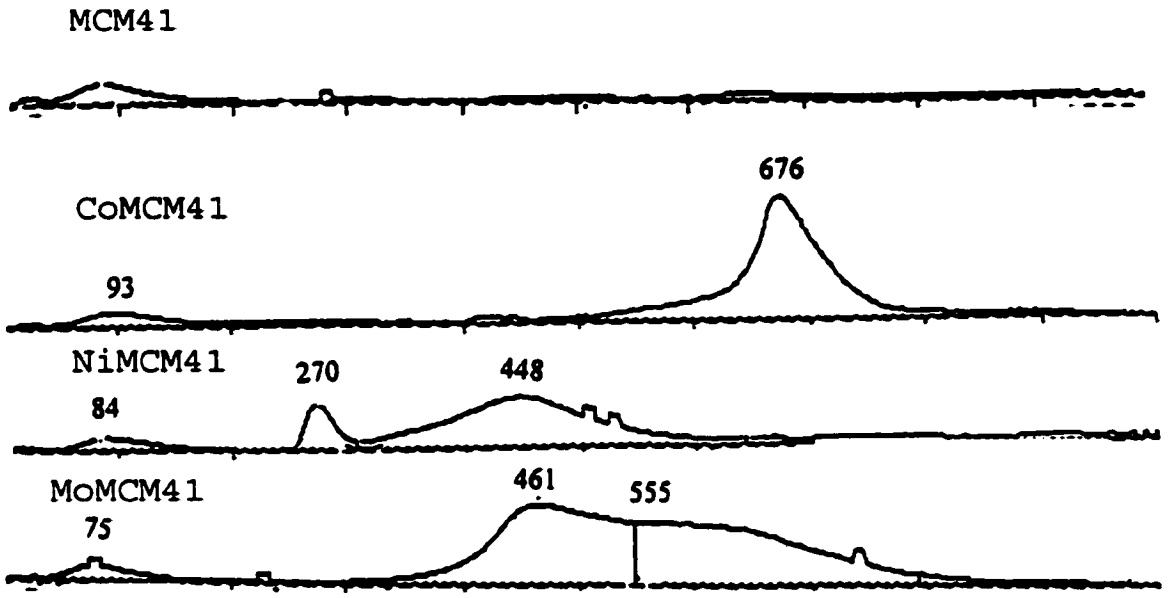

FIGURE 4-36 TPR spectra of MCM41 and metal incorporated MCM41 catalysts.

Figure 4-37 are TPR profiles of Mo/CoMCM41 and Co/MoMCM41 both in ionized form as well as calcined form one above the other. Figure 4-38 are TPR profiles of Mo/NiMCM41 and Ni/MoMCM41 both in ionized form as well as calcined form one above the other.

All the catalysts show multiple peak behavior. The first reduction appears in the region of 300 to 600 °C. The variation in the peak temperature can be attributed to the differences in the metal support interactions and multiple peak patterns might be due to the presence of the molybdenum at different sites of the support. The TPR pattern of all metal incorporated MCM41 indicates that the interaction between the metal species and MCM41 is quite different from that between the species and Al_2O_3.

When molybdenum is impregnated on CoMCM41 and NiMCM41 to get Mo/CoMCM41 and Mo/NiMCM41 respectively, there is good dispersion of molybdenum and it is reducing in the range of 458-466 °C. In Mo/NiMCM41, some intermediate species are being formed which is reducing at a very high temperature i.e 508 °C and 718 °C. Free nickel present in NiMCM41 reacts with molybdenum source at low temperature and thereby is getting reduced at a very high temperature. The shoulder peak in Mo/NiMCM41 (H^+ Form) at 304 °C which was not seen in calcined form indicates that nickel which was present in the pores came out of the pores during ion-exchange (Leeching of Metal). This peak can be reported as Ni (III) oxide. The shoulder peak in Mo/NiMCM41 (calcined) at 508 °C is not seen in H^+ form again indicating leeching of metal. The reducing temperature and close contact between Mo with Co or Ni atoms directly affects the hydrodesulfurization activity. It can be seen from the pulse

reactor results that the above catalysts (Mo/CoMCM41, Mo/NiMCM41) performed far better than the other catalysts.

When cobalt and nickel is impregnated on MoMCM41 to get Co/MoMCM41 and Ni/MoMCM41 respectively, the dispersion of cobalt and nickel is not good. It can be seen that peaks are broad and metal is getting reduced at broad temperature range and the reduction directly affects the performance of the catalyst as can be seen from pulse reactor results. The characteristic reduction temperature of the Mo sites as noticed in the MoMCM41 shifts to lower temperature in Ni/MoMCM41, suggesting a strong interaction between Ni and Mo species. The shift is from 460 °C to 410 °C. There are some intermediate species formed which are reducing at a very high temperature i.e 607 °C.

By comparing the areas of TPR spectra of ion exchanged and calcined catalyst, conclusion can be made that some of the metal got leached out, which was confirmed by atomic absorption. Molybdenum in MoMCM41 got leached out the most from 2.5 wt % to 1.7 wt%, which can be seen by comparing areas of Ni/MoMCM41, Co/MoMCM41 in H^+ form with calcined form. Cobalt in CoMCM41 got leached out from 1.6 wt% to 1.5 wt%, which can be seen by comparing Mo/CoMCM41 with calcined Mo/CoMCM41. Similarly nickel in NiMCM41 got leached out from 1.6 wt% to 1.4 wt%, which was seen, when comparing the areas of Mo/NiMCM41 (H^+ Form) and calcined Mo/NiMCM41. It can be concluded from TPR results that no free metal is available on the surface of the catalyst and metal is incorporated in the structure and is getting leached out during ionexchange.

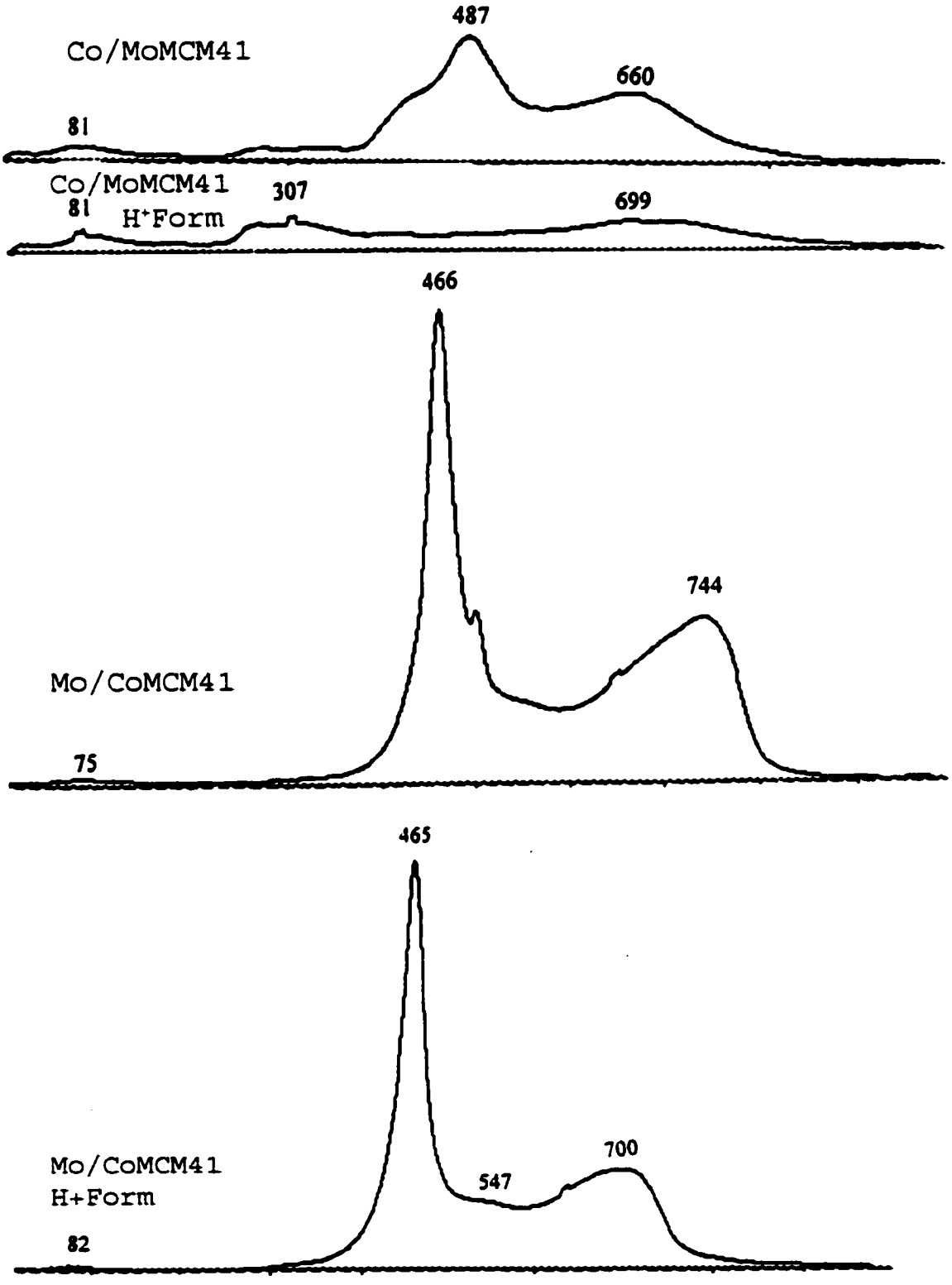

FIGURE 4-37 TPR spectra of Metal Impregnated on metal incorporated MCM41.

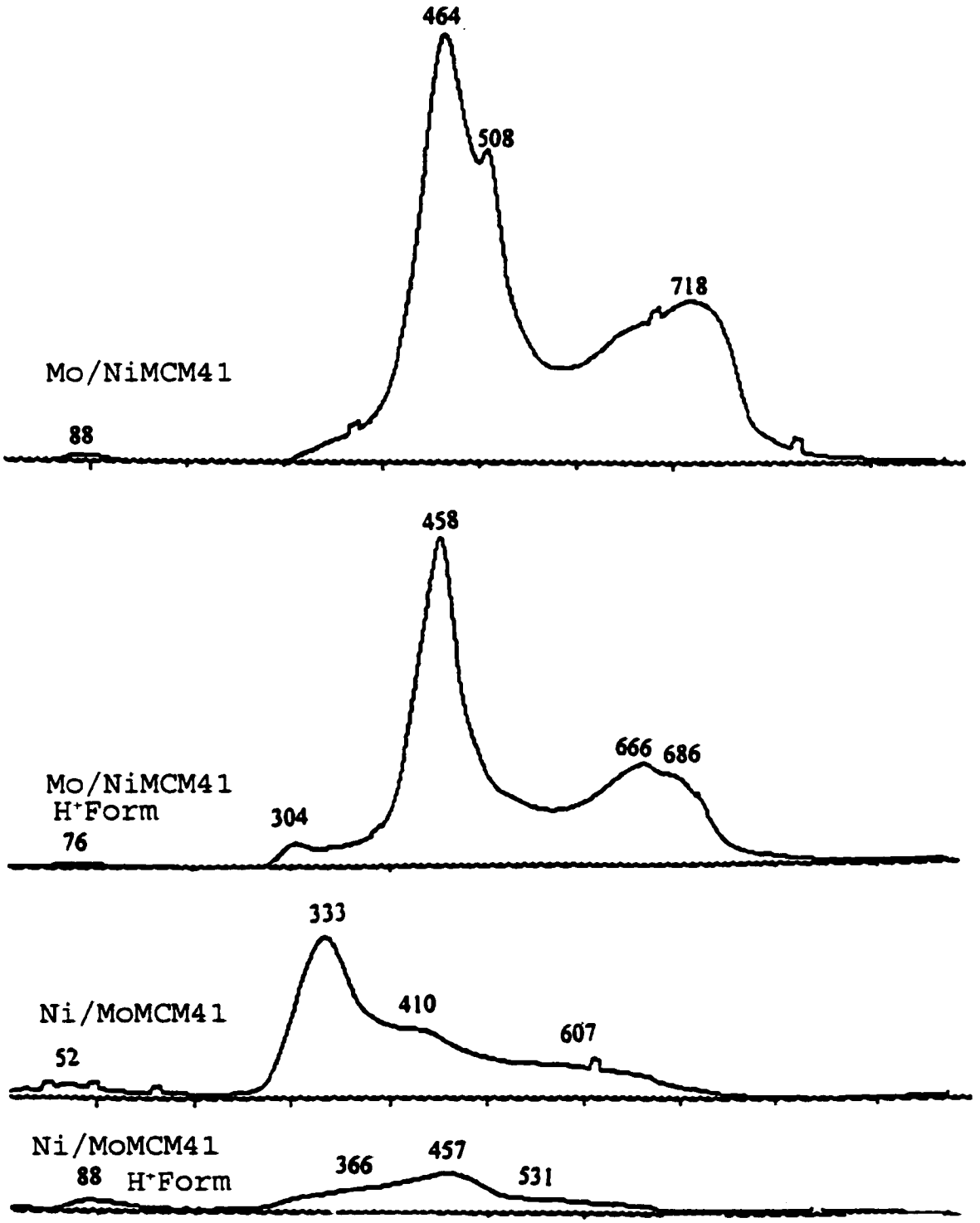

FIGURE 4-38 TPR spectra of Metal Impregnated on Metal Incorporated MCM41.

4.4 Elemental Analysis

Elemental analysis is one of the common methods for the estimation of the different elements on the catalyst. It is very necessary to balance the amount of different metals incorporated in and loaded on the catalyst as it affects life of the catalyst and the product distribution. Thus elemental analysis plays an important role during the synthesizing the catalyst.

4.4.1 Leaching of metals in Catalyst

In this study elemental analysis was carried out mainly to find out cobalt, nickel, molybdenum incorporated in the catalyst or supported on the catalyst. Table 4-4 lists the elemental analysis of different catalysts. From the table it is noticed that amount of metal was less in ion exchanged (H^+ form) samples as compared to calcined samples. While ion exchanging these catalysts, some of the metal were leeched out. Molybdenum based catalyst seems to be one which got leeched away the most 32 wt% as compared to cobalt and nickel based catalyst which was 6.25 wt% Co and 12.5 wt% Ni respectively. Reproducibility based on metal content in the catalyst was carried out as represented in table 4-4.

TABLE 4-4 Elemental analysis of fresh catalysts for different metal incorporations

No.	Catalysts	Metal Loaded (Wt%)			Metal Wt % Loss
		Ni	Co	Mo	
01	CoMCM41	-	1.5	-	6.25 wt% Co Loss
02	CoMCM41 (Calcined)	-	1.6	-	
03	NiMCM41	1.4	-	-	12.5 wt% Ni Loss
04	NiMCM41 (Calcined)	1.6	-	-	
05	MoMCM41	-	-	1.7	32.0 wt% Mo Loss
06	MoMCM41 (Calcined)	-	-	2.5	
07	CoMCM41	-	1.6	-	Reproducibility
08	MoMCM41	-	-	2.4	Reproducibility

4.5 Pulse Microreactor Evaluation

Small-scale testing of heterogeneous catalysts plays an important role during the development of a catalyst, especially at the early stages. Microreactors not only increases the rate of catalyst screening but also saves time and labor with isothermal operation assurance. These rapid screening tests are carried out at atmospheric pressure. Usually model compounds are employed as reactant in this type of reactors. The model compounds such as thiophene, benzothiophene and dibenzothiophene etc. representative of sulfur compound and pyridine, quinoline, alkyl-pyridines etc. are the representative of nitrogen compound in petroleum feed are widely used in pulse reactor evaluation. In this work thiophene and benzothiophene were chosen as a model compound because of its less reactivity and these sulfur compounds belong to the family of sulfur compounds that comprises the majority of the sulfur content in petroleum feedstocks. In fact all proposed catalysts in this work were evaluated in the pulse reactor for hydrodesulfurization (HDS) reaction. Results are presented and discussed as follows:

- Hydrodesulfurization (HDS) of Thiophene
- Hydrodesulfurization (HDS) of Benzothiophene.

4.5.1 Hydrodesulfurization (HDS) of Thiophene

The results are grouped and discussed as metal incorporated MCM41 and metal impregnated on metal incorporated MCM41.

4.5.1.1 Metal Incorporated MCM41

Molecular sieves containing transition metal ions in the framework positions exhibit remarkable properties as catalysts for oxidation reactions as found out by Notari[66].

Incorporation of Mo in the framework is limited because of the strain involved in the insertion of large transition metal ions in the framework position. However, incorporation of Mo in the framework of MCM41 is likely because of the greater flexibility of the structure as well as due to the differences in the mechanism of the formation of these materials. Rohit and Vishwananthan[45] in their work incorporated Mo in MCM41 gave evidences that the Mo is incorporated in the structure and the catalysts are stable and active and tested it for cyclohexanol and cyclohexane oxidation reactions. Similarly Deung Hee[46] incorporated Mo in MCM41 (so called direct synthesis) and found the catalyst active by testing the catalytic performance on oxidation of propylene. Nickel was incorporated before by Zhixiang *et. al.*[41] but its catalytic activity was not tested. Similarly cobalt incorporation in MCM41 by Jentys *et. al.*[67] was done, but it was not catalytically tested.

As shown in table 4-5 MCM41 without any metal incorporation showed the least conversion for thiophene as compared to metal incorporated MCM41. Molybdenum incorporated MCM41 show less conversion for thiophene hydrodesulfurization but still conversion per metal mole is high as compared to cobalt incorporated MCM41 as shown in figure 4-39. Molybdenum is used for hydrodesulfurization and cobalt and nickel as promoter to molybdenum. This is the reason why MoMCM41 is performing better than nickel and cobalt. Cobalt incorporated MCM41 is performing better as compared to nickel incorporated MCM41 as the amount of cobalt present in the CoMCM41 is high i.e 1.5 wt% as compared to the amount of nickel present in the NiMCM41 i.e. 1.4 wt%.

TABLE 4-5 HDS activity of MCM41 and metal incorporated MCM41 catalysts, evaluated in pulse reactor.

S.No	Catalysts	HDS activity (Conversion of Thiophene at temperature °C)				
		250	275	300	325	350
1	MCM41	-	-	0.20	0.28	0.39
2	NiMCM41	0.33	0.44	0.74	1.39	2.40
3	MoMCM41	0.43	0.99	2.42	2.78	3.72
4	CoMCM41	0.86	1.54	2.76	4.41	6.73

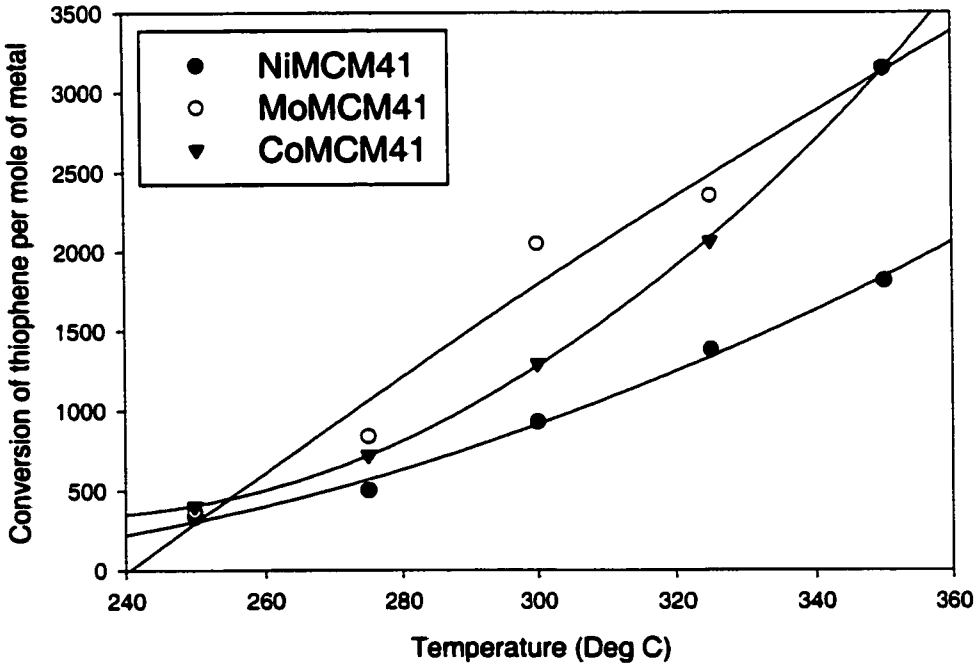

FIGURE 4-39 Conversion per metal mole for thiophene hydrodesulfurization as a function of temperature on metal incorporated MCM41 catalyst.

4.5.1.2 Metal Impregnated on metal incorporated MCM41

In this work thiophene HDS was conducted in pulse reactor to get the information about the HDS activity of the metal impregnated on metal incorporated MCM41 catalysts. As shown in table 4-6, it can be noticed that Mo-NiMCM41 thiophene conversion is high as compared to other impregnated catalyst. This result is inline with the result obtained by Klimova *et. al.*[54]. They studied Mo and MoNi HDS catalysts supported on γ-alumina to which various amounts (upto 30 wt%) of an MCM41 material (Si/Al:6.7) were added. Surprisingly, the MoNi catalyst (nickel first) had a higher thiophene HDS activity when the MCM41 content of the support was increased. From their investigations and this present study it can be interpreted that this increased activity is associated with a NiMo phase interacting with highly dispersed oxyaluminium species in MCM41 and that by impregnating nickel first and then molybdenum, changes in the dispersion of the Mo phase is caused which increases the thiophene hydrodesulfurization activity and HDS/hydrogenation ratio.

As shown in figure 4-40 and 4-41, Mo-NiMCM41 and Mo-CoMCM41 performed better as compared to Co-MoMCM41 and Ni-MoMCM41. Molybdenum when impregnated on nickel and cobalt incorporating MCM41 molecular sieves has good dispersion as seen in figures 4-37 and 4-38. Good dispersion of molybdenum on nickel impregnated MCM41 was also indicated by Klimova *et. a.l.*[54] which also showed high HDS activity. Similar to this result, molybdenum has good dispersion on cobalt and nickel incorporated MCM41 and hence it is showing high hydrodesulfurization activity. It can be said that molybdenum when impregnated on the promoted layer of Ni or Co,

NiMoS layer or CoMoS layer is getting formed, which is directly affecting the hydrodesulfurization activity.

Nickel and cobalt when impregnated on molybdenum incorporated MCM41 showed less dispersion as shown in figures 4-37 and 4-38. Hence Ni/MoMCM41 and Co/MoMCM41 showed less HDS activity. Commercial catalyst has less thiophene conversion as compared to impregnated MCM41 catalyst. The main reason behind this is the large difference between surface area and pore volume of the commercial catalyst and MCM41 based catalyst.

In zeolites, the catalysts were ion-exchanged to make it more catalytically active. Similarly MCM41 based catalyst were ion exchanged keeping in mind that it will create H^+ ion on the surface and hence increase the acidity of the catalyst. Ion exchanging the catalyst made a negative impact on the catalyst as during ion exchange some of the metal was getting leached as discussed in elemental analysis results. Due to reduction in metal content by leaching, ion-exchanged catalyst did not performed as good as compared to commercial and other MCM41 based catalyst.

TABLE 4-6 HDS activity (Conversion of thiophene) of metal impregnated on metal incorporated MCM41 catalyst, evaluated in pulse reactor.

S.No	Catalysts	HDS activity (Conversion of thiophene as a function of temperature °C)				
		250	275	300	325	350
1	Mo-NiMCM41-2 (Cal)	17.23	25.31	33.06	40.84	48.05
2	Mo-NiMCM41-4 (Ion)	14.82	23.21	32.10	35.27	41.45
3	Mo-CoMCM41-2 (Cal)	17.32	25.77	29.58	37.05	44.14
4	Mo-CoMCM41-2 (Ion)	17.00	25.33	31.49	36.67	43.31
5	Co-MoMCM41-2 (Cal)	3.01	5.26	7.45	9.21	11.03
6	Co-MoMCM41-3 (Ion)	1.02	1.72	3.00	3.97	5.52
7	Ni-MoMCM41-2 (Cal)	11.98	19.51	23.21	28.59	34.30
8	Ni-MoMCM41-1 (Ion)	1.45	2.25	4.03	7.00	9.90
9	Commercial Catalyst	8.72	10.34	11.17	13.83	19.14

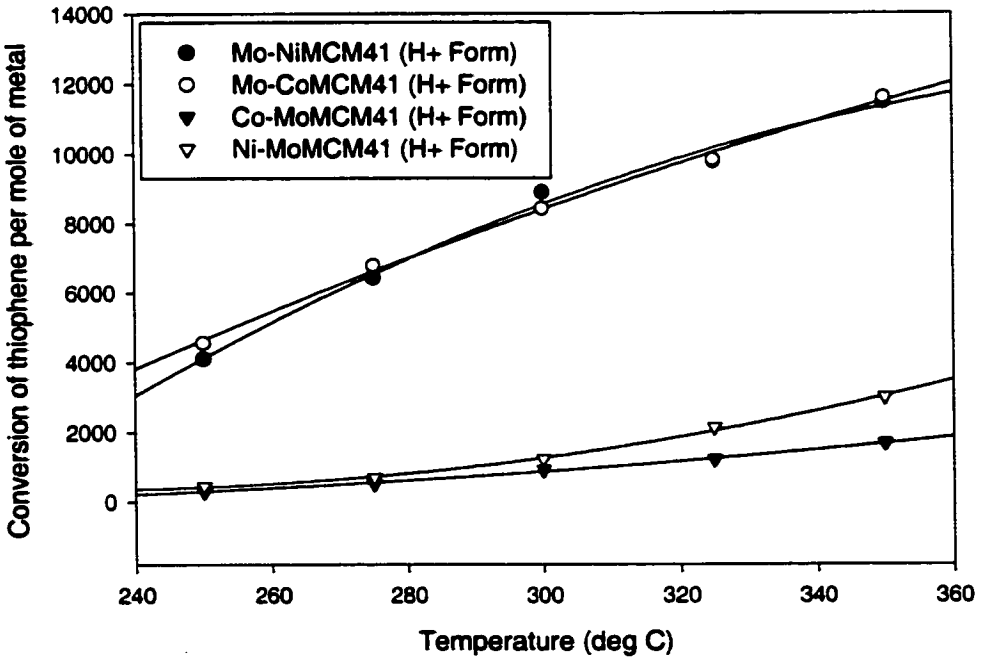

FIGURE 4-40 Conversion per metal mole for thiophene hydrodesulfurization as a function of temperature on metal impregnated on metal incorporated MCM41 catalyst. (H^+ Form)

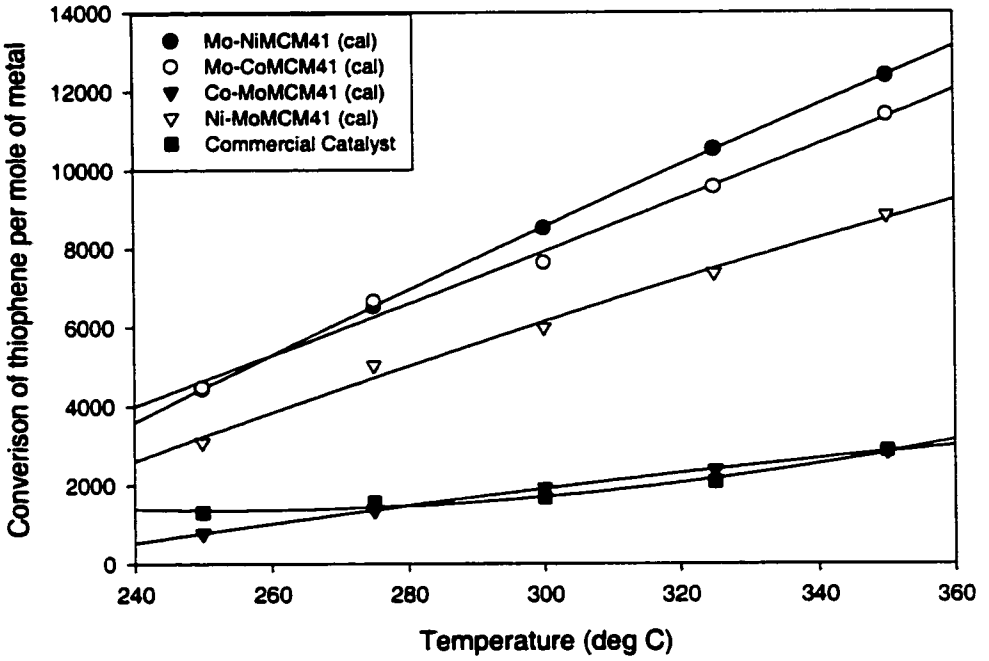

FIGURE 4-41 Conversion per metal mole for thiophene hydrodesulfurization as a function of temperature on metal impregnated on metal incorporated MCM41 catalyst. (Calcined)

4.5.2 Hydrodesulfurization (HDS) of Benzothiophene

The results are grouped as metal incorporated MCM41 and metal impregnated on metal incorporated MCM41.

4.5.2.1 Metal Incorporated MCM41

As shown in table 4-7 MCM41 without any metal incorporation showed the least conversion of benzothiophene as compared to metal incorporated MCM41. Similar to thiophene conversion, Molybdenum incorporated MCM41 catalysts showed higher conversion per metal mole as compared to nickel and cobalt incorporated MCM41 catalysts. Comparison of cobalt incorporated MCM41 catalysts and nickel incorporated MCM41, CoMCM41 has shown higher conversion per mole for benzothiophene hydrodesulfurization similar to thiophene hydrodesulfurization activity. Reason is as discussed in section 4.5.1.1 of hydrodesulfurization of thiophene.

4.5.2.2 Metal Impregnated on metal incorporated MCM41

As shown in table 4-8 and figures 4-43, 4-44 the trend is similar to what we got for thiophene conversion. Mo-NiMCM41 and Mo-CoMCM41 performed better as compared to Co-Mo and Ni-Mo. Commercial catalyst has less benzothiophene conversion and even it has very less activity per metal mole as compared to impregnated MCM41 catalyst. Reason for all the results of HDS of Benzothiophene of impregnated catalyst are as discussed in section 4.5.1.2 of hydrodesulfurization of thiophene.

TABLE 4-7 HDS activity (Conversion of Benzothiophene) of MCM41 ad metal incorporated MCM41 catalysts, evaluated in pulse reactor.

S.No	Catalysts	HDS activity (Conversion of Benzothiophene at temperature °C)				
		250	275	300	325	350
1	MCM41	--	0.30	0.50	0.52	0.70
2	NiMCM41	0.60	0.80	1.55	2.35	3.16
3	MoMCM41	1.09	2.95	4.60	5.99	7.20
4	CoMCM41	0.85	1.52	2.91	5.09	5.98

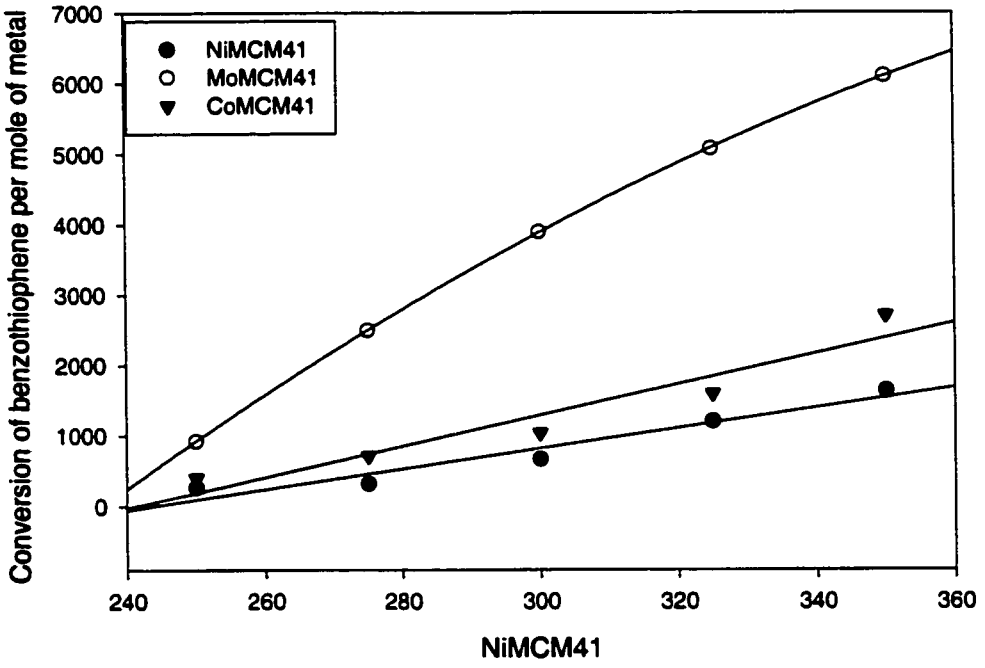

FIGURE 4-42 Activity per metal mole for benzothiophene hydrodesulfurization as a function of temperature on metal incorporated MCM41 catalyst.

TABLE 4-8 HDS activity (Conversion of benzothiophene) of metal impregnated on metal incorporated MCM41 catalyst, evaluated in pulse reactor.

S.No	Catalysts	(Conversion of Benzothiophene at temperature °C)				
		250	275	300	325	350
1	Mo-NiMCM41 (Cal)	14.86	21.47	23.26	24.28	24.40
2	Mo-NiMCM41 (Ion)	3.10	5.50	6.61	6.78	7.61
3	Mo-CoMCM41 (Cal)	13.40	17.07	18.52	19.64	20.00
4	Mo-CoMCM41 (Ion)	3.20	5.30	6.05	6.60	7.30
5	Co-MoMCM41 (Cal)	8.60	9.12	9.61	9.95	10.71
6	Co-MoMCM41 (Ion)	3.32	4.80	5.21	5.93	6.46
7	Ni-MoMCM41 (Cal)	5.01	6.40	7.35	7.38	7.90
8	Ni-MoMCM41 (Ion)	2.98	4.18	4.84	5.50	6.40
9	Commercial catalyst	10.11	11.50	13.10	15.10	17.10

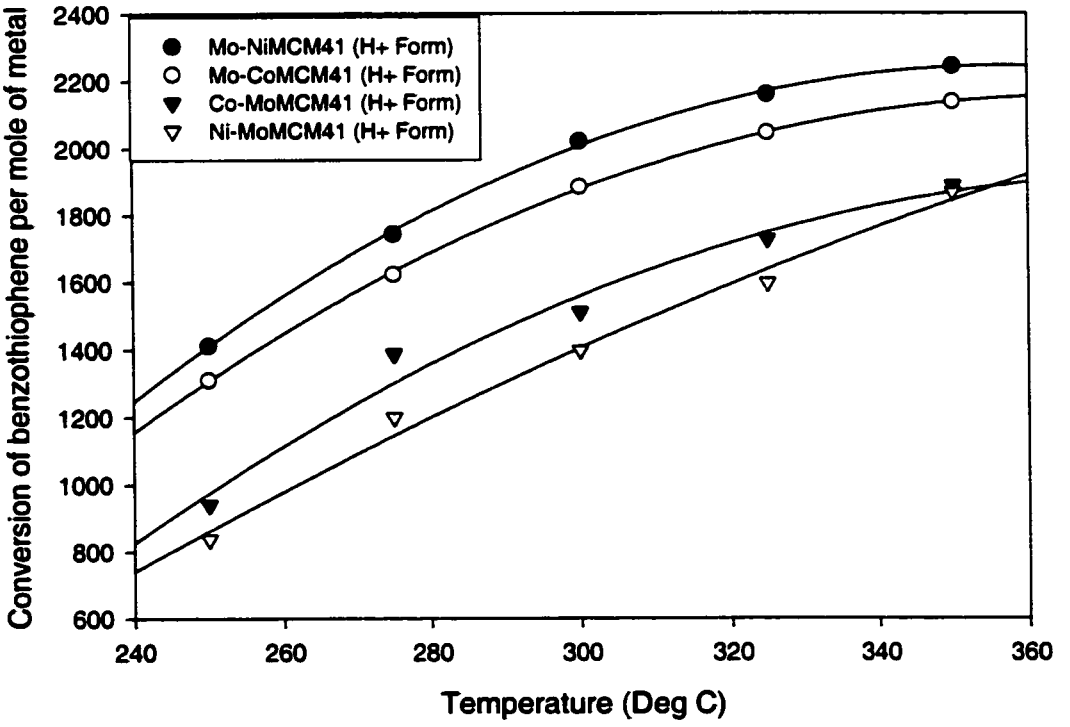

FIGURE 4-43 Activity per metal mole for benzothiophene hydrodesulfurization as a function of temperature on metal impregnated on metal incorporated MCM41 catalyst.

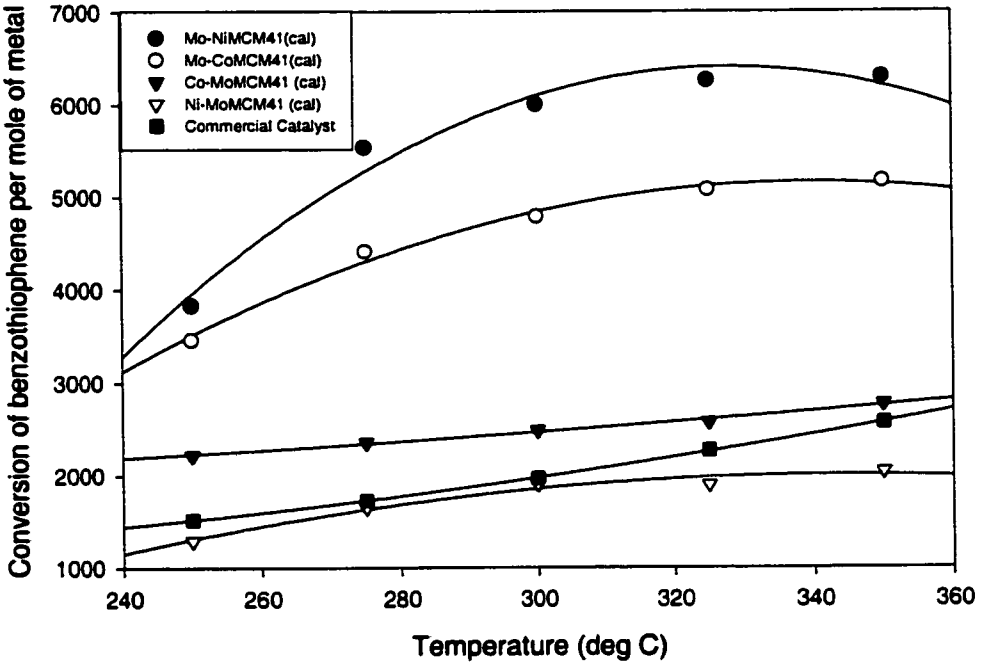

FIGURE 4-44 Activity per metal mole for benzothiophene hydrodesulfurization as a function of temperature on metal impregnated on metal incorporated MCM41 catalyst.

4.6 Batch Evaluation

Hydrodesulfurization (HDS) of petroleum fractions to lower their sulfur content down to specified levels is widely applied in today's refineries. It is well known based on the detailed analysis of sulfur compounds in petroleum heavy oils that dibenzothiophene (DBT) and it's derivatives are the ones which are big in size and are unable to access the active sites of the catalyst. These sulfur containing model compounds also tend to show high resistivity towards deep desulfurization. Therefore, DBT becomes a typical target molecule. Because the zeolites have limited accessibility for large molecules like DBTs, there was need of catalyst having bigger pores.

In this section batch reactor evaluation results of the promising catalysts are presented and discussed. Promising catalysts were selected from the pulse reactor evaluation results and gas sorption analyzer results. From the pulse reactor results it was observed that Mo-NiMCM41 (calcined) and Mo-CoMCM41 (calcined) showed the highest activity. Ni-MoMCM41 also showed comparable conversion per mole with the above two catalysts but higher as compared to commercial catalyst.

From the gas sorption analyzer results, Ni-MoMCM41 showed highest pore radius as compared to all catalyst and highest surface area as compared to Mo-NiMCM41 and Mo-CoMCM41.

Experimental details and the operating conditions have been given in chapter 3. After completion of the reaction for specified time, gas was purged out and liquid product was collected. Liquid sample was analyzed by GC for the amount of sulfur remaining in the product as dibenzothiophene.

To set the system temperature and pressure conditions, several runs were made with commercial catalyst. Initially the temperature was kept at 380 °C and feed as 1000 ppm of dibenzothiophene in dodecane and 3wt% catalyst. Table 4-9 represents the batch reactor results for 3 wt% catalysts. From the above table it is noticed that Mo-NiMCM41 showed less conversion as compared to commercial catalyst. If conversion is looked per metal mole, Mo-NiMCM41 is performing high as compared to commercial catalyst. Cobalt incorporated MCM41 showed less activity as compared to impregnated MCM41 and commercial catalyst but still it is high in terms of conversion. Conversion of all the catalysts were almost in the same range and difficult to compare. In order to differentiate the catalysts, the catalyst wt% was reduced from 3% to 2%. Table 4-10 represents the batch reactor results for 2 wt% catalysts. Results showed that commercial catalyst, Ni-MoMCM41, Mo-NiMCM41 and Co-MoMCM41 have very high activity and the conversions of the catalysts were distinguishable. To have a better comparison and for showing the effect of pore radius, Mo-Ni/Yzeolite was prepared and tested at the same conditions. Mo-Ni/Yzeolite showed less conversion as compared to MCM41 based molecular sieves. The reason of low conversion of DBT in zeolites can be attributed to the inaccessibility to the active sites of the zeolites as the pore radius is small in comparison to the size of the DBT molecule. Since the reactant composition was less i.e 1000 ppm, pore size effect was not clear. Whatever conversion is there in zeolite can be attributed to the surface reaction on the catalyst and in the mesopores formed during the treatment to the catalyst. i.e. impregnation and calcination.

To have better comparison, reactant composition DBT in dodecane was increased from 1000ppm to 2500 ppm and catalyst weight percentage was decreased from 2wt% to

0.5wt%. Table 4-11 clearly shows us the effect of the using a mesopores material like MCM41 with high surface area and high pore volume and high pore radius.

Ni-MoMCM41 are performing at par with commercial catalyst with almost 70% conversion. Comparison of impregnated nickel and molybdenum on Y-zeolite with Ni-MoMCM41 clearly indicates that low surface area and low pore volume and less pore radius accounts for the less conversion.

The conversion of Co-MoMCM41 and Ni-MoMCM41 supported is comparable to commercial catalyst. If the conversion per metal mole is looked, then for commercial catalyst, conversion per metal mole is very low as the amount of metal present in commercial catalyst is almost three times the amount of metal present in Co-MoMCM41 and Ni-MoMCM41. Results are inline with the result obtained by Song and Reddy[50] where they proved that cobalt and molybdenum when impregnated on MCM41 is active for hydrodesulfurization of DBT in n-tridecane. The results are also inline with results of work done by Corma *et. al.*[48], where he proved that MCM41 combination of large surface area, uniform pore size distribution, large enough to allow diffusion of large molecules produces a superior HDS performance than either amorphous silica or unit cell size USY zeolite. Ni/MoMCM41 and Co/MoMCM41 have compatible conversion per metal mole, which is in contrast with the result obtained by Wang *et. al.*[58, 56] . They impregnated molybdenum and nickel on MCM41 with 20 wt% MoO_3 and Ni/Mo atomic ratio of 0.75 and tested at high pressure and at temperatures ranging from 240 °C –380 °C. Ni-Mo/MCM41 showed better performance than Co-Mo/MCM41 in the HDS of DBT due to enhanced hydrogenation ability of Ni-Mo sulfides.

TABLE 4-9 Batch reactor evaluation results using 1000 ppm dibenzothiophene in dodecane as feed.

Catalyst	Wt%	Temperature °C	ppm of sulfur in the product
Commercial Catalyst	3	380	0
CoMCM41	3	380	108
Mo-NiMCM41	3	380	2
Commercial Catalyst	3	380	0

TABLE 4-10 Batch reactor evaluation results using 1000 ppm dibenzothiophene in dodecane as feed and 2 wt% catalyst.

Catalyst	Wt%	Temperature °C	ppm of sulfur in the product
Commercial Catalyst	2	360	0
Mo-NiMCM41	2	360	18
Co-MoMCM41	2	360	0
Ni-MoMCM41	2	360	0
Mo-CoMCM41	2	360	5
Mo-Ni/Yzeolite	2	360	52
Commercial Catalyst	2	360	0
Ni-MoMCM41	2	360	0

TABLE 4-11 Batch reactor evaluation results using 2500 ppm dibenzothiophene in dodecane as feed and 0.5wt%catalyst.

Catalyst	Wt%	Temperature °C	ppm of sulfur in the product	Conversion (%)
Commercial Catalyst	0.5	360	750	70.0
Ni-MoMCM41	0.5	360	810	67.6
Co-MoMCM41	0.5	360	770	69.2
MoNi-Yzeolite	0.5	360	1770	29.2

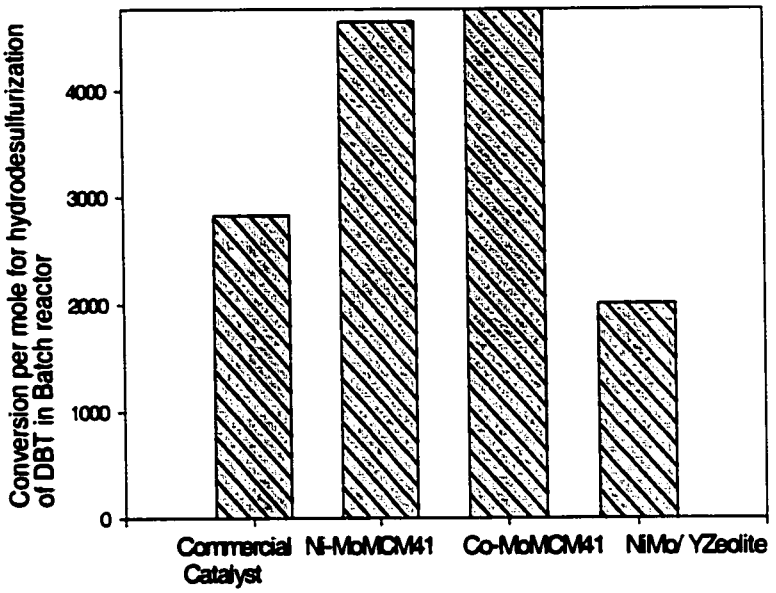

FIGURE 4-45 Conversion per metal mole for hydrodesulfurization of dibenzothiophene in batch reactor.

Conclusions and Recommendations

5.1 Conclusions

From this study the following conclusions are drawn:

1. Metal containing MCM41 has been successfully synthesized. Properties of these materials resemble similar to the properties as given in the literature. Cobalt incorporated MCM41 and nickel incorporated MCM41 molecular sieves synthesized are crystalline and resemble all the typical characteristics of mesoporous molecular sieve MCM41. Molybdenum incorporated MCM41 is comparatively less crystalline as compared to nickel and cobalt incorporated MCM41 molecular sieves.

2. Elemental analysis showed that metal content in H^+ form of catalyst is less as compared to calcined form, indicating leaching of metal during ion exchange, which was confirmed by comparing the areas in TPR results.

3. Molybdenum incorporated MCM41 has high activity in pulse reactor as compared to nickel and cobalt for thiophene and benzothiophene HDS. During ion exchange metal is getting leached out from metal incorporated MCM41.Molybdenum is getting leached out the most as compared to cobalt and nickel incorporated MCM41 molecular sieves.

4. All bi metallic catalyst has shown high HDS as compared to single incorporated MCM41 in HDS reaction of thiophene and benzothiophene in pulse reactor.

5. Mo-NiMCM41 and Mo-CoMCM41 has shown high activity for thiophene and benzothiophene HDS in pulse reactor as compared to commercial catalyst and other MCM1 based catalyst.

6. Mo-Ni/Yzeolite showed very less conversion for DBT in dodecane as compared to MCM41 based catalyst and commercial catalyst.

7. MCM41 based catalyst have shown high conversion per metal mole as compared to commercial catalyst in batch reactor as the conversion for DBT was almost the same with more than 3 times of metal content in commercial catalyst.

5.2 Recommendations

After conducting detailed investigations of the metal incorporation in MCM41, the following recommendations for future research are presented

1. Morphological characterizations like transmission electron microscopy (TEM) and X-ray photoelectron spectra (XPS) can be conducted to observe the ionic state of the metals and dispersion of the different metal on MCM41.

2. In this study batch autoclave reactor was employed for catalysts evaluation due to its simplicity and short time required conducting the experiments. A microflow reactor can be used for further studies. Such a reactor will enable a steady state operation and catalyst deactivation and studies for long time.

3. Metal incorporated MCM41 can be mixed with other supports like alumina or Y-zeolites and then should be tested for hydrodesulfurization.

4. In this study, D.B.T. in dodecane as a feed was used in batch autoclave reactor. Other feed can also be used like 4, 6, di methyl dibenzothiophene in dodecane.

5. Catalyst should be tested on real feed i.e. V.G.O. for hydrodesulfurization.

6. Ramirez *et. al.*[55] reported that the strong acidity in MCM41 was detrimental to the HDS activity of the catalyst. Wang *et. al.*[56,68] confirmed the fact by reporting that high surface area and mild acidity of the support improves the HDS activity. Hence metal (Ni or Co or Mo) incorporated MCM41 should be prepared without simultaneously incorporating aluminium with it, which will result in high surface area and high pore volume and high crystallanity.

APPENDIX A

TPR MEASUREMENTS

<< P A R A M E T E R >>

(1) DATA NAME	=	211024
(2) INITIAL TEMP(℃)	=	30
(3) INITIAL TEMP HOLDING TIME (min)	=	1
(4) TIME BY TARGET TEMP (min)	=	100
(5) FINAL TEMP(℃)	=	1030
(6) FINAL TEMP HOLDING TIME (min) .	=	10
(7) CALIBRATION = (μmol) / (COUNT)	=	1
(8) SAMPLE WEIGHT (g)	=	1
(9) MEMO	=	CoM41-1(CALCINED)
(10) X-AXIS(TIME:'0' / TEMP:'1') .	=	1

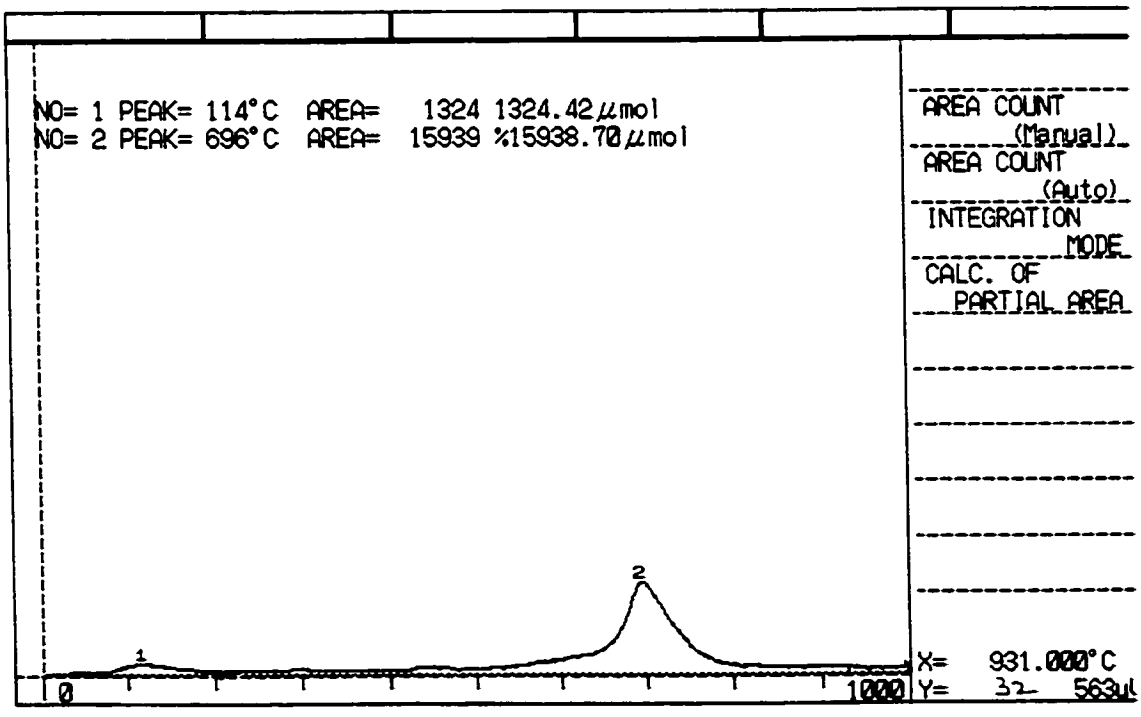

APPENDIX B

THIOPHENE GC RESULTS

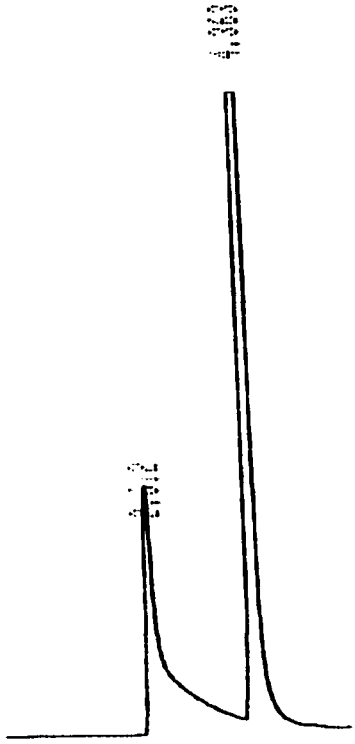

Chromatopac	C-60	File	0	
Sample No.	0	Method	41	
Report No	5073			
PKNO	TIME	AREA	MK	CONC
1	2.612	33497	V	18.7795
2	4.363	144872	V	81.2205
	TOTAL	178369		100

APPENDIX C

SAMPLE CALCULATION OF CONVERSION PER METAL MOLE IN PULSE REACTOR FOR THIOPHENE

Sample calculation for hydrodesulfurization (HDS) activity of thiophene for metal incorporated MCM41 are as follows

$$\% \text{ conversion} = (A_{product} / (A_{product}+A_{thiophene})) * 100 \quad (5\text{-}1)$$

where $A_{thiophene}$ is area under the peak for unreacted thiophene, $A_{product}$ is area under the peak of product. For example, $A_{product} = 36672$, $A_{thiophene} = 158967$

$$\% \text{ conversion} = (36672 / (36672+158967)) * 100 = 18.74$$

$$\text{Conversion per mole metal} = x/(\text{atom-metal}) = 100*x/(M*\text{Factor})$$

where x is conversion of thiophene(18.74), M is the weight of catalyst loaded into the reactor,0.1 gm, and

$$\text{Factor} = (W_{CoO} / MW_{CoO})$$

where MW_{CoO} is molecular weight of CoO (74.93 gm/mol), W_{CoO} is weight percent of CoO on the catalyst (1.5), therefore Factor is equal to 0.02. Now, the conversion per mole metal is equal to 9370.

Sample calculation for hydrodesulfurization (HDS) activity of thiophene for metal impregnated MCM41 are as follows (Mo-CoMCM41)

$$\% \text{ conversion} = (A_{product} / (A_{product} + A_{thiophene})) * 100 \quad (5\text{-}2)$$

where $A_{thiophene}$ is area under the peak for unreacted thiophene, $A_{product}$ is area under the peak of product. For example, $A_{product} = 89171$, $A_{thiophene} = 119164$

$$\% \text{ conversion} = (89171 / (89171 + 119164)) * 100 = 42.80$$

$$\text{Conversion per mole metal} = x/(\text{atom-metal}) = 100 * x/(M * \text{Factor})$$

where x is conversion of thiophene(42.80), M is the weight of catalyst loaded into the reactor,0.1 gm, and

$$\text{Factor} = (W_{CoO} / MW_{CoO}) + (W_{MoO3} / MW_{MoO3})$$

where MW_{CoO} is molecular weight of CoO (74.93 gm/mol), MW_{MoO3} is molecular weight of MoO_3 (143.94 gm/mol), W_{CoO} is weight percent of CoO on the catalyst (1.5), W_{MoO3} is weight percent of MoO_3 on the catalyst (2.5), therefore Factor is equal to 0.03738. Now, the conversion per mole metal is equal to 501337.61.

APPENDIX D

SAMPLE CALCULATION FOR HDS ACTIVITY OF BENZOTHOPHENE FOR METAL IMPREGNATED CATALYST

Sample calculation for hydrodesulfurization (HDS) activity of benzothiophene for metal incorporated MCM41 are as follows

$$\% \text{ conversion} = (A_{product} / (A_{product} + A_{benzothiophene})) * 100$$

where $A_{benzothiophene}$ is area under the peak for unreacted benzothiophene, $A_{product}$ is area under the peak of product. For example, $A_{product} = 15399$, $A_{benzothiophene} = 39117$

$$\% \text{ conversion} = (15399 / (15399+39117)) * 100 = 18.74$$

$$\text{Conversion per mole metal} = x/(\text{atom-metal}) = 100*x/(M*\text{Factor})$$

where x is conversion of benzothiophene(18.74), M is the weight of catalyst loaded into the reactor,0.1 gm, and

$$\text{Factor} = (W_{CoO} / MW_{CoO}) + (W_{MoO3} / MW_{MoO3})$$

where MW_{CoO} is molecular weight of CoO (74.93 gm/mol), MW_{MoO3} is molecular weight of MoO_3 (143.94 gm/mol), W_{CoO} is weight percent of CoO on the catalyst (1.5), W_{MoO3} is weight percent of MoO_3 on the catalyst (2.5), therefore Factor is equal to 0.03738. Now, the conversion per mole metal is equal to 5013.61.

Sample calculation for hydrodesulfurization (HDS) activity of benzothiophene for metal impregnated MCM41 are as follows

$$\% \text{ conversion} = (A_{product} / (A_{product}+A_{benzothiophene})) * 100 \quad (5\text{-}1)$$

where $A_{benzothiophene}$ is area under the peak for unreacted benzothiophene, $A_{product}$ is area under the peak of product. For example, $A_{product} = 34496$, $A_{benzothiophene} = 158967$

$$\% \text{ conversion} = (34496/ (34496+158967)) * 100 = 17.83$$

$$\text{Conversion per mole metal} = x/(\text{atom-metal})=100*x/(M*\text{Factor})$$

where x is conversion of benzothiophene(17.83), M is the weight of catalyst loaded into the reactor,0.1 gm, and

$$\text{Factor} = (W_{CoO}/ MW_{CoO}) + (W_{MoO3} /MW_{MoO3})$$

where MW_{CoO} is molecular weight of CoO (74.93 gm/mol), MW_{MoO3} is molecular weight of MoO_3 (143.94 gm/mol), W_{CoO} is weight percent of CoO on the catalyst (1.5), W_{MoO3} is weight percent of MoO_3 on the catalyst (2.5), therefore Factor is equal to 0.03738. Now, the conversion per mole metal is equal to 4769.9.

APPENDIX E

RECIPE FOR PREPARATION OF METAL INCORPORATED MCM41 CATALYSTS

Silica sources: Ludox (40 wt% silica, **[Alfa]**)

Aluminium source: Aluminium sulfate **[Alfa]**

Metal source: e.g. Nickel nitrate **[Fisher Scientific Company]**

Metal source: e.g. HexaAmmonium Heptamolybdate **[Mallin Ckrodt]**

Metal source: e.g. Cobalt Nitrate **[Mallin Ckrodt]**

Organic Template: 25 wt% aqueous solution of cetyl tri methyl ammonium bromide (CTABr, **[Aldrich]**)

Solution A:

1. Take 12.5 gm of CTABr and dissolve it in 38 gm of deionized water.
2. Dissolve desired amount of nickel nitrate in deionized water.
3. Dissolve the 2 solutions got in step 1 and 2 slowly with continuous stirring. Keep on stirring in PP bottle applying gentle heat. In case it gets thick then add solution of NaOH so as to make gel.

Solution B:

1. Take 1 gm NaOH and dissolved it in 13.5 gm water.
2. Add 1.55 gm $NaAlO_2$ to the solution and stir it for long time till it gets dissolved.

Solution C:

1. Dissolve 3.83 gm NaOH in 100gm water.
2. Add 33.5gm ludox HS-40 and heat for ½ hour with continuous stirring till clear solution is obtained.

PROCEDURE:

1. Add solution A and solution B at room temperature.
2. Cool C to RT & Mix C to solution obtained from step 1 and stir it ½ hour.
3. Adjust pH with 30% acetic acid to 10.5.
4. Allow to cool the solution for 1 hour and again adjust pH to 10.5.
5. After every 24 hour pH was adjusted to 10.5 and allowed to react for 4 days at 373 K in reactor bottle.
6. After 4 days, product was filtered and washed with ethanol and dried overnight at 323°C.

LITERATURE CITED

1. Srinivasan R, Hydrodesulfurization. *Business Line*, (May 1999).

2. Knudsen K.G., B. H. Cooper, and H. Topsoe, *Applied Catalysis A:General*, **189**, 205 (1999).

3. C. T. Kresge, M. E. Leonowicz, W. J. Roth, J. C. Vartuli, K. M. Keville, S. S. Shih, T. F. Degnan, F.G. Dwyer, and M. E. Landis, Demetallation of hydrocarbon feedstocks with a synthetic mesoporous crystalline material. *US Patent*, **5183561**, (1993).

4. M. R. Apelian, T. F. Degnan, D. O. Marler, D. N. Mazzone, Hydroprocessing catalyst composition. *US Patent*, **5227353**, (1993).

5. S. S. Shih, Upgrading of a hydrocarbon feedstock utilizing a graded, mesoporous catalyst system. *US Patent*, **5344553**, (1994).

6. T. F. Degnan, K. M. Keville, M. E. Landis, D. O. Marler, D. N. Mazzone, Hydrocracking process using ultra-large pore size catalysts. *US Patent*, **5183557**, (1993).

7. T. F. Degnan, K. M. Keville, M. E. Landis, D. O. Marler, D. N. Mazzone, Hydrocracking process using ultra-large pore size catalysts. *US Patent*, **5290744**, (1993).

8. N. A. Bhore, I. D. Johnson, K. M. Keville, Q. N. Le, G. H. Yokomizo, Catalytic oligomerization process using modified mesoporous crystalline material. *US Patent*, **5260501**, (1993).

9. Xiaoliang Ma and Harold Schobert, *Journal of Molecular Catalysis*, **160**, 409-427 (2000).

10. C. N. Satterfield, *Hetrogeneous catalysis in industrial practice*, Vol. 2, McGraw-Hill International Editions, 1993.

11. D. Duayne Whitehurst, Takaaki Isoda, and Isao Mochida, *Advances in Catalysis*, **42**, 345-467 (1998).

12. H. Pine, *The Chemistry of catalytic hydrocarbon conversion*, Academic Press, New York, 1981.

13. T. Kabe, A. Ishihara, and W. Qian., *Hydrodesulfurization and Hydrodenitrogenation*, Kodansha Ltd., 1999.

14. D. Chadwick, and M. Breysse, *Journal of Catalysis*, **71**, 226 (1981).

15. R. Chianelli, and S. Tauster, *Journal of Catalysis*, **71**, 228 (1981).

16. H. Topsoe, R. Canadia, Y. Topsoe, and B. Clausen, *Bull. Soc. Chim. Belg.*, **93**, 783 (1984).

17. S. Tauster, T. Pecoraro, and R. Chianelli, *Journal of Catalysis*, **63**, 515 (1980).

18. M. Daage, and R. Chianelli, *Journal of Catalysis*, **149**, 414 (1994).

19. J. Lipsch, A. Schuit , *Journal of Catalysis*, **15**, 179 (1969).

20. F. Massoth, *Journal of Catalysis*, **36**, 164 (1975).

21. R. Voorhoeve and J. Stuiver, *Journal of Catalysis*, **23**, 243 (1971).

22. G. Hagenbach, P. Courty and B. Delmon, *Journal of Catalysis*, **23**, 295 (1971).

23. G. Hagenbach, P. Courty and B. Delmon, *Journal of Catalysis*, **31**, 264 (1973).

24. H. Topsoe, B. Ckausen, R. Candia, C. Wivel and S. Morup, *Journal of Catalysis*, **68**, 433 (1981).

25. C. Wivel, R. Candia, B. Clausen, S. Morup and H. Topsoe, *Journal of Catalysis*, **68**, 453 (1981).

26. H. Topsoe, B. Clausen and F. Massoth, *Hydrotreating Catalysis: Science and Technology*, Berlin (1996).

27. Vasudevan, and J.L.Fierro, *Catalysis Reviews-Science and Engineering*, **38**(2), 161-188 (1996).

28. E. Hensen, J. Lardinois, H. de Beer, V. H. J., J. Veen and V. Santen, *J. Catal*, **187**, 95 (1999).

29. M. Nagai, H. Koyama, S. Sakamoto and S. Omi, *Stud. Surf. Sci. Catal*, **127**, 195 (1999).

30. Fierro, J. C. Conesa, and Lopez Agudo, *Journal of Catalysis*, **108**, 334-345 (1987).

31. Leglise, A. Janin, J. C. Lavalley, and D. Cornet, *Journal of Catalysis*, **114**, 388-397 (1988).

32. Cid Ruby, F. Orellana, and Lopez Agudo, *Applied Catalysis*, **32**, 327-336 (1987).

33. D. Yitzhaki, M.V. Landua, D. Berger, and M. Herskowitz, *Applied Catalysis*, **122**, 99-110 (1995).

34. Avelino Corma, *Chemical Reviews*, **97**(6), 2373-2419 (1997).

35. J. S. Beck, J. C. Vartuli, W. J. Roth, M. E. Leonowicz, C. T. Kresge, K. D. Schmitt, C. T. Chu, D. H. Olson, E. W. Sheppard, S. B. McCullen, J.B. Higgins, and J. L. Schlenker , *J. Am. Chem. Soc.*, **114**(27), 10834-10843 (1992).

36. Y. C. Cong, L. B. Sandra, Hong Xin Li, and Mark Davis , *Microporous Materials*, **2**, 27-34 (1993).

37. N. A. Raman, M. T. Anderson, C. J. Brinker, *Chem. Mater*, **8**, 1682-1701 (1996).

38. C. Y. Chen, H. Y. Li, M. E. Davis, *Microporous. Mater.*, **2**, 27-34 (1993b).

39. S. Jaenicke, L. Y. Chen, and G. K. Chuah, *Microporous Materials*, **12**, 323-330 (1997).

40. Ryong Roo and Shinae Jun, *J. Phys. Chem. B*, **101**, 317-320 (1997).

41. Zhixiang Chang, Zhidong Zhu, and Larry Kevan, *J. Phys. Chem. B*, **103**, 9442-9449 (1999).

42. Thomson, *US Patent*, **5232580**, - (1993).

43. Y. Cesteros and G. L. Haller, *Microporous and Mesoporous Materials*, **43**, 171-179 (2001).

44. Dong Ho Park, Sung Soo Park, and Sang Joon Choe, *Bull. Korean Chem. Soc.*, **20**(6), 715-719 (1999).

45. Rohit Kumar Rana and B. Vishwanathan, *Catalysis Letters*, **52**, 25-29 (1998).

46. Deung-Hee Cho, Tae-Sun Chang, Seung-Kon Ryu, and Young K. Lee, *Catalysis Letters*, **64**, 227-232 (2000).

47. A. Corma, V. Fornes, M. T. Navarro, and J. Perez-Pariente, *Journal of Catalysis* , **148**, 569-574 (1994).

48. A. Corma, A. Martinez, V. Martinez-Soria, and J. B. Monton, *Journal of Catalysis*, **153**, 25-31 (1995).

49. Chunshan Song and Kondam Madhusudan Reddy, *Applied Catalysis*, **176**, 1-10 (1999).

50. C. Song, K. M. Reddy, *Am. Chem. Soc.,Div. Petro. Chem. Prep.*, **41**(3), 567 (1996).

51. Kondam Madhusudan Reddy, Boli Wei, Chunshan Song, *Catalysis Today*, **43**, 261-272 (1998).

52. J. C. Vartuli, S. S. Shih, C. T. Kresge, and J. S. Beck, *Studies of Surface Science and Catalysis*, **117**, 13 (1998).

53. J. Cui, Y. N. Yue, Y. Sun, W. Y. Dong, and Z. Gao, *Studies of Surface Science and Catalysis*, **105A**, 687 (1997).

54. T. Klimova, J. Ramirez, M. Calderon, and J. M. Dominguez, *Studies in Surface Science and Catalysis*, **117**, 493-500 (1998).

55. Jorge Ramirez, Roberto Contreras, Perla Castillo, Tatiana Klimova, Rene Zarate, and Rosario Luna, *Applied Catalysis*, **197**, 69-78 (2000).

56. A. Wang, Y. Wang, T. Kabe, Y. Chen, A. Ishihara, and W. Qian, *Journal of Catalysis*, **199**, 19-29 (2001).

57. A. Wang, Y. Wang, T. Kabe, Y. Chen, A. Ishihara, W. Qian, and P. Yao, *Journal of Catalysis*, **210**, 319-327 (2002).

58. Paul A. Webb and Clyde Orr, *Analytical methods in fine particle technology*, Micromeritics Instrument Corporation, 1997.

59. J. S. Beck, *US patent*, **5057296**, 1 (1991).

60. Z. Luan, C. Cheng, W. Zhou, and J. Klinowski, *J. Phys. Chem*, **99**, 1018-1024 (1995).

61. Z. Luan, H. He., C. Cheng, W. Zhou, and J. Klinowski, *J. Chem. Soc. Faraday Trans.*, **91**, 2955-2959 (1995).

62. S. Brauner, L. S. Deming, and E. Teller, *J. Am. Chem. Soc.*, **62**, 1723 (1940).

63. P. Arnoldy and J. A. Moulijn , *Journal of catalysis* , **93**, 38-54 (1985).

64. B. Mile, D. Stirling, M. Zammitt, A. Lovell, and M. Webb, *Journal of Catalysis*, **114**, 217-229 (1988).

65. P. Arnoldy, M. Franken, B. Scheffer, and J. Moulijn, *Journal of catalysis*, **96**, 381-395 (1985).

66. B. Notari, *Catalysis Today*, **18**, 163 (1993).

67. A. Jentys, N. H. Pham, H. Vinek, Englisch, J. A. Lercher, *Microporous Materials*, **6**, 13-17 (1996).

68. A. Wang, X. Li, Y. Wang, T. Kabe, Y. Chen, Y. Hu, and D. Han, *Chem. Lett.*, **5**, 474 (2001).

VITA

Name	Rizwan Ahmed Khan
Date & Place of Birth	29-Aug-1977, Aurangabad (India)
Nationality	Indian
Religion	Islam
Marital Status	Single
Educational qualifications	B. E. in Petroleum Engineering from Maharashtra Institute of Technology, Pune, India (1994-98). M. B. A. from Indira Institute of Management, Pune, India (1999-2000).[Ist year completed] M. Sc. in Chemical Engineering from King Fahd University of Petroleum & Minerals, Dhahran, Saudi Arabia (2000-todate).